NOVEL ADAPTIVE STRATEGIES FOR NON-LINEAR SYSTEM IDENTIFICATION

Naveed Ishtiaq Chaudhary

60-FET/PHDEE/F13

Submitted in partial fulfillment of the requirements for the PhD degree in Electronic Engineering at the Department of Electrical Engineering

Faculty of Engineering and Technology

International Islamic University,

Islamabad

Supervisor

Dr. Syed Zubair

May, 2018

1- Adaptive strategies
2- Neutral networks
3- Nonlinear control theory
4- Theses

DEDICATED TO

My Teachers,

Parents,

Wife, Kids,

and Sisters

CERTIFICATE OF APPROVAL

Title of Thesis: Novel Adaptive Strategies for Non-linear System Identification

Name of Student: Naveed Ishtiaq Chaudhary

Registration No: 60-FET/PHDEE/F13

Accepted by the Department of Electrical Engineering, Faculty of Engineering and Technology, International Islamic University, Islamabad, in partial fulfillment of the requirements for the Doctor of Philosophy degree in Electronic Engineering.

Viva voce committee:

Dr. Suheel Abdullah Malik (Chairman)
Associate Professor
Department of Electrical Engineering
International Islamic University, Islamabad.

Prof. Dr. Ijaz Mansoor Qureshi (External Examiner)
Department of Electrical Engineering
Air University, Islamabad.

Dr. Aamer Saleem Choudhry (External Examiner)
Associate Professor
Hamdard Institute of Engineering & Technology
Hamdard University, Islamabad.

Prof. Dr. Muhammad Amir (Internal Examiner)
Dean, Faculty of Engineering & Technology
International Islamic University, Islamabad.

Dr. Syed Zubair (Supervisor)
Assistant Professor
Department of Electrical Engineering
International Islamic University, Islamabad

May 3, 2018

ABSTRACT

The Hammerstein model in which a static nonlinear function is followed by a linear dynamic block has been used extensively to model a variety of nonlinear problems. The traditional algorithms for Hammerstein system identification are based on stochastic gradient and least squares methods. The present work may consider to be an advancement in designing an accurate, alternate, and convergent computing mechanism based on deep rooted fractional calculus concepts for Hammerstein system identification. Fractional calculus is a branch of mathematics that deals with non-integer order derivatives and integrals. The concepts of fractional order calculus are exploited to develop fractional least mean square (FLMS), modified FLMS-1 and 2, normalized FLMS, sliding window based FLMS and momentum FLMS algorithms. The computational cost of FLMS is reduced in MFLMS-1 and 2, convergence made smoother in NFLMS, while SW-FLMS and mFLMS increases the convergence speed of standard FLMS by effectively utilizing the previous information. The correctness of the designed fractional adaptive algorithms is established by efficiently optimizing the parameters of different nonlinear system identification models based on Hammerstein structure. The effective application of proposed momentum FLMS for accurate parameter estimation of electrically stimulated muscle model, as well as, identification of power signals with unknown amplitude and phase further establishes the worth and efficacy of the method. Besides the accurate identification, the other advantages of proposed fractional adaptive strategies include, availability of more controlling parameters, wider applicability domain and flexibility in the design procedure based on fractional integrals or derivatives

LIST OF PUBLICATIONS AND SUBMISSIONS

[1]. **N. I. Chaudhary**, S. Zubair, and M. A. Z. Raja, "Design of momentum LMS adaptive strategy for parameter estimation of Hammerstein controlled autoregressive systems," *Neural Computing and Applications*, 2016. DOI: 10.1007/s00521-016-2762-1 **(IF 2.505)**

[2]. **N. I. Chaudhary**, and M. A. Z. Raja, "Identification of Hammerstein nonlinear ARMAX systems using nonlinear adaptive algorithms," *Nonlinear Dynamics* vol. 79, no. 2, pp. 1385-1397, 2015. **(IF 3.464)**

[3]. **N. I Chaudhary**, M. A. Z. Raja, and A. U. R Khan, "Design of modified fractional adaptive strategies for Hammerstein nonlinear control autoregressive systems," *Nonlinear Dynamics*, vol. 82, no. 4, pp. 1811-1830, 2015. **(IF 3.464)**

[4]. **N. I. Chaudhary,** S. Zubair, and M. A. Z. Raja, "A new computing approach for power signal modeling using fractional adaptive algorithms," *ISA transactions*, vol. 68, pp. 189-202, 2017. **(IF 3.394)**.

[5]. **N. I. Chaudhary**, M. Ahmed, Z. A. Khan, S Zubair and M. A. Z. Raja and N. Dedovic "Design of normalized fractional adaptive algorithms for parameter estimation of control autoregressive autoregressive systems," *Applied Mathematical Modeling*, vol. 55, pp. 698-715, 2018. **(IF 2.350)**

[6]. M. S. Aslam, **N. I. Chaudhary**, and M. A. Z. Raja, "A sliding-window approximation-based fractional adaptive strategy for Hammerstein nonlinear ARMAX systems," *Nonlinear Dynamics*, vol. 87, no. 1, pp. 519-533, 2017. **(IF 3.464)**

[7]. S. Zubair, **N. I. Chaudhary**, Z. A. Khan, and W. Wang, "Momentum fractional LMS for power signal parameter estimation," *Signal Processing*, vol. 142, pp. 441-449, 2018. **(IF 3.110)**

[8]. **N. I. Chaudhary**, M. S Aslam, and M. A. Z. Raja, "Modified Volterra LMS algorithm to fractional order for identification of Hammerstein non-linear system,"

IET Signal Processing, vol. 11, no. 8, pp. 975-985, 2017. **(IF 1.298)**

[9]. **N. I. Chaudhary**, M. A. Manzar and M. A. Z. Raja, "Fractional Volterra LMS algorithm with application to Hammerstein control autoregressive model identification," *Neural Computing and Applications*, 2018. **(IF 2.505)**

[10]. **N. I. Chaudhary**, M. A. Z. Raja, M. S. Aslam, and N. Ahmed, "Novel generalization of Volterra LMS algorithm to fractional order with application to system identification," *Neural Computing and Applications*, 2016. DOI: 10.1007/s00521-016-2548-5 **(IF 2.505)**

[11]. **N. I. Chaudhary** and M. A. Z. Raja, "Adaptive strategies for parameter estimation of Box–Jenkins systems," *IET Signal Processing,* vol. 8, no. 9, pp. 968-980, 2014. **(IF 1.298)**

[12]. M. A. Z. Raja, A. A. Shah, A. Mehmood, **N. I. Chaudhary**, and M. S. Aslam, "Bio-inspired computational heuristics for parameter estimation of nonlinear Hammerstein controlled autoregressive system," *Neural Computing and Applications,* 2016. DOI: 10.1007/s00521-016-2677-x **(IF 2.505)**

[13]. M. A. Z. Raja, J. A. Khan, **N. I Chaudhary**, and E. Shivanian, "Reliable numerical treatment of nonlinear singular Flierl–Petviashivili equations for unbounded domain using ANN, GAs, and SQP," *Applied Soft Computing*, vol. 38 pp. 617-636, 2016. **(IF 3.541)**

[14]. M. A. Z. Raja, U. Farooq, **N. I. Chaudhary**, and A. M. Wazwaz, "Stochastic numerical solver for nanofluidic problems containing multi-walled carbon nanotubes," *Applied Soft Computing*, vol. 38, pp. 561-586, 2016. **(IF 3.541)**

[15]. M. A. Z. Raja, M. A. R. Khan, T. Mahmood, U. Farooq, and **N. I Chaudhary**, "Design of bio-inspired computing technique for nanofluidics based on nonlinear Jeffery–Hamel flow equations," *Canadian Journal of Physics*, vol. 94, no. 5, pp. 474-489, 2016. **(IF 0.877)**

[16]. M. A. Z. Raja, U. Ahmed, A. Zameer, A. K. Kiani, and **N. I. Chaudhary**, "Bio-inspired heuristics hybrid with sequential quadratic programming and interior-point methods for reliable treatment of economic load dispatch problem," *Neural Computing and Applications*, 2017. DOI: 10.1007/s00521-017-3019-3 **(IF 2.505)**

[17]. M. A. Z. Raja, M. S. Aslam, **N. I. Chaudhary**, M. Nawaz and S. M. Shah, "Design of hybrid nature-inspired heuristics with application to active noise control systems," *Neural Computing and Applications*, 2017. DOI: 10.1007/s00521-017-3214-2 **(IF 2.505)**

[18]. A. Mehmood, A. Zameer, M. A. Z. Raja, R. Bibi, **N. I. Chaudhary** and M. S. Aslam, "Nature-inspired heuristic paradigms for parameter estimation of control autoregressive moving average systems," *Neural Computing and Applications*, 2018. DOI: 10.1007/s00521-018-3406-4 **(IF 2.505)**

SUBMITTED PAPERS

[1]. **N. I. Chaudhary,** Z. A. Khan, S Zubair and M. A. Z. Raja, "Normalized Fractional Adaptive Algorithms for Nonlinear Control Autoregressive Systems," *Nonlinear Dynamics* (Major Revision) 2017.

[2]. **N. I. Chaudhary**, S. Zubair and M. A. Z. Raja, "Momentum fractional LMS algorithm for Hammerstein nonlinear system identification," *IET Control Theory & Applications* (submitted) 2017.

The research work presented in this dissertation is based on the accepted publications 1 to 7 and the submitted publications 1 to 2. 8

ACKNOWLEDGEMENTS

In the name of Allah (Subhanahu Wa Ta'ala), who is the most gracious and the merciful. I would like to thank Allah for giving me strength and patience to complete this research work. Peace and blessings of Allah be upon His last Prophet Muhammad (Sallulah-o-Alaihihe-Wassalam) and all his Sahaba (Razi-Allah-o-Anhu) who dedicated their lives for Dawah and spread of Knowledge.

I am truly grateful to my supervisor Dr. Syed Zubair whose inspiration, ideas and efforts make it possible for me to complete my higher studies. He has been a role model for me and many others in teaching, research and other aspects of life. I would also like to thank Dr. Muhammad Asif Zahoor Raja for his time, support and guidance during my research work.

I offer my sincere thanks to my colleagues Engr. Zeshan Aslam Khan, Engr. Khizer Mehmood, Engr. Baber Khan Jadoon, Engr. Rehan and Engr. Sharjeel Abid Butt for their never-ending support during last few years. I would like to acknowledge the support of International Islamic University Islamabad, Pakistan for providing me full fee waiver during the PhD studies. I am thankful to administration at department, as well as university level for their kind support.

I am really grateful to my father (late), mother and sisters for their love and support throughout my life. I am also very thankful to my wife for her patience, encouragement and prayers during every stage of my PhD degree. Finally, I am thankful to my kids, whose innocent gestures were source of inspiration for me.

(Naveed Ishtiaq Chaudhary)

TABLE OF CONTENTS

LIST OF FIGURES

LIST OF ABBREVIATIONS

AM	Auxiliary Model
FLMS	Fractional Least Mean Square
HCAR	Hammerstein Control Autoregressive
HCARMA	Hammerstein Control Autoregressive Moving Average
LTI	Linear Time Invariant
mFLMS	Momentum Fractional Least Mean Square
mLMS	Momentum Least Mean Square
MFLMS-1	Modified Fractional Least Mean Square -1
MFLMS-2	Modified Fractional Least Mean Square -2
MIN	Minimum
MIT	Multi Innovation Theory
MSE	Mean Square Error
NFLMS	Normalized Fractional Least Mean Square
NMFLMS-1	Normalized Modified Fractional Least Mean Square-1
NMFLMS-2	Normalized Modified Fractional Least Mean Square-2
NSE	Nash Sutcliffe Efficiency
SD	Standard Deviation
SNR	Signal to Noise Ratio
SW-FLMS	Sliding Window Fractional Least Mean Square
VAF	Variance Account For

LIST OF SYMBOLS

A list of commonly used symbols in this dissertation are given below.

L	Length of a window
J	Cost function
$\mathbf{I}$	Identity matrix
$\mathbf{R}$	Autocorrelation matrix
fr	Fractional order
δ	Fitness function
α	Proportion of previous gradients
β	Adjustable gain parameter
λ	Eigen value
μ	Step size
μ_1	Step size related to first order gradient
μ_f	Step size related to fractional order gradient
ϕ	Phase
$\mathbf{w}$	Weight vector
$\mathbf{p}$	Cross correlation vector
$\boldsymbol{\theta}$	Parameter vector
$\boldsymbol{\psi}$	Information vector
σ^2	Variance
σ	Standard deviation
t	Time

Chapter 1.

Introduction

In this chapter, significance of nonlinear system identification problem in signal processing and control is briefly overviewed along with the need of exploring and exploiting strong mathematical concepts of fractional calculus in developing an alternate, accurate, reliable, and robust computing mechanism. The main contributions of the study are presented in terms of designing novel adaptive strategies for parameter estimation of nonlinear systems, as well as, their applications to muscle modeling and power signal estimation.

1.1 Background

System identification or parameter estimation deals with learning internal details that govern overall characteristics of a system. Most practical systems exhibit nonlinear characteristics outside a limited linear range and these characteristics are frequently encountered in the form of hysteresis, limit cycle, harmonic distortion, bifurcation and chaos [1], [2]. Nonlinear dynamic processes are considered as inherently complex and can be approximated by nonlinear block oriented models such as Wiener and Hammerstein models. In Wiener models, a linear dynamic block is followed by a static nonlinear function, while a static nonlinear function is followed by a linear dynamic block for

Hammerstein models [3]. Applications of Hammerstein models have been reported in diverse fields such as, identification of nonlinear biological systems [4], nonlinear model predictive control [5], modelling and identification of heat processes [6], vibrating devices [7], fuel control of gas turbine engine [8], emulation of electro-thermal models for power electronic devices [9], wind speed prediction [10] and peak load forecasting [11].

1.2 Research Problem

Many algorithms are used for identification purpose that adaptively learn parameters of Hammerstein nonlinear systems. For instance, least squares and stochastic gradient based algorithms using multi-innovation theory [12], [13], data filtering approach [14], [15], hierarchical principle [16], [17] and parameter separation idea [18]. The increasing complexity of these systems require continuous search for the development of alternate algorithms that could identify the system in a more accurate and reliable way. The commonly used algorithms for Hammerstein systems are based on first order gradient. Recently, the concepts of fractional calculus are applied in different areas of engineering, science and technology to achieve better results [19]–[23]. Therefore, the present study aims to investigate in fractional order adaptive algorithms by exploiting the strong mathematical foundations of fractional calculus for Hammerstein nonlinear system identification and their application to practical parameter estimation problems of power signal modeling.

1.3 Philosophy of the Work

The exploitation of fractional calculus concepts provides better performance for solving different engineering problems in comparison with traditional integer order calculus. Thus, developing fractional gradient based adaptive algorithms for nonlinear system identification may give more accurate and robust performance.

1.4 Research Hypothesis

The research hypotheses formulated for the study are:

- The addition of fractional calculus concepts in standard adaptive strategies may results in faster convergence and better estimation accuracy.
- The fractional calculus based novel adaptive methods may provide an alternate, accurate, reliable and robust computing mechanism for parameter estimation of nonlinear systems.

1.5 Research Methodology

The standard adaptive methods for system identification such as, least mean squares algorithm is based on steepest descent approach and uses the first order gradient to estimate the unknown parameters. While the fractional adaptive algorithms use the concept of fractional order gradient in their optimization mechanism.

- The fractional least mean squares (FLMS) adaptive algorithm is proposed for parameter estimation of Hammerstein systems. FLMS algorithm exploits the strength of both first and fractional order gradients to optimize the system parameters.

- Modified FLMS-1 and 2 methods are proposed to reduce the computational cost of standard FLMS without compromising the accuracy.
- Normalized FLMS is proposed for automatic adjustment of the step size parameter.
- Sliding window based FLMS algorithm is developed by using finite length of recent data instead of current data to increase the rate of convergence of standard FLMS.
- Momentum FLMS is designed by incorporating the concept of momentum term to increase the convergence speed and avoid trapping in local minima.

1.6 Contribution of the Research

Our research contributions are in two directions.

1. Design of novel fractional adaptive algorithms based on strong mathematical foundations of fractional calculus for nonlinear system identification.
    - Fractional Least Mean Squares (FLMS)
    - Modified FLMS-1
    - Modified FLMS-2
    - Normalized FLMS
    - Sliding window based FLMS
    - Momentum FLMS
2. Applications of proposed fractional algorithms to parameter estimation of different nonlinear systems.

- The designed fractional adaptive techniques are applied on Hammerstein models for different noise and fractional order variations.
- The fractional adaptive algorithms are applied for identification of electrically stimulated muscle model required for rehabilitation of paralyzed muscles.
- The proposed fractional adaptive strategies are also employed for parameter estimation of power signals with unknown amplitude and phase.

1.7 Research Scope

The present study utilizes the strength of fractional calculus for developing adaptive algorithms to estimate the parameters of nonlinear systems based on block oriented Hammerstein structure. This research does not cover the identification of other block oriented structures such as Wiener and Hammerstein-Wiener models.

1.8 Thesis Organization

The organization of the thesis is as follows; the introduction, problem statement, scope of the research and contribution of the dissertation are given in Chapter 1. Chapter 2 provides the brief description of nonlinear system identification problem based on Hammerstein structure. The proposed fractional adaptive strategies for parameter estimation of Hammerstein nonlinear systems are introduced in Chapter 3. The results of the simulations for different case studies of Hammerstein systems are given in Chapter 4 along with necessary discussion. Application of the proposed methodology for parameter estimation of the power signals is presented in Chapter 5. We conclude our finding in the last chapter 6 along with few future research directions in this domain.

Chapter 2.

Critical Literature Review

2.1 Introduction

This chapter presents necessary details about nonlinear systems based on block oriented structures (BOS). The applications of BOS to model variety of nonlinear problems arising in engineering, science and technology are given in this chapter. Moreover, the existing methods for parameter estimation of BOS are presented here. At the end of this chapter, identification model for parameter estimation of BOS based on Hammerstein control autoregressive (HCAR) and HCAR moving average (HCARMA) systems are presented before going to introduce novel adaptive strategies in the next chapter.

2.2 Nonlinear System Identification

Nonlinear systems are more complex and hard to analyze because many basic questions are difficult to answer in nonlinear paradigm. For example, linear superposition theorem is no longer available, solution existence and uniqueness are not sure and numerical approximations are not always adequately accurate in nonlinear regime. Nonlinearity is ubiquitous in physical phenomena. Numerous physical processes like fluid mechanics, gas dynamics, ecology, plasma physics, relativity, combustion, chemical reactions, elasticity and biomechanics etc. are described by nonlinear equations [24]. In general, most real-life systems are nonlinear in nature and their parameter estimation/identification is more challenging due to inherent stiffness, complex system representation and applications to real time environment. The graphical representation of general nonlinear system identification problem is given in Fig. 2.1

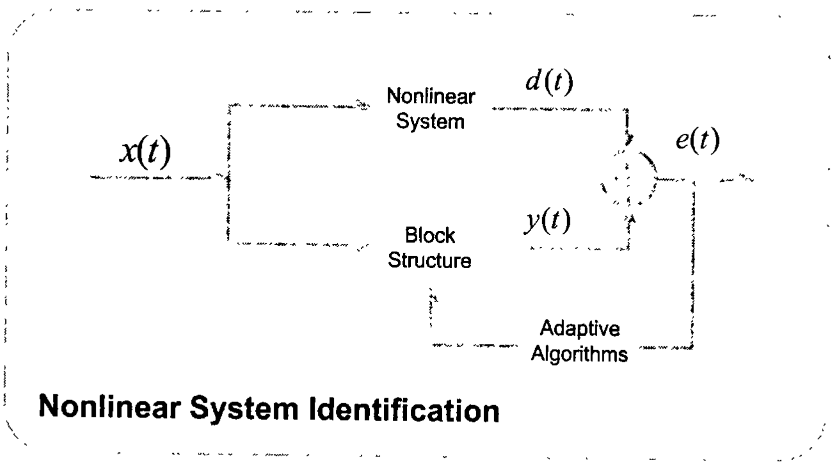

Fig. 2.1 Block diagram of nonlinear system identification

2.2.1 Block Oriented Models

Nonlinear processes can be effectively modelled through BOS that are composed of a concatenation of static nonlinear blocks and linear time invariant (LTI) dynamic subsystems. The linear subsystems are normally parametric (transfer functions, state space representations, input/output models), whereas the nonlinear blocks can be with or without memory [18].

The BOS are categorized into four major types; Hammerstein, Wiener, Hammerstein-Wiener and Weiner-Hammerstein. Hammerstein type, a class of input nonlinear systems consisting of a static nonlinear block followed by a linear dynamic subsystem. Wiener type, a class of output nonlinear systems consisting of linear block preceding some static nonlinear block. Hammerstein-Wiener model, a class of input-output nonlinear systems consisting of linear block sandwiched by two static nonlinear blocks and Wiener-Hammerstein model which consists of a static nonlinearity sandwiched between two dynamic linear elements. In this dissertation, we shall restrict our study to Hammerstein model. Block diagram of Hammerstein structure is given in Fig. 2.2

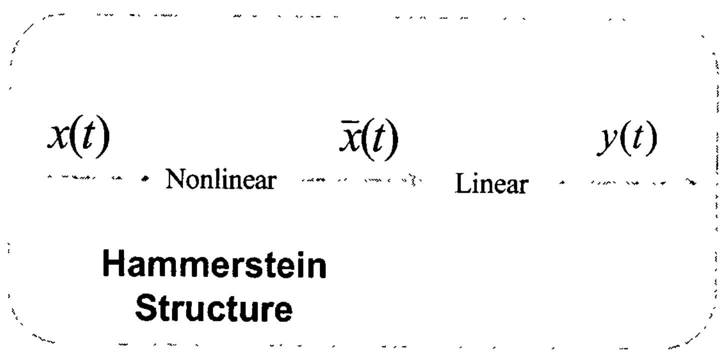

Fig. 2.2 Block diagram of Hammerstein structure

2.2.2 Applications of Hammerstein Model

The BOS based Hammerstein systems have been used effectively to model different nonlinear problems arising in a spectrum of fields. Few potential applications are biological processes [4], model predictive control [25], wind speed forecasting [10], peak load forecasting [11], gas turbines [8], chemical processes [26][27], turntable servo system [28], power electronic devices [9], mechanical systems [29], physiological processes [30], vibrating devices [7], software systems [31] and electrically stimulated muscle modeling [32]. These illustrative applications of Hammerstein model motivate to investigate and develop alternate, accurate, robust and reliable computing platforms for its identification.

2.3 Hammerstein Control Autoregressive Model

In this section, identification model for Hammerstein control autoregressive systems (HCAR) is presented. In HCAR structure, normally the nonlinear block is given through polynomial and linear dynamics are represented with exogenous noise autoregressive model. The block diagram of the HCAR model is given in Fig. 2.3

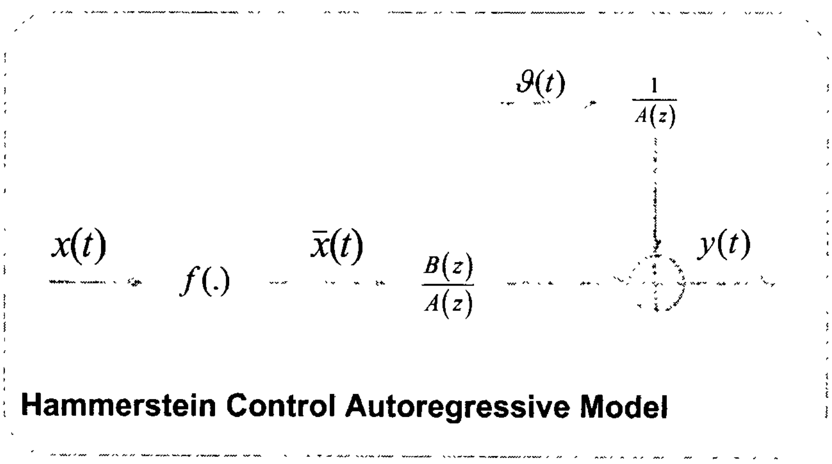

Fig. 2.3 Hammerstein Control Autoregressive Model

The governing mathematical relation for HCAR model is written as [33], [34]:

$$A(z)y(t) = B(z)\bar{x}(t) + \vartheta(t), \tag{2.1}$$

here $y(t)$ represents the output of system, $\vartheta(t)$ is the disturbance noise, $\bar{x}(t)$ is defined as a nonlinear function of m known basis ($f_1, f_2, \ , f_m$) of the system input $x(t)$:

$$\bar{x}(t) = f[x(t)] = c_1 f_1[x(t)] + c_2 f_2[x(t)] + \cdots + c_m f_m[x(t)]. \tag{2.2}$$

A(z) and B(z) are predefined polynomials and their expression in term of unit backward shift operator z^{-1} $[z^{-1}y(t) = y(t-1)]$, are given as:

$$A(z) = 1 + a_1 z^{-1} + a_2 z^{-2} + \cdots + a_{n_a} z^{-n_a}, \tag{2.3}$$

$$B(z) = b_1 z^{-1} + b_2 z^{-2} + \cdots + b_{n_b} z^{-n_b}, \tag{2.4}$$

where $\mathbf{a} = [a_1, a_2, \cdots, a_{n_a}]^T$ and $\mathbf{b} = [b_1, b_2, \cdots, b_{n_b}]^T \in R^n$ are the constant coefficient vectors. Rearranging equation (2.1) as:

$$y(t) = [1 - A(z)]y(t) + B(z)\bar{x}(t) + \vartheta(t). \tag{2.5}$$

Using (2.2) to (2.4) in (2.5) then

$$y(t) = -\sum_{i=1}^{n_a} a_i y(t-i) + \sum_{i=1}^{n_b}\sum_{j=1}^{m} b_i c_j f_j[x(t-i)] + \vartheta(t). \tag{2.6}$$

Expanding (2.6) one gets

$$\begin{aligned} y(t) = &-\sum_{i=1}^{n_a} a_i y(t-i) + b_1 c_1 f_1[x(t-1)] + b_1 c_2 f_2[x(t-1)] + \cdots + b_1 c_m f_m[x(t-1)] \\ &+ b_2 c_1 f_1[x(t-2)] + b_2 c_2 f_2[x(t-2)] + \cdots + b_2 c_m f_m[x(t-2)] + \cdots \\ &+ b_{n_b} c_1 f_1[x(t-n_b)] + b_{n_b} c_2 f_2[x(t-n_b)] + \cdots + b_{n_b} c_m f_m[x(t-n_b)] + \vartheta(t) \end{aligned} \tag{2.7}$$

Equation (2.7) in vector form is written as:

$$y(t) = \boldsymbol{\psi}^T(t)\boldsymbol{\theta} + \vartheta(t), \tag{2.8}$$

where the parameter vector $\boldsymbol{\theta}$ and information vector $\boldsymbol{\psi}(t)$ are defined as:

$$\boldsymbol{\theta} = [\mathbf{a}^T, b_1\mathbf{c}^T, b_2\mathbf{c}^T, \cdots, b_{n_b}\mathbf{c}^T]^T \in R^{n_a+n_b m}, \tag{2.9}$$

$$\boldsymbol{\psi}(t) = [\boldsymbol{\psi}_0^T(t), \boldsymbol{\psi}_1^T(t), \boldsymbol{\psi}_2^T(t), \cdots, \boldsymbol{\psi}_m^T(t)]^T \in R^{n_a+n_b m}, \tag{2.10}$$

$$\psi_0(t) = [-y(t-1), -y(t-2), \cdots, -y(t-n_a)]^T \in R^{n_a}, \tag{2.11}$$

$$\psi_j(t) = \{f_j[x(t-1)], f_j[x(t-2)], \cdots, f_j[x(t-n_b)]\}^T \in R^{n_b}, j = 1,2, \ldots, m. \tag{2.12}$$

Equation (2.8) represents the generic identification model for HCAR systems.

2.4 Hammerstein Control Autoregressive Moving Average Model

In this section, the identification model for Hammerstein control autoregressive moving average (HCARMA) model is presented. In HCARMA structure, normally the nonlinear block is given through polynomial and linear dynamics are represented with exogenous noise autoregressive moving average model. The block diagram of HCARMA structure is given in Fig. 2.4

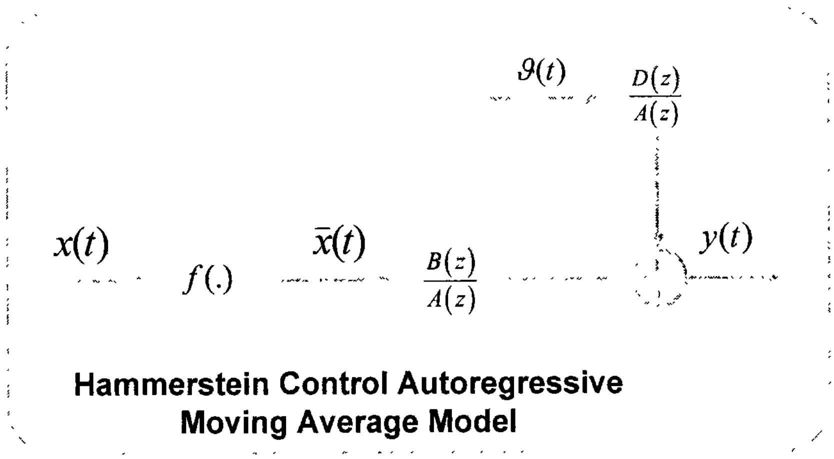

Fig. 2.4 Hammerstein Control Autoregressive Moving Average Model

The governing mathematical relation for HCARMA model is written as [35], [36]:

$$A(z)y(t) = B(z)\bar{x}(t) + D(z)\vartheta(t), \tag{2.13}$$

here $y(t)$ represents the output of system, $\vartheta(t)$ is the disturbance noise, $\bar{x}(t)$ is defined as a nonlinear function of m known basis ($f_1, f_2, \ldots, f_m$) of the system input $x(t)$ and given in Eq. (2.2). A(z) and B(z) are given in Eq. (2.3) and (2.4) respectively, while $D(z)$ is defined as:

$$D(z) = 1 + d_1 z^{-1} + d_2 z^{-2} + \cdots + d_{n_d} z^{-n_d}. \tag{2.14}$$

Rearranging equation (2.13) as:

$$y(t) = [1 - A(z)]y(t) + B(z)\bar{x}(t) + D(z)\vartheta(t). \tag{2.15}$$

Using (2.2) to (2.4) and (2.14) in (2.15), then

$$y(t) = -\sum_{i=1}^{n_a} a_i y(t-i) + \sum_{i=1}^{n_b}\sum_{j=1}^{m} b_i c_j f_j[x(t-i)] + \sum_{i=1}^{n_d} d_i \vartheta(t-i) + \vartheta(t). \tag{2.16}$$

The main equation for identification model of HCARMA system is same as HCAR model that is given in Eq. 2.8, except that parameter vector and information vector in case of HCARMA model are respectively defined as:

$$\boldsymbol{\theta} = [\mathbf{a}^T, b_1\mathbf{c}^T, b_2\mathbf{c}^T, \cdots, b_{n_b}\mathbf{c}^T, \mathbf{d}^T]^T \in R^{n_a+n_b m+n_d}, \tag{2.17}$$

$$\boldsymbol{\psi}(t) = [\boldsymbol{\psi}_0^T(t), \boldsymbol{\psi}_1^T(t), \boldsymbol{\psi}_2^T(t), \cdots, \boldsymbol{\psi}_m^T(t), \boldsymbol{\psi}_n^T(t)]^T \in R^{n_a+n_b m}, \tag{2.18}$$

$$\boldsymbol{\psi}_0(t) = [-y(t-1), -y(t-2), \cdots, -y(t-n_a)]^T \in R^{n_a}, \tag{2.19}$$

$$\boldsymbol{\psi}_j(t) = \{f_j[x(t-1)], f_j[x(t-2)], \cdots, f_j[x(t-n_b)]\}^T \in R^{n_b}, j = 1, 2, \ldots, m. \tag{2.20}$$

$$\psi_n(t) = [\vartheta(t-1), \vartheta(t-2), \cdots, \vartheta(t-n_d)]^T \in R^{n_d} \qquad (2.21)$$

2.5 Adaptive Strategies for Non-linear System Identification

Parameter estimation or identification of BOS has been a field of great interest for researchers all around the world. The Hammerstein system identification has been studied extensively since 1960's [37]–[44]. The global search methodologies based on nature and bio-inspired heuristics have been proposed for parameter identification of Hammerstein systems. For instance, genetic algorithms [45], particle swarm optimization [46]–[48], cuckoo search optimization [49], hybrid backtracking search [50] and gravitational search algorithm [51]. The commonly used Hammerstein identification algorithms are based on gradient descent and least squares methods [35], [36], [52]–[55]. The gradient methods have less computational cost but suffer from slow convergence speed as compared to least squares [56]. Multi innovation theory (MIT) [56] is proposed to improve the convergence speed. MIT uses not only the current data but also the past data at each iteration, thus provides better estimation accuracy and convergence speed [12], [13], [34], [57], [58]. The over parameterization methods also estimate redundant parameters in addition to useful parameters and are computationally heavy [59]. To avoid identifying redundant parameters, key term separation procedure is proposed but the parameterized system contains the unmeasurable internal variables [14], [15]. The auxiliary model (AM) idea [60] deals with identification problems having unknown internal variables in information vector. The basic idea in AM is to replace the unknown internal variables with the output of auxiliary model [33], [60]–[62]. The hierarchical identification algorithm requires reduced computational burden by decomposing a nonlinear system into several subsystems with smaller dimension [16], [17], [63], [64].

In this thesis, we apply fractional calculus concepts to develop alternate and accurate adaptive algorithms for nonlinear system identification based on Hammerstein structure. We apply the proposed fractional adaptive algorithms for parameter estimation of HCAR and HCARMA systems to demonstrate their worth and effectiveness.

2.6 Summary

This chapter presented the detailed overview of nonlinear system identification problem based on block-oriented Hammerstein structure. The comprehensive review of modeling nonlinear identification problems using HCAR and HCARMA structures was given along with the standard identification procedures to identify parameters of these Hammerstein structures. Finally, the need for developing alternate identification algorithms based on fractional calculus concepts was discussed.

Chapter 3.

Adaptive Strategies for Hammerstein Systems

In this chapter, design of novel adaptive strategies based on fractional calculus is presented for parameter estimation of Hammerstein systems.

3.1 Introduction

Fractional calculus is a branch of mathematics that deals with non-integer order derivatives and integrals [65] [66]. It has equally evolved in parallel with integer order calculus in the field of mathematics [67]. Chen explored its applications in the field of control engineering [21], [23], [68], [69], while Machado and Ortigueira presented the idea of fractional signal processing [20], [70]–[73]. Raja gave the new concept of fractional adaptive algorithms in the domain of fractional order control and signal processing by using the fractional gradient in standard adaptive methods [74].

3.2 Fractional adaptive algorithms

The newly evolved fractional adaptive algorithms borrow their ideas from LMS algorithm and its variants by introducing different ways for step size calculation and weights updating mechanisms. For example, fractional least mean square (FLMS) identification algorithm was developed by exploiting the theories of fractional calculus for weights update in standard LMS [75]. The standard FLMS update equation includes integer order gradient as well as the fractional order gradient. The trade-off between these two gradients is suggested in [76] that adds a proportion of each gradient according to the value of adjustable gain parameter. This results in better convergence as compared to the original FLMS in [75]. A variable power FLMS (VP-FLMS), and further a robust VP-FLMS methods are given in [77], [78] that dynamically adapt the fractional power of the FLMS to obtain high rate of convergence with low steady state error. A complex variant of FLMS is developed in [79] to deal with the problem of complex system identification. A fractional variant of Volterra LMS is also proposed for system identification [80], [81].

The fractional order used in the algorithms so far lies in the range $\in (0,1)$. An innovative fractional order LMS (IFLMS) based on variable initial value and gradient order is proposed in [82] for fractional order $\in (0,1.5)$. A variable initial value is suggested to guarantee the convergence of IFLMS by attenuating the non–local property of fractional calculus. A larger value of the gradient order provides faster convergence rate but at the cost of more steady state error. A variable gradient order concept is incorporated in IFLMS to remove this contradiction between rapidity and accuracy. This behavior of rapidity and accuracy was further studied in [83], [84] for fractional order $\in (0,2)$. A novel variable order FLMS algorithm is developed for spline adaptive filter in [85]. Modified LMS [86] is extended to fractional version in [87]. A fractional steepest descent method is proposed and fractional quadratic energy norm is studied in [88]. A comprehensive study on convergence behavior of different fractional methods including standard FLMS [75] is presented in [89].

These fractional adaptive strategies have been exploited to solve different signal processing, communication and control problems including parameter estimation [90], [91], channel equalization [92]–[94], echo cancellation [95], speech enhancement [96]–[98], chaotic time series prediction [76], [99], neural network optimization [100] and active noise control [101]–[103]. The fractional adaptive methods outperform standard adaptive approaches in these illustrative applications.

In this dissertation, first, standard FLMS [75] is applied to Hammerstein system identification, then different variants of standard FLMS are developed to increase the convergence rate and estimation accuracy. All the algorithms presented in this chapter are based on our published research articles.

The algorithms exploited for parameter estimation of Hammerstein systems are:

1. Fractional Least Mean Squares (FLMS)
2. Modified FLMS-1
3. Modified FLMS-2
4. Normalized FLMS
5. Sliding window based FLMS
6. Momentum FLMS

3.3 Fractional LMS

In this section, the detail of fractional LMS is given for Hammerstein system identification. The FLMS algorithm is developed by using the concept of fractional derivative in standard LMS method. The recursive parameter update expression of standard FLMS incorporates the strength of both integer order and fractional order gradients to minimize the cost function.

3.3.1 Mathematical Formulation

The objective function for the system is given below:

$$J(t) = \mathrm{E}[e^2(t)], \tag{3.1}$$

where $\mathrm{E}(\cdot)$ is an expectation operator, $e(t)$ is the error term, *i.e.*, difference between the desired and estimated response, and is given by:

$$e(t)=d(t)-y(t), \tag{3.2}$$

where $d(t)$ is the desired response of the system and the estimated output $y(t)$ is written as:

$$y(t)=\boldsymbol{\psi}^T(t)\hat{\boldsymbol{\theta}}, \tag{3.3}$$

where $\boldsymbol{\psi}$ is the information vector and $\hat{\boldsymbol{\theta}}$ is the estimated parameter vector. The iterative update rule of FLMS uses both integer and fractional order derivatives and is given as:

$$\hat{\boldsymbol{\theta}}(t+1)=\hat{\boldsymbol{\theta}}(t)-\frac{1}{2}\left[\mu_1\frac{\partial J(t)}{\partial\hat{\boldsymbol{\theta}}}+\mu_f\frac{\partial^{fr}J(t)}{\partial\hat{\boldsymbol{\theta}}^{fr}}\right], \tag{3.4}$$

where, μ_1 and μ_f are the leaning rates corresponding to the first order and fractional order gradients, respectively while *fr* is the order of fractional derivative. Taking the first order derivative of cost function (3.1) with respect to $\hat{\boldsymbol{\theta}}$ gives

$$\frac{\partial}{\partial\hat{\boldsymbol{\theta}}}[J(t)]=2e(t)\frac{\partial}{\partial\hat{\boldsymbol{\theta}}}\left[d(t)-\boldsymbol{\psi}^T(t)\hat{\boldsymbol{\theta}}(t)\right]. \tag{3.5}$$

Simplifying (3.5) as in [104], then obtains

$$\frac{\partial}{\partial\hat{\boldsymbol{\theta}}}(J(t))=-2e(t)\boldsymbol{\psi}(t). \tag{3.6}$$

The iterative parameter update relation for parameter estimation of Hammerstein systems using LMS is written as:

$$\hat{\theta}(t+1)=\hat{\theta}(t)+\mu e(t)\psi(t). \tag{3.7}$$

A variety of fractional order derivative definitions are available in the fractional calculus literature including Caputo, Riesz, Riemann-Liouville, Hadamard and Grünwald-Letnikov [19], [66], [105], [106] and accordingly, the fractional derivative of a function $g(t)=t^p$ is generally defined as

$$D^{fr}g(t)=\frac{\Gamma(p+1)}{\Gamma(p-fr+1)}t^{p-fr}, fr>0, p>-1, \tag{3.8}$$

where, D^{fr} is the fractional derivative operator of order fr and Γ is the gamma function, defined as:

$$\Gamma(t)=(t-1)!. \tag{3.9}$$

Now, computing the fractional order derivative of a cost function, with the assumption that the fractional derivative of a constant is zero, then fractional derivative in (3.5) is calculated as:

$$\frac{\partial^{fr}J(t)}{\partial\hat{\theta}^{fr}}=-2(e(t)\psi(t))\frac{\partial^{fr}}{\partial\hat{\theta}^{fr}}\hat{\theta}(t). \tag{3.10}$$

Using (3.8) and (3.9) in (3.10), the fractional derivative of the cost function is written as

$$\frac{\partial^{fr}J(t)}{\partial\hat{\theta}^{fr}}\cong-2(e(t)\psi(t))\frac{1}{\Gamma(2-fr)}\hat{\theta}(t)^{1-fr}. \tag{3.11}$$

Substituting the values of the integer order derivative (3.6) and fractional order derivative (3.11) in (3.4), the weight update relation of FLMS is written as

$$\hat{\theta}(t+1)=\hat{\theta}(t)+\mu_1 e(t)\psi(t)+\frac{\mu_f}{\Gamma(2-fr)}e(t)\psi(t)\circ\left|\hat{\theta}(t)\right|^{1-fr}, \tag{3.12}$$

where the symbol $\circ$ denotes an element-by-element multiplication of vectors and the absolute value of the vector $\hat{\boldsymbol{\theta}}$ is used to avoid complex values.

3.3.2 Convergence Analysis

Define the parameter error vector for performing convergence analysis of the FLMS algorithm as:

$$\Delta\boldsymbol{\theta}(t) = \hat{\boldsymbol{\theta}}(t) - \boldsymbol{\theta}_{\text{opt}}, \tag{3.13}$$

where $\boldsymbol{\theta}_{\text{opt}}$ represents the optimum value of the parameter vector. For simplicity, suppose $\mu_f / \Gamma(2-fr) = \mu_1 = \mu$ in (3.12), and rearranging as

$$\hat{\boldsymbol{\theta}}(t+1) = \hat{\boldsymbol{\theta}}(t) + \mu e(t)\boldsymbol{\psi}(t)\left[1 + \left|\hat{\boldsymbol{\theta}}(t)\right|^{1-fr}\right]. \tag{3.14}$$

The parameter update relation in terms of the parameter error vector is then given by

$$\Delta\boldsymbol{\theta}(t+1) = \Delta\boldsymbol{\theta}(t) + \mu\boldsymbol{\psi}(t)\{d(t) - \boldsymbol{\psi}(t)^T[\boldsymbol{\theta}_{\text{opt}} + \Delta\boldsymbol{\theta}(t)]\}\{1 + [\boldsymbol{\theta}_{\text{opt}} + \Delta\boldsymbol{\theta}(t)]^{1-fr}\}. \tag{3.15}$$

Expanding (3.15) obtains

$$\begin{aligned}\Delta\boldsymbol{\theta}(t+1) &= \Delta\boldsymbol{\theta}(t) + \mu\boldsymbol{\psi}(t)d(t) + \mu\boldsymbol{\psi}(t)y(t)[\boldsymbol{\theta}_{\text{opt}} + \Delta\boldsymbol{\theta}(t)]^{1-fr} \\ &- \mu\boldsymbol{\psi}(t)\boldsymbol{\psi}(t)^T\boldsymbol{\theta}_{\text{opt}} - \mu\boldsymbol{\psi}(t)\boldsymbol{\psi}(t)^T\Delta\boldsymbol{\theta}(t) - \mu\boldsymbol{\psi}(t)\boldsymbol{\psi}(t)^T[\boldsymbol{\theta}_{\text{opt}} + \Delta\boldsymbol{\theta}(t)]^{2-fr}.\end{aligned} \tag{3.16}$$

Using the binomial expansion

$$\{\boldsymbol{\theta}_{\text{opt}} + \Delta\boldsymbol{\theta}(t)\}^j = \sum_{k=0}^{\infty}\binom{j}{k}(\boldsymbol{\theta}_{\text{opt}}^k)^T\Delta\boldsymbol{\theta}(t)^{j-k}. \tag{3.17}$$

and

$$\binom{j}{k} = \frac{j(j-1)\ldots(j-k+1)}{k!}. \tag{3.18}$$

Using (3.17) in (3.16),

$$\begin{aligned}\Delta\boldsymbol{\theta}(t+1) &= \Delta\boldsymbol{\theta}(t) + \mu\boldsymbol{\psi}(t)d(t) - \mu\boldsymbol{\psi}(t)\boldsymbol{\psi}(t)^T\boldsymbol{\theta}_{\text{opt}} - \mu\boldsymbol{\psi}(t)\boldsymbol{\psi}(t)^T\Delta\boldsymbol{\theta}(t) \\ &+ \mu\boldsymbol{\psi}(t)d(t)\Delta\boldsymbol{\theta}(t)^{1-fr} + \mu\boldsymbol{\psi}(t)d(t)\sum_{k=1}^{\infty}\binom{1-fr}{k}(\boldsymbol{\theta}_{\text{opt}}^{k})^T\Delta\boldsymbol{\theta}(t)^{1-fr-k} \\ &- \mu\boldsymbol{\psi}(t)\boldsymbol{\psi}(t)^T\Delta\boldsymbol{\theta}(t)^{2-fr} - \mu\boldsymbol{\psi}(t)\boldsymbol{\psi}(t)^T\binom{2-fr}{1}(\boldsymbol{\theta}_{opt}^{1})^T\Delta\boldsymbol{\theta}(t)^{1-fr} \\ &- \mu\boldsymbol{\psi}(t)\boldsymbol{\psi}(t)^T\sum_{k=1}^{\infty}\binom{1-fr}{k}(\boldsymbol{\theta}_{\mathbf{opt}}^{k+1})^T\Delta\boldsymbol{\theta}(t)^{1-fr-k}\end{aligned} \qquad (3.19)$$

If the parameters are statistically independent of output and input, and the output and input are uncorrelated, then applying expectation on both sides of (3.19) and equating $E[\Delta\boldsymbol{\theta}(\cdot)] = \mathbf{w}(\cdot)$,

$$\begin{aligned}\mathbf{w}(t+1) &= \mathbf{w}(t) + \mu\mathbf{p} - \mu\mathbf{R}\boldsymbol{\theta}_{\text{opt}} - \mu\mathbf{R}\mathbf{w}(t) \\ &+ \mu\mathbf{p}E\left[\Delta\boldsymbol{\theta}(t)^{1-fr}\right] + \mu\mathbf{p}\sum_{k=1}^{\infty}\binom{1-fr}{k}\boldsymbol{\theta}_{\text{opt}}^{k}E\left[\Delta\boldsymbol{\theta}(t)^{1-fr-k}\right] - \mu\mathbf{R}E\left[\Delta\boldsymbol{\theta}(t)^{2-fr}\right], \\ &- \mu\mathbf{R}\binom{2-fr}{1}\boldsymbol{\theta}_{\text{opt}}^{1}E\left[\Delta\boldsymbol{\theta}(t)^{1-fr}\right] - \mu\mathbf{R}\sum_{k=1}^{\infty}\binom{1-fr}{k}\boldsymbol{\theta}_{\text{opt}}^{k+1}E\left[\Delta\boldsymbol{\theta}(t)^{1-fr-k}\right]\end{aligned} \qquad (3.20)$$

where $\mathbf{R}$ is the auto-correlation matrix, and $\mathbf{p}$ is the cross-correlation vector between the input and desired parameters. For optimal values of the parameters, $\mathbf{p} - \mathbf{R}\boldsymbol{\theta}_{\text{opt}} = 0$, and (3.20) becomes:

$$\begin{aligned}\mathbf{w}(t+1) &= \mathbf{w}(t) - \mu\mathbf{R}\mathbf{w}(t) + \mu\mathbf{p}E\left[\Delta\boldsymbol{\theta}(t)^{1-fr}\right] \\ &- \mu\mathbf{R}E\left[\Delta\boldsymbol{\theta}(t)^{2-fr}\right] - \mu\mathbf{R}\binom{2-fr}{1}\boldsymbol{\theta}_{\text{opt}}^{1}E\left[\Delta\boldsymbol{\theta}(t)^{1-fr}\right].\end{aligned} \qquad (3.21)$$

Let

$$\begin{aligned}&\mu\mathbf{p}E\left[\Delta\boldsymbol{\theta}(t)^{1-fr}\right] - \mu\mathbf{R}E\left[\Delta\boldsymbol{\theta}(t)^{2-fr}\right] - \mu\mathbf{R}\binom{2-fr}{1}\boldsymbol{\theta}_{\text{opt}}^{1}E\left[\Delta\boldsymbol{\theta}(t)^{1-fr}\right] \\ &= \mu E[\Delta\boldsymbol{\theta}(t)]\mathbf{F}[\Delta\boldsymbol{\theta}(t), fr]\end{aligned}, \qquad (3.22)$$

so that using (3.22) in (3.21) gives

$$\mathbf{w}(t+1)=\mathbf{w}(t)-\mu\mathbf{R}\mathbf{w}(t)+\mu E[\Delta\boldsymbol{\theta}(t)]\mathbf{F}[\Delta\boldsymbol{\theta}(t),fr]$$
$$\mathbf{w}(t+1)=\mathbf{w}(t)-\mu\mathbf{R}\mathbf{w}(t)+\mu\mathbf{w}(t)\mathbf{F}[\Delta\boldsymbol{\theta}(t),fr] \quad (3.23)$$

Simplifying (3.23),

$$\mathbf{w}(t+1)=\mathbf{w}(t)\{1-\mu[\mathbf{R}-\mathbf{F}(\Delta\boldsymbol{\theta}(t),fr)]\}. \quad (3.24)$$

The condition for stability or convergence of the algorithm is

$$-1<1-\mu[\mathbf{R}-\mathbf{F}(\Delta\boldsymbol{\theta}(t),fr)]<1, \quad (3.25)$$

which results in

$$0<\mu<\frac{2}{\mathbf{R}-\mathbf{F}[\Delta\boldsymbol{\theta}(t),fr]}, \quad (3.26)$$

or

$$0<\mu<\frac{2}{\lambda_{\max}-\mathbf{F}[\Delta\boldsymbol{\theta}(t),fr]_{\min}}, \quad (3.27)$$

where $\lambda_{\max}$ is the maximum eigenvalue of the covariance matrix and $\mathbf{F}[\Delta\boldsymbol{\theta}(t),fr]$ is the factor affecting the learning rate of the fractional LMS and it is a function of instantaneous error.

3.4 Modified Fractional LMS-1

The standard FLMS algorithm provides better convergence performance than LMS [96], [98], but suffers from computational burden because of evaluating the complex gamma function in its weight update mechanism. Therefore, to avoid the gamma function evaluation at each iteration, a modified form of standard FLMS is proposed. In modified fractional LMS-1 (MFLMS-1) adaptive algorithm, two changes are introduced in the standard FLMS method

1. A new parameter *i.e.*, adjustable gain parameter β is introduced in the weight update relation of the standard FLMS method.

2. The Gamma function of the standard FLMS approach is absorbed in the fractional step size parameter due to which the MFLMS-1 method requires less computational cost while not compromising the performance.

3.4.1 Mathematical Formulation

The weight update expression of MFLMS-1 is given as:

$$\hat{\boldsymbol{\theta}}(t+1)=\hat{\boldsymbol{\theta}}(t)+\beta\mu_1 e(t)\boldsymbol{\psi}(t)+(1-\beta)\mu_{fr}e(t)\boldsymbol{\psi}(t)\circ\left|\hat{\boldsymbol{\theta}}(t)\right|^{1-fr}, \quad (3.28)$$

where

$$\mu_{fr}=\frac{\mu_f}{\Gamma(2-fr)}, \quad (3.29)$$

and β is an adjustable parameter between 0 and 1. If $\beta < 0.5$, fractional part of the equation (3.28) is dominant while, if $\beta > 0.5$, integer order derivative prevails.

Now, if $\beta = 1$ in (3.28), the MFLMS-1 algorithm reduces to the standard LMS algorithm (3.7). The weight adaptation procedure of MFLMS-1 requires less computational budget that makes it an efficient alternative fractional adaptive method.

3.5 Modified Fractional LMS-2

The standard FLMS algorithm is better than LMS in accuracy but requires more computational burden [96], [98]. To address this limitation of the FLMS algorithm, another modification in the standard FLMS is proposed. In this modified FLMS-2 (MFLMS-2) algorithm, instead of taking both first and fractional order derivatives of cost function, only fractional order derivative is used. This reduces the computational cost of the FLMS while not compromising the accuracy.

3.5.1 Mathematical Formulation

The weight update expression in case of the MFLMS-2 algorithm is given by:

$$\hat{\boldsymbol{\theta}}(t+1)=\hat{\boldsymbol{\theta}}(t)-\frac{1}{2}\left[\mu_f\frac{\partial^{fr}J(t)}{\partial\hat{\boldsymbol{\theta}}^{fr}}\right]. \tag{3.30}$$

Putting equation (3.11) in (3.30), the recursive weight update relation in case of the MFLMS-2 is written as:

$$\hat{\boldsymbol{\theta}}(t+1)=\hat{\boldsymbol{\theta}}(t)+\frac{\mu_f}{\Gamma(2-fr)}e(t)\boldsymbol{\psi}(t)\circ\left|\hat{\boldsymbol{\theta}}(t)\right|^{1-fr}. \tag{3.31}$$

If we put fr = 1 in equation (3.31), the recursive expression of the MFLMS-2 algorithm reduces to the standard LMS method (3.7).

3.6 Normalized FLMS

The implementation of standard FLMS adaptive scheme and its modified versions require an appropriate value of the step size parameter that affects the stability, convergence speed and steady state performance of the method. It is difficult to select a step size that is guaranteed to lie within the stability region. We design normalized versions of FLMS, MFLMS-1 and MFLMS-2 algorithms *i.e.*, NFLMS, NMFLMS-1 and NMFLMS-2 methods to address the problem of step size selection by choosing a time varying learning rate as NLMS is developed from standard LMS algorithm [107]–[110].

3.6.1 Mathematical Formulation

The parameter update rule of NFLMS for Hammerstein system identification is given as:

$$\hat{\boldsymbol{\theta}}(t+1)=\hat{\boldsymbol{\theta}}(t)+\mu_1 e(t)\frac{\boldsymbol{\psi}(t)}{\|\boldsymbol{\psi}(t)\|}+\frac{\mu_f}{\Gamma(2-fr)}e(t)\frac{\boldsymbol{\psi}(t)}{\|\boldsymbol{\psi}(t)\|}\circ\left|\hat{\boldsymbol{\theta}}(t)\right|^{1-fr}. \quad (3.32)$$

The update rules of NMFLMS-1 and NMFLMS-2 algorithms for Hammerstein system identification are respectively given as:

$$\hat{\boldsymbol{\theta}}(t+1)=\hat{\boldsymbol{\theta}}(t)+\beta\mu_1 e(t)\frac{\boldsymbol{\psi}(t)}{\|\boldsymbol{\psi}(t)\|}+(1-\beta)\mu_{fr}e(t)\frac{\boldsymbol{\psi}(t)}{\|\boldsymbol{\psi}(t)\|}\circ\left|\hat{\boldsymbol{\theta}}(t)\right|^{1-fr}, \quad (3.33)$$

$$\hat{\boldsymbol{\theta}}(t+1)=\hat{\boldsymbol{\theta}}(t)+\frac{\mu_f}{\Gamma(2-fr)}e(t)\frac{\boldsymbol{\psi}(t)}{\|\boldsymbol{\psi}(t)\|}\circ\left|\hat{\boldsymbol{\theta}}(t)\right|^{1-fr}. \quad (3.34)$$

3.7 Sliding window based FLMS

The standard FLMS algorithm (3.12) is a memory-less algorithm, as it uses the data available at the current iteration only. This results in poor convergence rate of the algorithm. We propose a sliding window approximation based FLMS (SW-FLMS) algorithm to increase the convergence rate of the standard FLMS. The SW-FLMS method uses not only the current data points but also the past data at each iteration. The SW-FLMS uses sliding-window approximation of the expectation where the length of data used by SW-FLMS algorithm determines the size of sliding window.

3.7.1 Mathematical Formulation

For FLMS algorithm, the criterion function is to reduce the error in mean square sense as:

$$J(t)=\mathrm{E}\left[e^2(t)\right]=\mathrm{E}\left[d(t)-\boldsymbol{\psi}^T(t)\hat{\boldsymbol{\theta}}\right]^2 \quad (3.35)$$

In the early 1960s, Windrow-Hoff introduced an approximation of averaging operator. This popular approximation is a memory-less estimation based only on the current data points [104], [111]:

$$J(t) = e^2(t) = \left[d(t) - \psi^T(t)\hat{\theta}\right]^2. \quad (3.36)$$

An alternative to time-averaging operator is the incorporation of sliding-window approximation [112]–[114]. In sliding-window approximation, we use the recent L data points $\{d(i),\, \psi\,(i) : t - L + 1 \le i \le t\}$:

$$J(t) = \frac{1}{L}\sum_{i=t-L+1}^{t} e^2(i) = \frac{1}{L}\sum_{i=t-L+1}^{t}\left[d(i) - \psi^T(i)\hat{\theta}\right]^2, \quad (3.37)$$

where L represents the memory of the approximation or the size of the window. Taking the gradient of cost function (3.37) with respect to $\hat{\theta}$, given as:

$$\frac{\partial}{\partial\hat{\theta}}[J(t)] = -\frac{2}{L}\sum_{i=t-L+1}^{t}\psi(i)\left[d(i) - \psi^T(i)\hat{\theta}(t)\right]. \quad (3.38)$$

Taking the fractional derivative of the cost function (3.38) using (3.11):

$$\frac{\partial^{fr}}{\partial\hat{\theta}^{fr}}[J(t)] = -\frac{2}{L}\sum_{i=t-L+1}^{t}\psi(i)\left[d(i) - \psi^T(i)\hat{\theta}(t)\right]\frac{1}{\Gamma(2-fr)}\hat{\theta}(t)^{1-fr}. \quad (3.39)$$

Since FLMS uses both first and fractional order derivatives for parameter update, substituting (3.38) and (3.39) in equation (3.4) results in:

$$\hat{\theta}(t+1) = \hat{\theta}(t) + \frac{\mu}{L}\sum_{i=t-L+1}^{t}\psi(i)\left[d(i) - \psi^T(i)\hat{\theta}(t)\right]\left[1 + \frac{\hat{\theta}(t)^{1-fr}}{\Gamma(2-fr)}\right], \quad (3.40)$$

where it is assumed that $\mu_1 = \mu_f = \mu$. Equation (3.40) can be written as:

$$\hat{\theta}(t+1) = \hat{\theta}(t) + \frac{\mu}{L}\sum_{i=t-L+1}^{t}\psi(i)e(i)\left[1 + \frac{\hat{\theta}(t)^{1-fr}}{\Gamma(2-fr)}\right]. \quad (3.41)$$

Equation (3.41) is the parameter update rule of SW-FLMS algorithm.

3.8 Momentum Fractional LMS

An alternative way to increase the convergence speed of the standard FLMS is to use the concepts of momentum term for gradient calculation, as has been used for standard LMS [115], [116]. The momentum term takes care of the proportion of previous updates and adds it to the current weights. This helps in speeding up the optimum search and avoids trapping in local minima. The momentum FLMS updates the weights by incorporating the proportion of the previously calculated gradients in the current update step. Thus, increasing the rate of convergence of standard FLMS.

3.8.1 Mathematical Formulation

The parameter update expression of the momentum FLMS (mFLMS) method is written as:

$$\hat{\boldsymbol{\theta}}(t+1)=\hat{\boldsymbol{\theta}}(t)+\mathbf{v}(t+1), \tag{3.42}$$

where $\mathbf{v}(t+1)$ is the velocity term which contains previously calculated gradients

$$\mathbf{v}(t+1)=\alpha\,\mathbf{v}(t)+\mathbf{g}(t), \tag{3.43}$$

while, $\mathbf{g}(t)$ is the gradient part of the FLMS equation given by:

$$\mathbf{g}(t)=\mu_1 e(t)\boldsymbol{\psi}(t)+\frac{\mu_f}{\Gamma(2-fr)}e(t)\boldsymbol{\psi}(t)\circ\left|\hat{\boldsymbol{\theta}}(t)\right|^{1-fr}. \tag{3.44}$$

Here α is between 0 and 1. It controls the proportion of previous gradients that is added in the current update. In case of standard momentum LMS, (3.42) and (3.43) remain same but the gradient term $\mathbf{g}(t)$ is computed as:

$$\mathbf{g}(t)=\mu_1 e(t)\boldsymbol{\psi}(t). \tag{3.45}$$

3.8.2 Convergence analysis

For simplicity, suppose $\mu_f / \Gamma(2-fr) = \mu_1 = \mu$ in (3.12), and rearranging as

$$\hat{\boldsymbol{\theta}}(t+1) = \hat{\boldsymbol{\theta}}(t) + \alpha\left[\hat{\boldsymbol{\theta}}(t) - \hat{\boldsymbol{\theta}}(t-1)\right] + \mu e(t)\boldsymbol{\psi}(t)\left[1 + \left|\hat{\boldsymbol{\theta}}(t)\right|^{1-fr}\right]. \tag{3.46}$$

Now, defining the parameter error vector, as defined for standard FLMS in (3.13), then the parameter update relation of mFLMS in terms of the parameter error vector is given by

$$\begin{aligned}\Delta\boldsymbol{\theta}(t+1) &= \Delta\boldsymbol{\theta}(t) + \alpha[\Delta\boldsymbol{\theta}(t) - \Delta\boldsymbol{\theta}(t-1)] \\ &+ \mu\boldsymbol{\psi}(t)\left\{d(t) - \boldsymbol{\psi}(t)^T\left[\boldsymbol{\theta}_{\text{opt}} + \Delta\boldsymbol{\theta}(t)\right]\right\}\left\{1 + \left[\boldsymbol{\theta}_{\text{opt}} + \Delta\boldsymbol{\theta}(t)\right]^{1-fr}\right\}.\end{aligned} \tag{3.47}$$

Expanding (3.47) obtains:

$$\begin{aligned}\Delta\boldsymbol{\theta}(t+1) &= \Delta\boldsymbol{\theta}(t) + \alpha[\Delta\boldsymbol{\theta}(t) - \Delta\boldsymbol{\theta}(t-1)] + \mu\boldsymbol{\psi}(t)d(t) \\ &+ \mu\boldsymbol{\psi}(t)^T d(t)\left\{\boldsymbol{\theta}_{\text{opt}} + \Delta\boldsymbol{\theta}(t)\right\}^{1-fr} - \mu\boldsymbol{\psi}(t)\boldsymbol{\psi}(t)^T\boldsymbol{\theta}_{\text{opt}} \\ &- \mu\boldsymbol{\psi}(t)\boldsymbol{\psi}(t)^T\Delta\boldsymbol{\theta}(t) - \mu\boldsymbol{\psi}(t)\boldsymbol{\psi}(t)^T\left[\boldsymbol{\theta}_{\text{opt}} + \Delta\boldsymbol{\theta}(t)\right]^{2-fr}.\end{aligned} \tag{3.48}$$

Using the binomial expansion (3.17), the equation (3.48) updates as:

$$\begin{aligned}\Delta\boldsymbol{\theta}(t+1) &= \Delta\boldsymbol{\theta}(t) + +\alpha[\Delta\boldsymbol{\theta}(t) - \Delta\boldsymbol{\theta}(t-1)] + \mu\boldsymbol{\psi}(t)d(t) \\ &- \mu\boldsymbol{\psi}(t)\boldsymbol{\psi}(t)^T\boldsymbol{\theta}_{\text{opt}} - \mu\boldsymbol{\psi}(t)\boldsymbol{\psi}(t)^T\Delta\boldsymbol{\theta}(t) + \mu\boldsymbol{\psi}(t)^T d(t)\Delta\boldsymbol{\theta}(t)^{1-fr} \\ &+ \mu\boldsymbol{\psi}(t)d(t)\sum_{k=1}^{\infty}\binom{1-fr}{k}\left(\boldsymbol{\theta}_{\text{opt}}^{k}\right)^T\Delta\boldsymbol{\theta}(t)^{1-fr-k} - \mu\boldsymbol{\psi}(t)\boldsymbol{\psi}(t)^T\Delta\boldsymbol{\theta}(t)^{2-fr} \\ &- \mu\boldsymbol{\psi}(t)\boldsymbol{\psi}(t)^T\binom{2-fr}{1}(\boldsymbol{\theta}_{\text{opt}}^{1})^T\Delta\boldsymbol{\theta}(t)^{1-fr} \\ &- \mu\boldsymbol{\psi}(t)\boldsymbol{\psi}(t)^T\sum_{k=1}^{\infty}\binom{1-fr}{k}(\boldsymbol{\theta}_{\text{opt}}^{k+1})^T\Delta\boldsymbol{\theta}(t)^{1-fr-k}\end{aligned}. \tag{3.49}$$

If the parameters are statistically independent of output and input, and the output and input are uncorrelated, then applying expectation on both sides of (3.49) and equating $E[\Delta\boldsymbol{\theta}(\cdot)] = \mathbf{w}(\cdot)$,

$$\begin{aligned}\mathbf{w}(t+1) &= \mathbf{w}(t)+\alpha[\mathbf{w}(t)-\mathbf{w}(t-1)]+\mu\mathbf{p}-\mu\mathbf{R}\boldsymbol{\theta}_{\text{opt}}-\mu\mathbf{R}\mathbf{w}(t)\\ &+\mu\mathbf{p}E\{\Delta\boldsymbol{\theta}(t)^{1-fr}\}+\mu\mathbf{p}\sum_{k=1}^{\infty}\binom{1-fr}{k}\boldsymbol{\theta}_{\text{opt}}^{k}E\left[\Delta\boldsymbol{\theta}(t)^{1-fr-k}\right]-\mu\mathbf{R}E\left[\Delta\boldsymbol{\theta}(t)^{2-fr}\right],\\ &-\mu\mathbf{R}\binom{2-fr}{1}\boldsymbol{\theta}_{\text{opt}}^{1}E\left[\Delta\boldsymbol{\theta}(t)^{1-fr}\right]-\mu\mathbf{R}\sum_{k=1}^{\infty}\binom{1-fr}{k}\boldsymbol{\theta}_{\text{opt}}^{k+1}E\left[\Delta\boldsymbol{\theta}(t)^{1-fr-k}\right]\end{aligned} \tag{3.50}$$

where **R** shows the auto correlation matrix, **p** is cross correlation vector between input and desired parameters. For optimal values of parameters; $\mathbf{p}-\mathbf{R}\boldsymbol{\theta}_{\text{opt}}=0$, (3.50) becomes:

$$\begin{aligned}\mathbf{w}(t+1) &= \mathbf{w}(t)+\alpha[\mathbf{w}(t)-\mathbf{w}(t-1)]-\mu\mathbf{R}\mathbf{V}(t)\\ &+\mu\mathbf{p}E\left[\Delta\boldsymbol{\theta}(t)^{1-fr}\right]-\mu\mathbf{R}E\left[\Delta\boldsymbol{\theta}(t)^{2-fr}\right]-\mu\mathbf{R}\binom{2-fr}{1}\boldsymbol{\theta}_{\text{op}t}^{1}E\left[\Delta\boldsymbol{\theta}(t)^{1-fr}\right]\end{aligned}\cdot \tag{3.51}$$

Let

$$\begin{aligned}&\mu\mathbf{p}E\left[\Delta\boldsymbol{\theta}(t)^{1-fr}\right]-\mu\mathbf{R}E\left[\Delta\boldsymbol{\theta}(t)^{2-fr}\right]-\mu\mathbf{R}\binom{2-fr}{1}\boldsymbol{\theta}_{\text{opt}}^{1}E\left[\Delta\boldsymbol{\theta}(t)^{1-fr}\right]\\ &=\mu E[\Delta\boldsymbol{\theta}(t)]\mathbf{F}[\Delta\boldsymbol{\theta}(t),fr]\end{aligned}, \tag{3.52}$$

using (3.52) in (3.51) gives

$$\begin{aligned}\mathbf{w}(t+1) &= \mathbf{w}(t)+\alpha[\mathbf{w}(t)-\mathbf{w}(t-1)]-\mu\mathbf{R}\mathbf{w}(t)+\mu E[\Delta\boldsymbol{\theta}(t)]\mathbf{F}[\Delta\boldsymbol{\theta}(t),fr]\\ \mathbf{w}(t+1) &= \mathbf{w}(t)+\alpha[\mathbf{w}(t)-\mathbf{w}(t-1)]-\mu\mathbf{R}\mathbf{w}(t)+\mu\mathbf{w}(t)\mathbf{F}[\Delta\boldsymbol{\theta}(t),fr]\end{aligned}. \tag{3.53}$$

Simplifying (3.53),

$$\mathbf{w}(t+1)=\mathbf{w}(t)(1+\alpha-\mu\{\mathbf{R}-\mathbf{F}[\Delta\boldsymbol{\theta}(t),fr]\})-\alpha\mathbf{w}(t-1). \tag{3.54}$$

Defining a $2N$ dimensional state vector as,

$$\mathbf{M}(t+1)=\begin{bmatrix}\mathbf{w}(t+1)\\ \mathbf{w}(t)\end{bmatrix}, \tag{3.55}$$

we have the following recursion

$$\mathbf{M}(t+1)=\begin{bmatrix}(1+\alpha)\mathbf{I}-\mu\{\mathbf{R}-\mathbf{F}[\Delta\boldsymbol{\theta}(t),fr]\} & -\alpha\mathbf{I}\\ \mathbf{I} & \mathbf{0}\end{bmatrix}\mathbf{M}(t). \tag{3.56}$$

The stability of the method is governed by the roots r of the determinant

$$\det\begin{bmatrix}(1+\alpha-r)\mathbf{I}-\mu\{\mathbf{R}-\mathbf{F}[\Delta\boldsymbol{\theta}(t),fr]\} & -\alpha\mathbf{I}\\ \mathbf{I} & -r\mathbf{I}\end{bmatrix}=0, \tag{3.57}$$

for which the necessary and sufficient condition is $|r_i| < 1, i = 1,2,\dots,2M$.

Using the following result for block matrices **A**, **B**, **C**, and **D** [117]

$$\det\begin{bmatrix}\mathbf{A} & \mathbf{B}\\ \mathbf{C} & \mathbf{D}\end{bmatrix}=\det[\mathbf{D}]\det[\mathbf{A}-\mathbf{B}\mathbf{D}^{-1}\mathbf{C}]=\det[\mathbf{A}]\det[\mathbf{D}-\mathbf{C}\mathbf{A}^{-1}\mathbf{B}] \tag{3.58}$$

Assuming that $\mathbf{D}^{-1}$ exists, we arrive at the following characteristics equation.

$$(-r)^n\det[\mathbf{D}]\det\left[(1+\alpha-r)\mathbf{I}-\mu\{\mathbf{R}-\mathbf{F}[\Delta\boldsymbol{\theta}(t),fr]\}-\frac{\alpha}{r}\mathbf{I}\right]=0. \tag{3.59}$$

The stability of the method is governed by the roots r of the determinant. To determine the $2N$ roots, we need to investigate the typical quadratic form

$$r_i^2-r_i\left(1+\alpha-\mu\{\lambda_i-\mathbf{F}[\Delta\boldsymbol{\theta}(t),fr]\}\right)+\alpha=0, \tag{3.60}$$

where λ_i are the eigen value of **R.** Applying the Jury's stability test to determine the step size bound [118]

$$0<\mu<\frac{1+\alpha}{\lambda_{\max}-\mathbf{F}[\Delta\boldsymbol{\theta}(t),fr]}. \tag{3.61}$$

Thus equation (3.61) gives the bound for the learning rate in case of mFLMS where $0 < \alpha < 1$.

3.9 Summary

In this chapter, first the latest literature of fractional adaptive algorithms was presented and then, the design of novel adaptive strategies based on variants of standard

FLMS, i.e., modified FLMS-1, modified FLMS-2, normalized FLMS, sliding-window FLMS and momentum FLMS is presented for Hammerstein system identification.

Chapter 4.

Simulation and Analytical Studies

In this chapter, results of simulations are presented for different case studies of Hammerstein system identification using proposed adaptive algorithms. The results presented in this chapter are mostly based on our published research articles.

4.1 Introduction

The parameter estimation of HCAR and HCARMA structures discussed in Chapter 2 is carried out using proposed adaptive algorithms by taking different levels of noise variance, learning rate parameter and fractional order. The input $x(t)$ is taken as a zero mean and unit variance signal, while noise $\vartheta(t)$ is a Gaussian signal with zero mean and constant variance σ^2. Simulations are performed in MATLAB software version 2012b in Windows 10 operating system running on HP ProBook model 4530s, with 2.30GHz Core-i3 processor and 4.00 GB RAM.

Performance indices based on fitness δ, mean square error (MSE), Nash-Sutcliffe efficiency (NSE) and Variance account for (VAF) are used for comparative study of the results. These performance measures are based on estimation error and are defined as:

$$\delta = \frac{\left\|\hat{\boldsymbol{\theta}}(t) - \boldsymbol{\theta}\right\|}{\left\|\boldsymbol{\theta}\right\|}, \tag{4.1}$$

$$\text{MSE} = \text{mean}\left[\hat{\boldsymbol{\theta}}(t) - \boldsymbol{\theta}\right]^2, \tag{4.2}$$

$$\text{NSE} = 1 - \left\{ \frac{\text{mean}\left[\hat{\boldsymbol{\theta}}(t) - \boldsymbol{\theta}\right]^2}{\text{mean}\left[\boldsymbol{\theta} - \text{mean}(\boldsymbol{\theta})\right]^2} \right\}, t \quad (4.3)$$

$$\text{ENSE} = 1 - \text{NSE}, \quad (4.4)$$

$$\text{VAF} = \left\{ 1 - \frac{\text{var}\left[\hat{\boldsymbol{\theta}}(t) - \boldsymbol{\theta}\right]}{\text{var}(\boldsymbol{\theta})} \right\} \times 100, \quad (4.5)$$

$$\text{EVAF} = 100 - \text{VAF}, \quad (4.6)$$

where, $\hat{\boldsymbol{\theta}}(t)$ is an estimated or adaptive parameter vector based on t^{th} iteration of the proposed algorithm and $\boldsymbol{\theta}$ is the desired parameter vector. In case of perfect model MSE, NSE and VAF values are zero, one and hundred, respectively, while, optimal values of ENSE, and EVAF are zero.

4.2 Case study 1: LMS and mLMS algorithms

In this case study, standard least mean square (LMS) and momentum LMS (mLMS) algorithms are applied to HCAR system identification. The iterative parameter update relation of standard LMS for HCAR systems is given in (3.7), while the update procedure of standard mLMS is given in (3.42), (3.43) and (3.45).

The HCAR system for simulation study is taken as follows [119]:

$$A(z)y(t) = B(z)\bar{x}(t) + \vartheta(t),$$

$$A(z) = 1 + a_1 z^{-1} + a_2 z^{-2} = 1 + 1.35 z^{-1} - 0.75 z^{-2},$$

$$B(z) = b_1 z^{-1} + b_2 z^{-2} = z^{-1} + 1.68 z^{-2},$$

$$\begin{aligned} \bar{x}(t) = f[x(t)] &= c_1 f_1[x(t)] + c_2 f_2[x(t)] + c_3 f_3[x(t)] \\ &= x(t) + 0.50 x^2(t) + 0.20 x^3(t) \end{aligned},$$

$$\boldsymbol{\theta} = [\theta_1, \theta_2, \theta_3, \theta_4, \theta_5, \theta_6, \theta_7, \theta_8]^T$$
$$\boldsymbol{\theta} = [a_1, a_2, c_1, c_2, c_3, b_2c_1, b_2c_2, b_2c_3]^T \quad . \tag{4.7}$$
$$\boldsymbol{\theta} = [-1.35, 0.75, 1.00, 0.50, 0.20, 1.68, 0.84, 0.336]^T$$

The mLMS algorithm is investigated for three different strategies of alpha α (proportion of previous gradients). Initially, for 10% of the iterations smaller value of α is taken and then larger value is used, *i.e.*, [0.1, 0.9], [0.3, 0.7] and [0.5, 0.5]. The step size for standard LMS and mLMS algorithms is selected after performing a set of trials to achieve the best MSE value after the convergence. For initial 10% iterations step size is taken as 10^{-3} for faster convergence and then 10^{-5} is used for stability purposes. The mLMS approach is examined for three values of noise variance *i.e.*, $\sigma^2 = 0.01^2$, 0.05^2 and 0.1^2.

The learning curves based on fitness (4.1) against iterations are given in Fig. 4.1 for all noise variations. The results presented in Fig. 4.1 are averaged on 10 iterations. It is observed that all variants of mLMS method are faster in convergence than standard LMS algorithm, while the mLMS with α = [0.5, 0.5] has faster convergence among all proposed variants of mLMS.

The performance comparison of proposed algorithm is also conducted based on number of iterations required to achieve the specific value of fitness. Two values of fitness *i.e.*, 0.1 and 0.01 are used to analyze the working of the design scheme and results are presented in Table 4.1 for all noise variances. It is seen that the LMS algorithm requires 7056 and 25294 iterations to achieve the fitness of 0.1 and 0.01 respectively while respective iterations in case of MLMS with α = [0.5, 0.5] are 3453 and 12750 for $\sigma^2 = 0.01^2$. It is observed that all mLMS variants require less number of iterations than standard LMS.

The design variables of HCAR system obtained by LMS and mLMS methods are presented in Appendix 4.1 for all noise variations. It is observed that the mLMS algorithm achieves the MSE values of the order 10^{-8}, 10^{-6} and 10^{-6} for $\sigma^2 = 0.01^2$, 0.05^2 and 0.1^2, respectively, while respective values in case of standard LMS are of the order 10^{-5}. Generally, it is seen that mLMS algorithm with $\alpha = [0.5, 0.5]$ gives more accurate results than other mLMS variants. It is observed that the methods are accurate and convergent for each scenario but the performance of mLMS algorithm with $\alpha = [0.5, 0.5]$ is better in terms of both convergence and accuracy.

In order to investigate the scheme in terms of initial convergence, the fitness (4.1) obtained in first 10000 iterations is given in Appendix 4.2 for all three noise variances. It is seen that the variants of mLMS algorithm have better rate of convergence than standard LMS and mLMS algorithm with $\alpha = [0.5, 0.5]$ has faster convergence rate among all mLMS variants for all noise variations.

The single good run of an algorithm is not enough for drawing concrete conclusions about the performance of the design scheme. Therefore, statistical analyses through 100 independent runs of the scheme are performed for HCAR system identification. The results of statistics based on minimum (MIN), mean and standard deviation (SD) through MSE and NSE performance measures using equations (4.2) and (4.4), respectively, are given in Appendix 4.3 for all variations. It is seen that if an algorithm achieves smaller value of MSE, then the corresponding value of ENSE is also small and vice versa. The MSE and E_{NSE} values of mLMS for $\alpha = [0.5, 0.5]$ are of the order 10^{-06}, while for LMS the corresponding values are of the order 10^{-04} for $\sigma^2 = 0.05^2$. It is observed that the values of both performance metrics are very close to desired values of HCAR system in each case, which validates the consistency of the mLMS approach for different performance indices.

Table 4.1 Performance comparison based on iterations required to achieve specific fitness value in case study 1

Method	α	$\delta = 0.1$			$\delta = 0.01$		
		$\sigma^2 = 0.01^2$	$\sigma^2 = 0.05^2$	$\sigma^2 = 0.1^2$	$\sigma^2 = 0.01^2$	$\sigma^2 = 0.05^2$	$\sigma^2 = 0.1^2$
LMS		7056	7031	7015	25294	25219	25151
mLMS	**(0.1, 0.9)**	4915	4912	4906	14031	14054	14062
mLMS	**(0.3, 0.7)**	4287	4285	4281	13118	13022	12989
mLMS	**(0.5, 0.5)**	3453	3411	3370	12750	12860	12371

4.3 Case study 2: FLMS, MFLMS-1 and MFLMS-2 algorithms

In this case study, FLMS, MFLMS-1 and MFLMS-2 algorithms are applied to parameter estimation of HCAR system given in equation (4.7). The step size is selected after performing a set of trials to achieve the best MSE value after the convergence. Same value is used for both μ_1 and μ_f parameters. For initial 10% iterations step size is taken as 10^{-3} for faster convergence and then 10^{-5} is used for stability purposes. The design approaches are evaluated for three different noise variances *i.e.*, $\sigma^2 = 0.1^2$, 0.5^2 and 0.9^2. Two values of fractional order (*fr*) are incorporated in the simulations for all three FLMS, MFLMS-1 and MFLMS-2 algorithms, *i.e.*, *fr* = 0.25 and 0.75, while two values of adjustable gain parameter β are used in MFLMS-1 algorithm, *i.e.*, $\beta = 0.25$ and 0.75.

Iterative results of proposed fractional adaptive algorithms based on values of fitness are shown in Figs. 4.2 and 4.3 for *fr* = 0.25 and 0.75 respectively. It is seen from learning curves that the final convergence of MFLMS-1 for $\beta = 0.25$ and MFLMS-2 algorithms are superior than FLMS and MFLMS-1 with $\beta = 0.75$ in almost all the cases, while these algorithms converge rapidly in initial iterations. There is no noticeable difference seen between the performance of MFLMS-1 for $\beta = 0.25$ and MFLMS-2 on the basis of learning curve.

In order to show the level of accuracy, the adaptive values of each algorithm are given in Appendices 4.4, 4.5 and 4.6 along with values of mean square error (MSE) for $\sigma^2 = 0.1^2$, 0.5^2 and 0.9^2, respectively. The results presented show that in terms of MSE values, MFLMS-2 algorithm provides relatively better from the rest of the algorithms. Moreover, with an increase in the value of noise variance, decrease in the performance of each algorithm is observed and still the results with reasonable accuracy are achieved by the proposed fractional adaptive algorithms.

Reliability and effectiveness of the proposed algorithms are examined through results of statistical analysis based on hundred independent runs of each fractional adaptive algorithm for parameters identification of HCAR model. Results in terms of MIN, mean and SD values calculated for 100 independent runs of each algorithm are given in Table 4.2 for MSE metric, while, for ENSE and EVAF performance measures, results are presented in Appendices 4.7 and 4.8 respectively. Generally, small values of statistical indicators are obtained which show that all three algorithms are consistently providing accurate results; however, relatively better results are obtained by MFLMS-2 algorithm in term of precision and convergence.

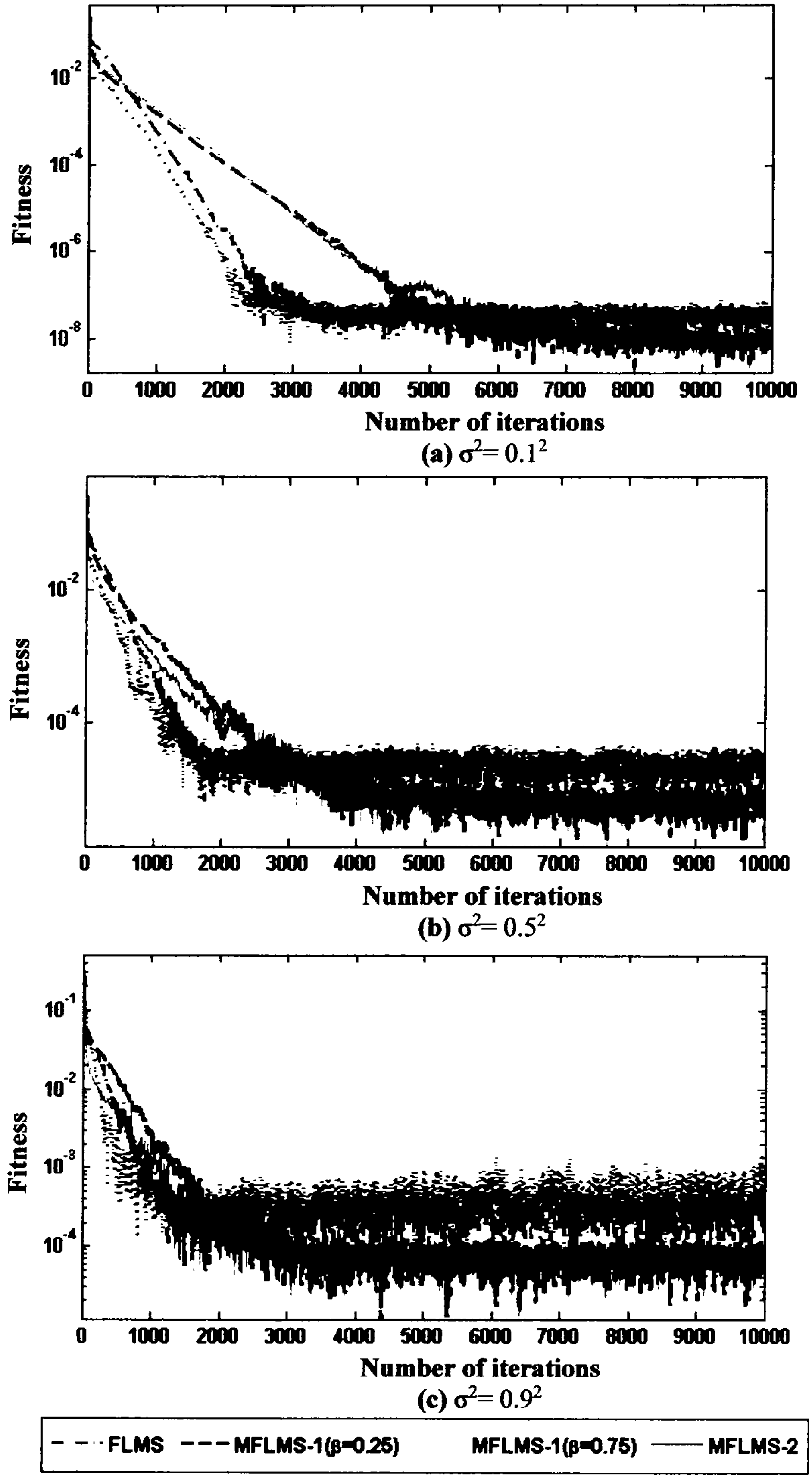

Fig. 4.2 Iterative adaptation of fitness function for *fr*=0.25 in case study 2

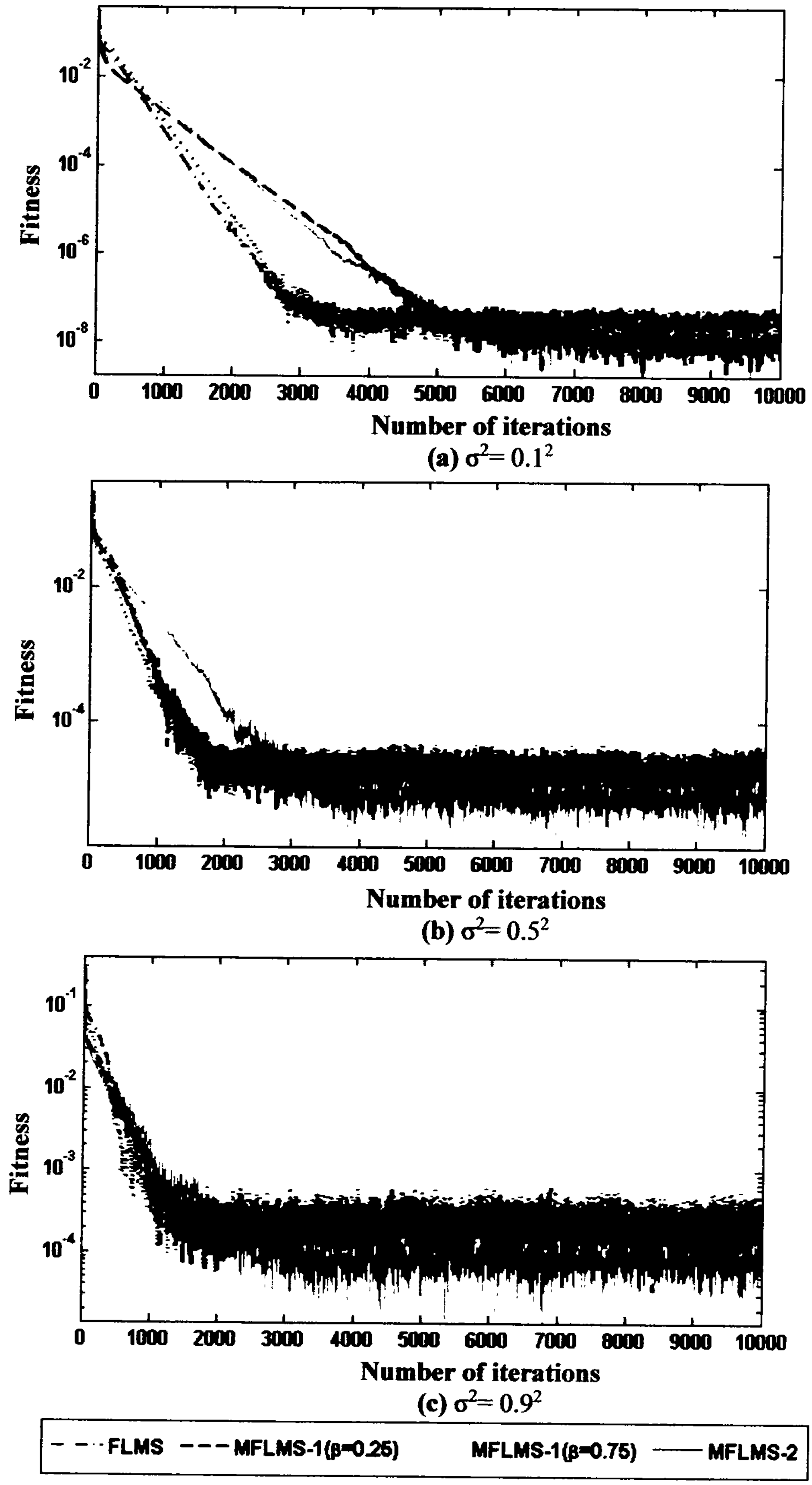

Fig. 4.3 Iterative adaptation of fitness function for fr = 0.75 in case study 2

Table 4.2 Performance comparison based on statistical parameters through MSE in case study 2

μ	METHOD	fr/β	$\sigma^2 = 0.1^2$			$\sigma^2 = 0.5^2$			$\sigma^2 = 0.9^2$		
			MIN	MEAN	STD	MIN	MEAN	STD	MIN	MEAN	STD
(10^{-03}, 10^{-05})	**FLMS**	**0.25**	3.48E-08	4.20E-07	6.92E-07	2.74E-05	2.81E-04	5.73E-04	3.47E-03	3.64E-03	2.35E-04
		0.75	3.50E-08	4.32E-07	7.23E-07	2.34E-05	2.31E-04	3.21E-04	2.73E-04	8.58E-03	4.96E-02
	MFLMS-1	**0.25/0.25**	8.00E-09	5.56E-08	3.17E-08	5.34E-06	3.47E-05	2.00E-05	7.86E-05	3.76E-04	2.23E-04
		0.75/0.25	3.29E-08	3.47E-07	5.30E-07	2.12E-05	1.83E-04	2.38E-04	3.19E-04	2.50E-03	2.55E-03
		0.25/0.75	3.03E-08	2.22E-07	2.64E-07	1.94E-05	1.24E-04	1.18E-04	1.42E-04	1.43E-03	1.44E-03
		0.75/0.75	3.35E-08	3.51E-07	5.33E-07	2.14E-05	1.95E-04	2.58E-04	2.31E-04	2.12E-03	3.30E-03
	MFLMS-2	**0.25**	6.18E-09	5.47E-08	3.27E-08	4.34E-06	3.41E-05	2.06E-05	7.09E-05	3.75E-04	2.32E-04
		0.75	1.07E-08	6.10E-08	3.38E-08	7.15E-06	3.80E-05	2.14E-05	9.37E-05	4.10E-04	2.37E-04

4.4 Case study 3: Normalized FLMS algorithms

In this case study, the proposed NFLMS, NMFLMS-1 and NMFLMS-2 algorithms are applied to estimate the parameters of HCAR system (4.7) for sufficient number of iterations *i.e.,* t = 20000. The proposed normalized adaptive strategies are evaluated for three values of noise variance *i.e.*, $\sigma^2 = 0.2^2$, 0.5^2 and 0.8^2. The NMFLMS-1 method is studied for two values of adjustable gain parameter *i.e.*, $\beta = 0.25$ and 0.75.

The step size plays a very important role in convergence and stability of adaptive algorithms. In order to select an appropriate value of step size parameter, the standard and normalized fractional algorithms are tested for four step size values *i.e.,* 10^{-02}, 10^{-03}, 10^{-04} and 10^{-05}. Ten independent runs of the methods are performed and results in terms of mean value and standard deviation are given in Appendix 4.9 for fractional order 0.5 and noise variance 0.5^2. It is evident from the results that 10^{-02} and 10^{-03} are the suitable step size values for standard and normalized fractional methods respectively. Same value is used for both μ_1 and μ_f parameters.

In proposed fractional adaptive algorithms, one important variable is fractional order. The proposed normalized methods are examined for nine different values of fractional orders *i.e.*, [0.1, 0.2, ..., 0.9] and results based on 10 independent runs of the algorithms in terms of MSE are given in Appendix 4.10. It is observed that all the proposed normalized fractional strategies are convergent for all values of fractional orders but standard FLMS provides divergent behavior for lower value of fractional order *i.e.,* $fr = 0.1$. It is seen that there is very small difference among different values of fractional orders for HCAR system identification (4.7) using normalized fractional adaptive strategies. So, it is reasonable to take $fr = 0.5$ in rest of this case study.

The iterative plots of fitness function (4.1) using NFLMS and NMFLMS-2 given in Fig. 4.4 while for NMFLMS-1 algorithm respective plots are given in Fig. 4.5 for all noise variations. It is seen that all the proposed fractional order adaptive methods are correct and convergent but the convergence speed of proposed normalized fractional strategies is faster than the standard counterparts.

The performance of the proposed methods is examined through MSE (4.2), and results are given in Appendices 4.11, 4.12 and 4.13 for $\sigma^2 = 0.2^2$, 0.5^2 and 0.8^2 respectively. It is observed that all schemes give better results for lesser standard deviation *i.e.,* $\sigma^2 = 0.2^2$ and relatively degraded results are obtained for higher noise deviation *i.e.,* $\sigma^2 = 0.8^2$. It is seen that the accuracy of NFLMS, NMFLMS-1 and NMFLMS-2 algorithms is better than standard FLMS, MFLMS1 and MFLMS2 methods. However, negligible difference is observed among proposed normalized algorithms.

The proposed normalized fractional adaptive algorithms are examined through statistics calculated for MSE, NSE and VAF (4.2) - (4.6) performance measures based on hundred independent runs. The results of statistical parameters based on MIN, mean and SD values are presented in Table 4.3 for MSE evaluation metric, while, for ENSE and EVAF performance measures results are presented in Appendices 4.14 and 4.15 respectively. Generally, it is seen that all the proposed normalized fractional algorithms are accurate and convergent, while standard FLMS algorithm provides few divergent runs. Moreover, it is observed that proposed normalized methods give better results than standard adaptive strategies which validates the performance of the normalized algorithms on different performance metrics.

In order to show the extent of divergence *i.e.,* number of divergent runs, results of statistical analyses are also plotted in ascending order in Fig 4.6 for standard FLMS and normalized FLMS algorithms. It is clear from Fig 4.6 that FLMS shows divergent behavior for all noise levels, but number of divergent runs increases with an increase in noise standard deviation *i.e.,* one, two and twelve divergent runs for $\sigma^2 = 0.2^2$, 0.5^2 and 0.8^2 respectively, while this behavior is not seen in normalized version.

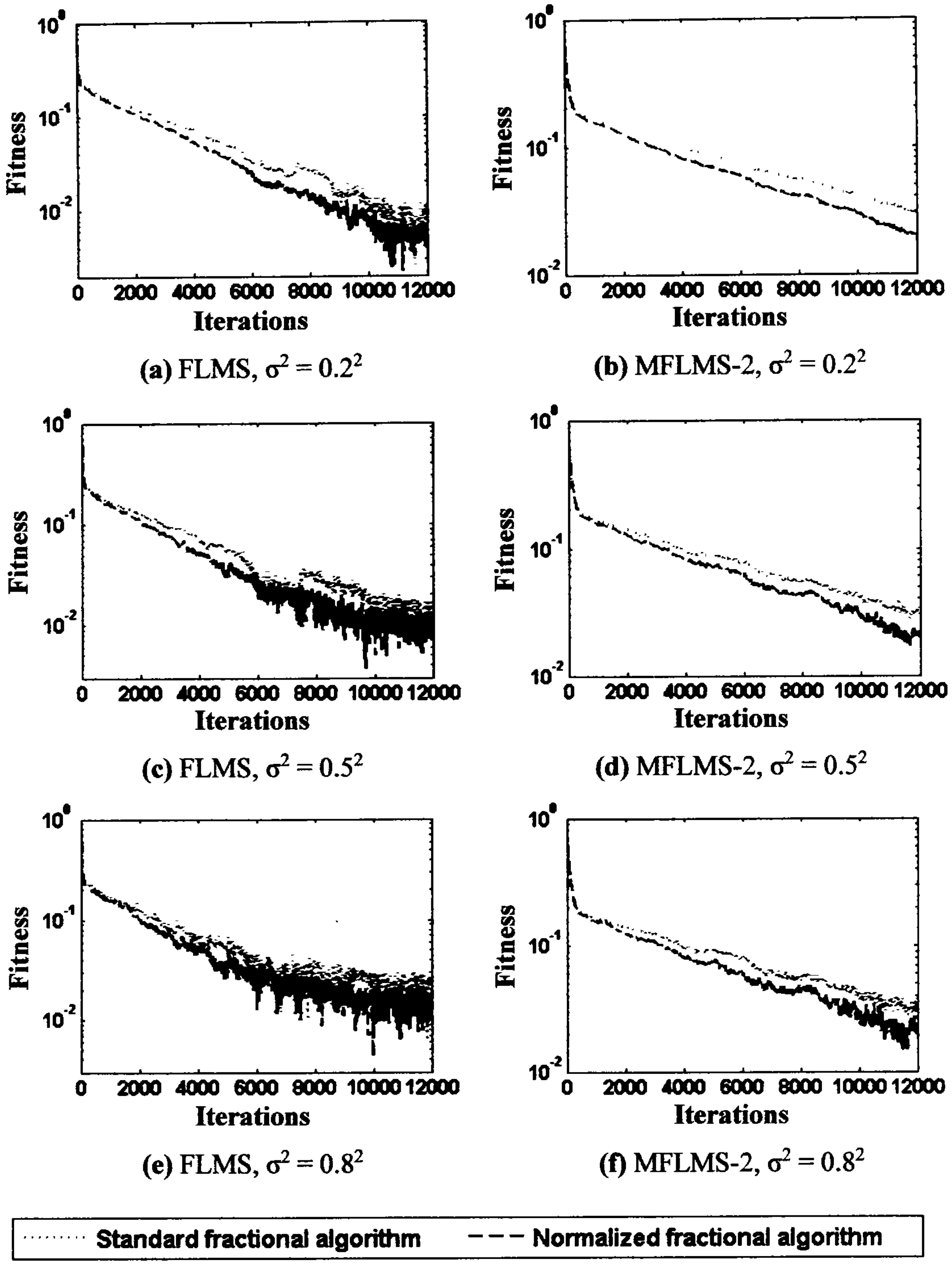

Fig. 4.4 Iterative adaptation of fitness using NFLMS and NFLMS-2 in case study 3

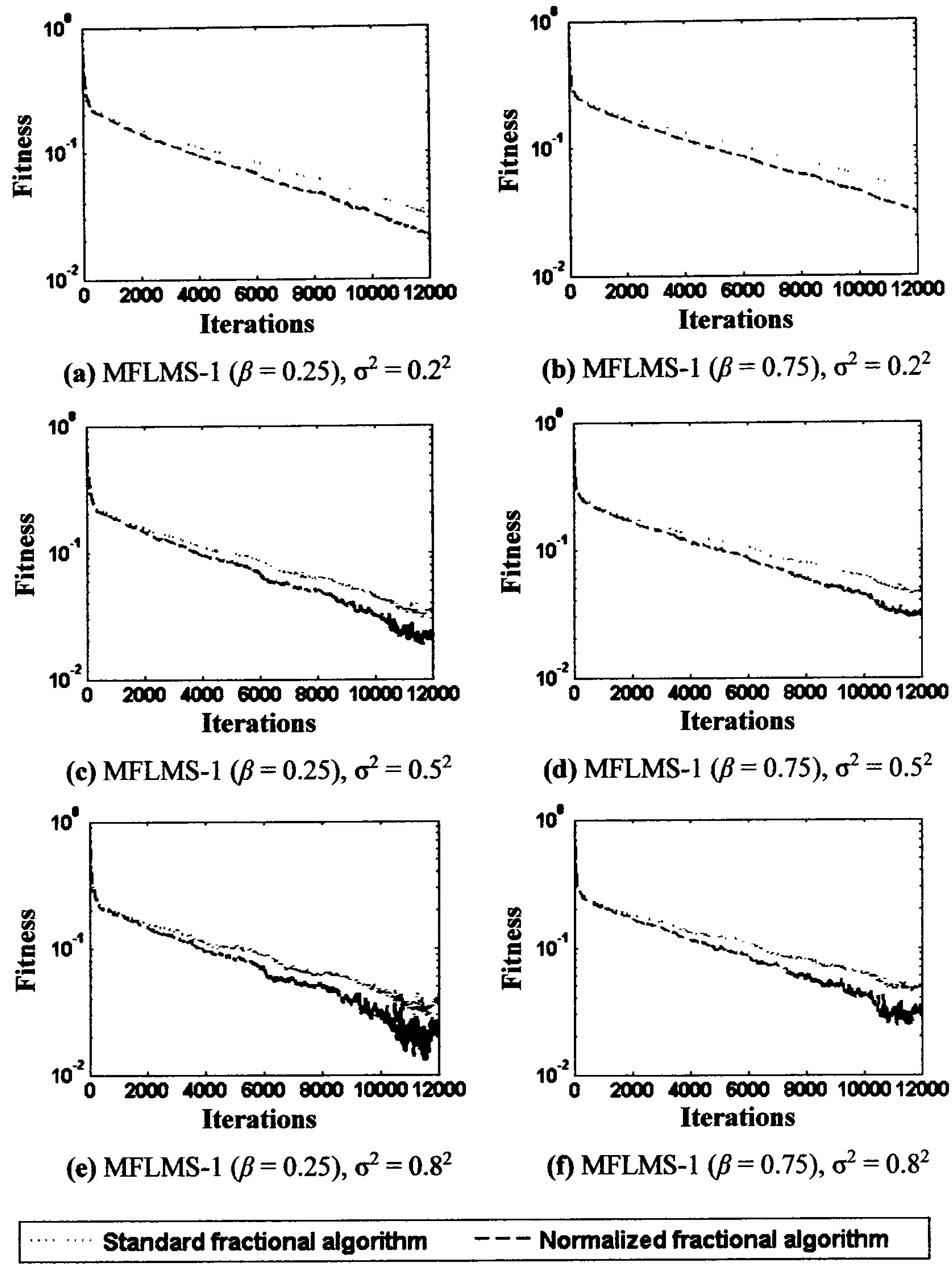

(a) MFLMS-1 ($\beta = 0.25$), $\sigma^2 = 0.2^2$

(b) MFLMS-1 ($\beta = 0.75$), $\sigma^2 = 0.2^2$

(c) MFLMS-1 ($\beta = 0.25$), $\sigma^2 = 0.5^2$

(d) MFLMS-1 ($\beta = 0.75$), $\sigma^2 = 0.5^2$

(e) MFLMS-1 ($\beta = 0.25$), $\sigma^2 = 0.8^2$

(f) MFLMS-1 ($\beta = 0.75$), $\sigma^2 = 0.8^2$

Fig. 4.5 Iterative adaptation of fitness using NMFLMS-1 in case study 3

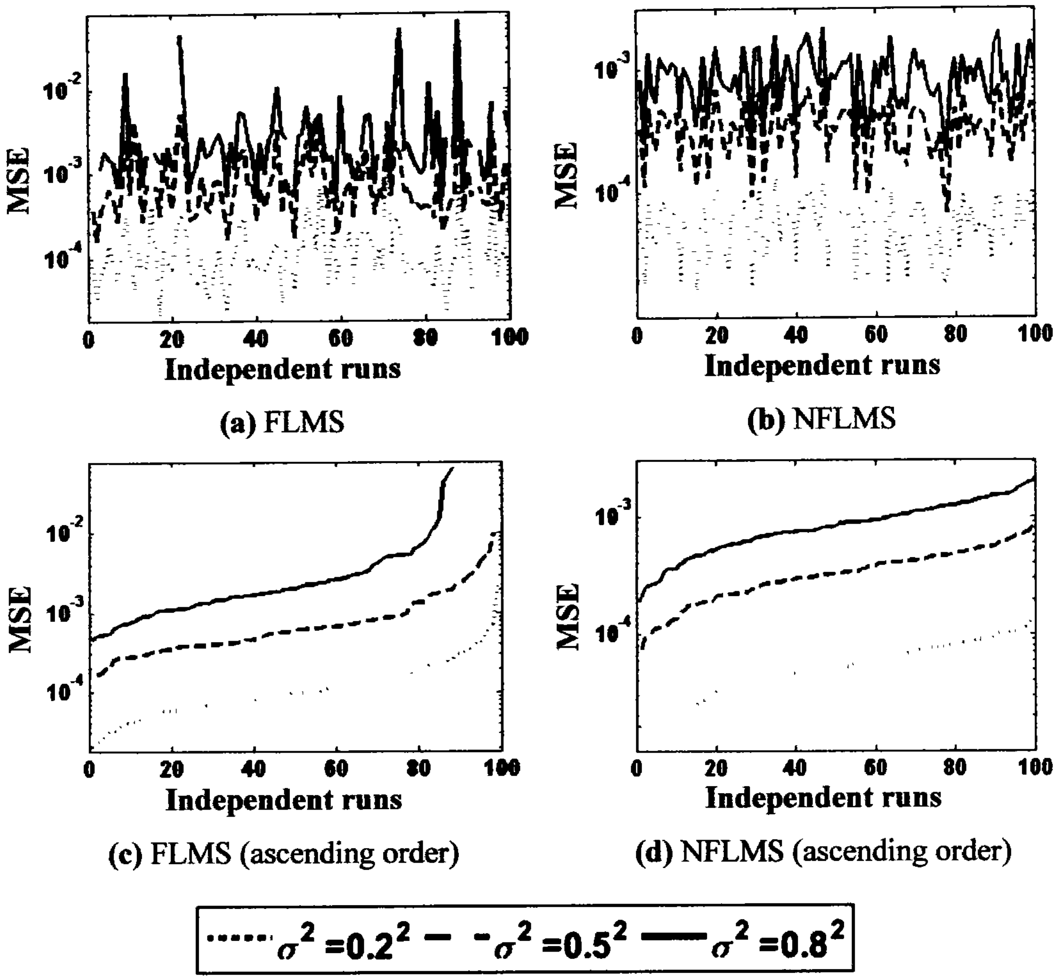

Fig. 4.6 Plot of statistical analyses based on MSE values in case study 3

Table 4.3 Performance comparison through statistics based on MSE values in case study 3

	Method	$\sigma^2 = 0.2^2$			$\sigma^2 = 0.5^2$			$\sigma^2 = 0.8^2$		
		MIN	**MEAN**	**SD**	**MIN**	**MEAN**	**SD**	**MIN**	**MEAN**	**SD**
MSE	**FLMS**	2.02E-05	NaN	NaN	1.60E-04	NaN	NaN	4.57E-04	NaN	NaN
	NFLMS	1.60E-05	5.68E-05	2.71E-05	6.74E-05	3.52E-04	1.67E-04	1.93E-04	9.12E-04	4.28E-04
	MFLMS-1($\beta = 0.25$)	6.89E-05	1.62E-03	1.05E-03	1.00E-04	1.67E-03	1.12E-03	1.99E-04	1.80E-03	1.22E-03
	MFLMS-1($\beta = 0.75$)	1.85E-04	1.60E-03	7.90E-04	2.08E-04	1.67E-03	8.53E-04	3.02E-04	1.83E-03	9.69E-04
	NMFLMS-1($\beta = 0.25$)	2.86E-05	4.07E-04	2.57E-04	5.50E-05	5.35E-04	3.23E-04	9.36E-05	7.85E-04	4.33E-04
	NMFLMS-1($\beta = 0.75$)	3.49E-05	4.12E-04	1.97E-04	5.36E-05	5.53E-04	2.73E-04	1.03E-04	8.25E-04	3.93E-04
	MFLMS-2	7.03E-05	1.87E-03	1.49E-03	1.14E-04	1.92E-03	1.57E-03	2.32E-04	2.02E-03	1.67E-03
	NMFLMS-2	3.39E-05	4.87E-04	3.86E-04	6.08E-05	6.10E-04	4.46E-04	8.39E-05	8.52E-04	5.51E-04

4.5 Case study 4: Sliding window based FLMS algorithm

In this case study, sliding window based FLMS (SW-FLMS) algorithm is applied to Hammerstein nonlinear system based on HCARMA model given in section 2.3. The HCARMA system for simulation study is taken as follows [35], [36]:

$$A(z)y(t) = B(z)\bar{x}(t) + D(z)\vartheta(t),$$

$$A(z) = 1 + a_1 z^{-1} + a_2 z^{-2} = 1 - 1.60z^{-1} + 0.8z^{-2},$$

$$B(z) = b_1 z^{-1} + b_2 z^{-2} = 0.85z^{-1} + 0.65z^{-2},$$

$$D(z) = 1 - d_1 z^{-1} = 1 - 0.64z^{-1}$$

$$\begin{aligned}\bar{x}(t) = f[x(t)] &= c_1 f_1[x(t)] + c_2 f_2[x(t)] + c_3 f_3[x(t)] \\ &= x(t) + 0.50x^2(t) + 0.25x^3(t)\end{aligned},$$

$$\boldsymbol{\theta} = [\theta_1, \theta_2, \theta_3, \theta_4, \theta_5, \theta_6, \theta_7, \theta_8, \theta_9]^T$$

$$\boldsymbol{\theta} = [a_1,\ a_2,\ b_1c_1,\ b_2c_1,\ b_1c_2,\ b_2c_2,\ b_1c_3,\ b_2c_3,\ d_1]^T$$

$$\boldsymbol{\theta} = [1.60, -0.80, 0.85, 0.65, 0.425, 0.325, 0.2125, 0.1625, -0.64]^T \tag{4.8}$$

Simulations are performed by taking different levels of noise variances *i.e.,* $\sigma^2 =$ 0.1, 0.4 and 0.8. The learning parameter is taken as 10^{-4} that is selected after performing a set of trials to obtain the best MSE after convergence. Moreover, comparative analyses of the results are also given with standard FLMS algorithm to determine the effectiveness of proposed modification. The fitness versus iterations are used for performance evaluation. We intend to use SW-FLMS algorithm with different window lengths to estimate the parameters of HCARMA system given in (4.8).

Fig. 4.7 shows the learning curves for FLMS and SW-FLMS. Each learning curve is obtained by averaging the results of 30 independent runs with stopping criteria of estimation errors $\delta < 0.05$. In this way, all algorithms are comparable in terms of mean behavior to reach an estimation error of 5 percent. Fig. 4.8 shows the number of iterations to reach an estimation error of 5 percent for 200 independent runs. Some interesting observations from Figs. 4.7 and 4.8 are:

- For $\sigma^2 = 0.1$, 0.4 and 0.8, the standard FLMS takes the most number iterations to reach an estimation error of 5 percent as can be seen in Figs. 4.7 and 4.8.
- It is clear from Fig. 1(a) and 2(a) that for $\sigma^2 = 0.1$, the standard FLMS requires almost 2.5 times more iterations than SW-FLMS with $L = 3$, and 6 times more iterations than SW-FLMS with $L = 7$.
- For $\sigma^2 = 0.4$ and 0.8, the standard FLMS requires 3 times more iterations than SW-FLMS with $L = 3$, and 6 times more iterations than SW-FLMS with $L = 7$ to reach an estimation error of 5 percent as shown in Fig. 4.7(b)-(c) and Fig. 4.8(b)-(c).
- For $\sigma^2 = 0.1$, 0.4 and 0.8, the standard FLMS takes the most number iterations to reach an estimation error of 5 percent.
- All the above-mentioned observations are equally valid for $fr = 0.5$ and 0.7. Also, the iterations with $fr = 0.5$ are more than the iterations for $fr = 0.7$ irrespective of the algorithm used.

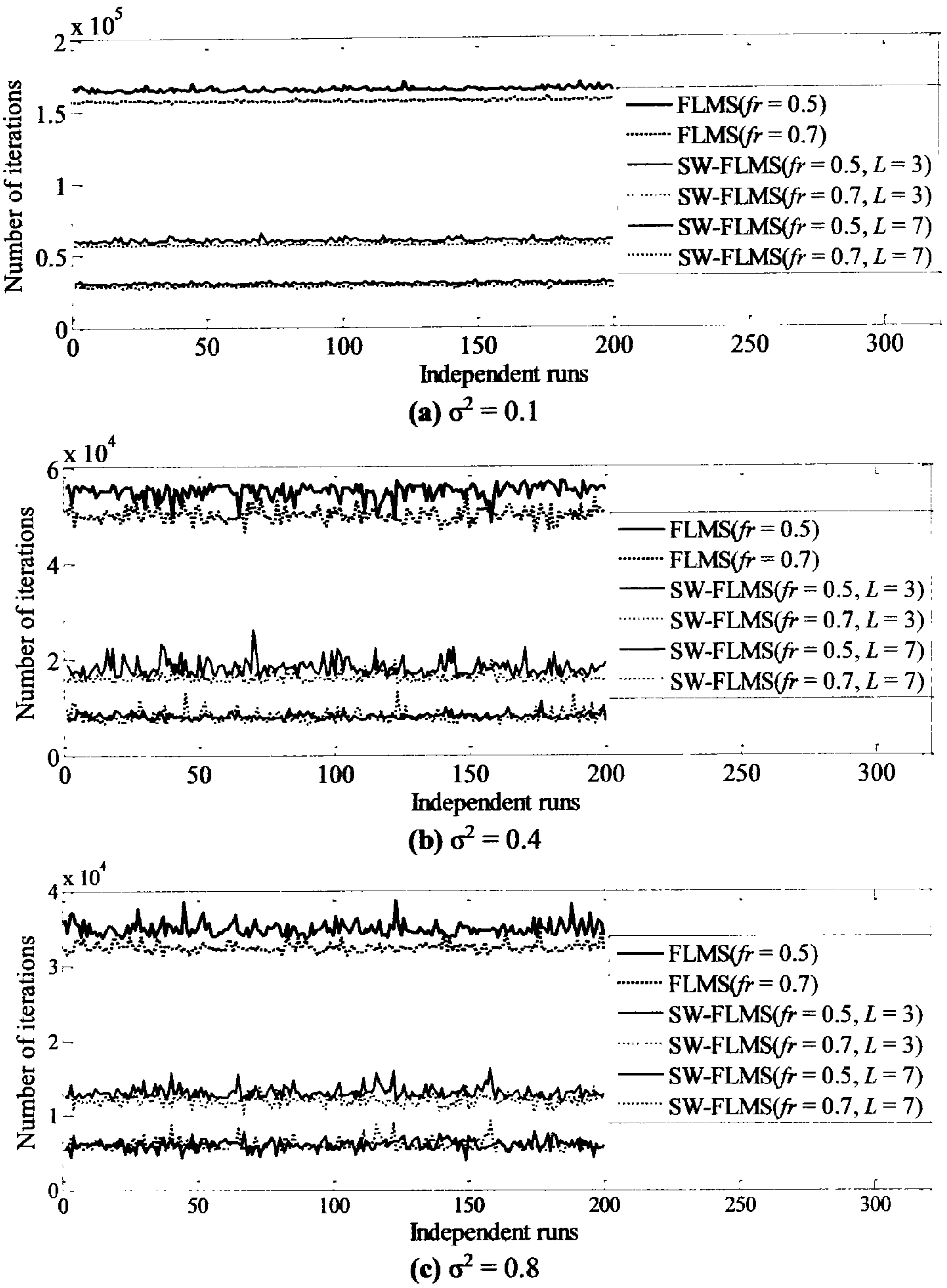

Fig. 4.8 Number of iterations for estimation error of 5 percent in case study 4.

4.6 Case study 5: Momentum FLMS algorithm

In this case study, momentum FLMS *i.e.,* mFLMS is applied to parameter estimation of HCAR system given in (4.7). The results obtained through mFLMS algorithm are compared with standard FLMS to show the effectiveness of the proposed modification. The learning parameters are taken as 10^{-3} that is selected after performing a set of trials to obtain the best MSE after convergence. Same value is used for both μ_1 and μ_f parameters. The robustness of the scheme is studied by taking the noise with different variance *i.e.,* $\sigma^2 = 0.01^2$, 0.05^2 and 0.1^2. The performance of the method is examined for different values of α and fractional order, *i.e.*, 0.2, 0.4, 0.6, and 0.25, 0.50, 0.75 respectively.

To study the convergence properties of mFLMS scheme, the fitness δ achieved in first 10000 iterations is presented in Appendices 4.16, 4.17 and 4.18 for $\sigma^2 = 0.01^2$, 0.05^2 and 0.1^2 respectively. It is seen from the results that proposed mFLMS method provides faster convergence than standard FLMS for all values of α. It is also observed that convergence speed increases by increasing the proportion of momentum term.

The performance of the design scheme is analyzed through iterations required for obtaining specific fitness value. The number of iterations required to achieve 0.1 and 0.05 fitness values are given in Table 4.4 for all noise and α variations. It is seen that the standard FLMS algorithm requires 4070 and 6352 iterations for 0.1 and 0.05 fitness values respectively, while the respective iterations for mFLMS algorithm with $\alpha = 0.6$ are 1127 and 2145, for $\sigma^2 = 0.1^2$. It is inferred from the results that proposed mFLMS algorithm has faster convergence and requires less iterations for specific fitness value.

The number of iterations required decreases with an increase in value of α, i.e. the convergence speed increases by increasing the α.

The performance of the method is investigated through MSE metric. The HCAR system parameters along with MSE values are given in Appendices 4.19, 4.20 and 4.21 for $\sigma^2 = 0.01^2$, 0.05^2 and 0.1^2, respectively. It is seen from Appendix 4.19 that MSE values given by FLMS are of the order 10^{-4} for all fractional orders. The MSE values through proposed mFLMS algorithm are of the order 10^{-5}, 10^{-6} and 10^{-7} for $\alpha = 0.2$, 0.4 and 0.6 respectively. It is inferred from the results that design scheme is accurate and convergent for all values of fractional orders. It is also inferred that proposed method is robust against different noise values. However, slight degradation in performance is seen for higher noise variance.

The learning curves based on fitness are presented in Fig. 4.9 for all noise variances and fractional order = 0.50. It is observed that mFLMS algorithm is faster in convergence than standard FLMS for all values of α. It is observed from the learning curves that higher value of α i.e., higher proportion of momentum term increases the speed of convergence but at the cost of steady state performance. It is inferred from the plots that the middle value of α i.e., α = 0.4 is a good compromise between fast convergence and minimum steady state error.

Table 4.4 Performance comparison based on iterations required for specific fitness value in case study 5

Method	α	$\delta = 0.1$			$\delta = 0.05$		
		$\sigma^2 = 0.01^2$	$\sigma^2 = 0.05^2$	$\sigma^2 = 0.1^2$	$\sigma^2 = 0.01^2$	$\sigma^2 = 0.05^2$	$\sigma^2 = 0.1^2$
FLMS		4019	4034	4070	6243	6275	6352
mFLMS	**0.2**	2882	2901	2912	4657	4761	4888
mFLMS	**0.4**	1909	1915	1945	3204	3215	3260
mFLMS	**0.6**	1139	1130	1127	2071	2095	2145

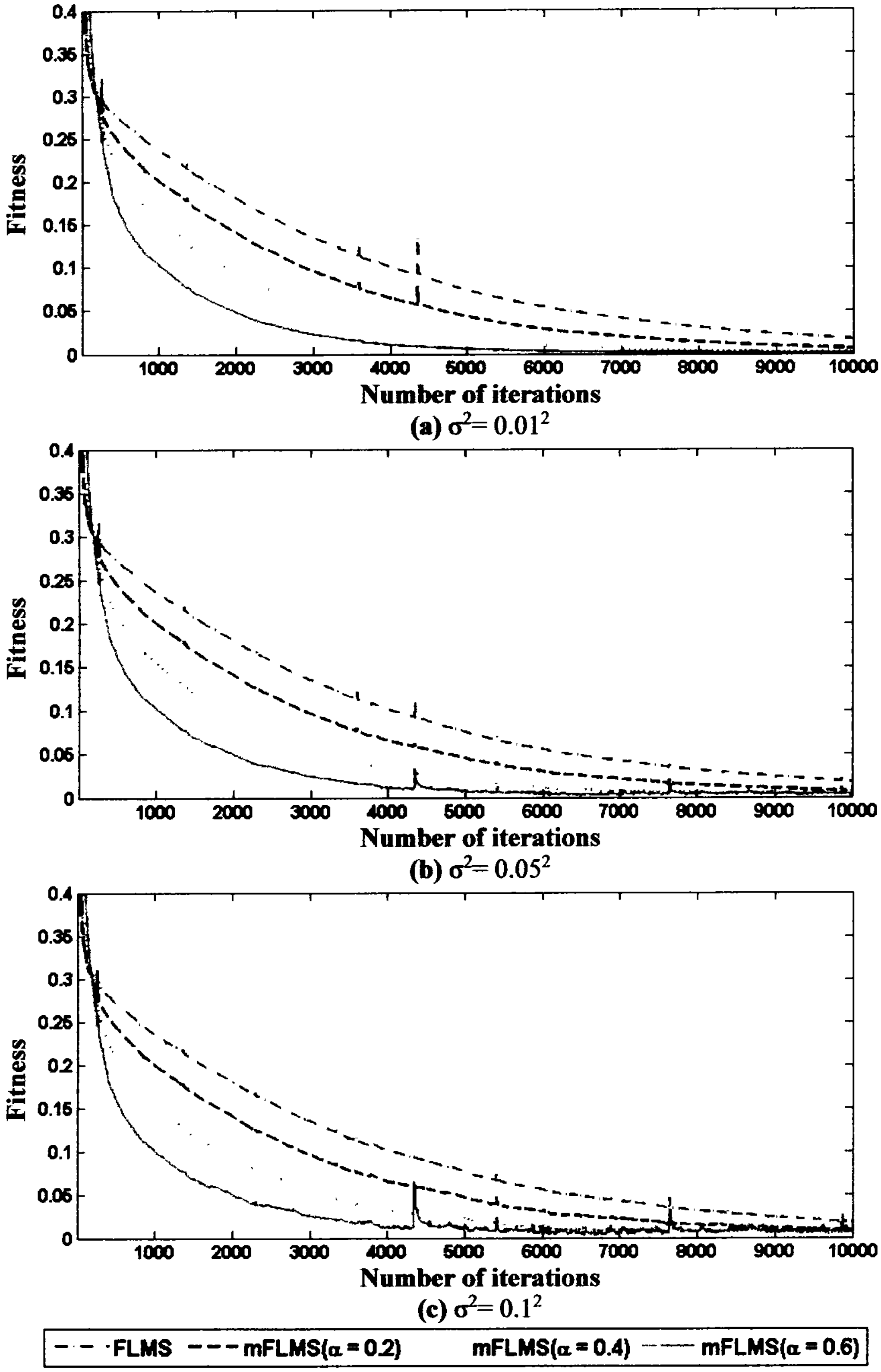

Fig. 4.9 Iterative adaptation of fitness function for $fr = 0.50$ in case study 5

4.7 Case study 6: Comparison of proposed fractional algorithms

In this case study, the comparison of proposed fractional adaptive strategies based on MFLMS-1, MFLMS-2, NFLMS, SW-FLMS and mFLMS is presented with standard FLMS for HCAR system identification (4.7) with $\sigma^2 = 0.5^2$.

The parameters of the proposed algorithms are selected based on the observations from the previous case studies. It is observed in the previous case studies that fractional adaptive algorithms normally provide relatively better results for higher values of fractional order. Therefore, the algorithms are compared for fractional order $fr = 0.75$. In case study 3, it is seen that mFLMS provides faster convergence rate for higher value of α, but with more steady state error. Therefore, in this case study, initially the higher value of α *i.e.,* 0.5 is used for faster convergence and then lower value of α *i.e.,* 0.1 is taken for better steady state performance. In SW-FLMS algorithm, the length of window used is 5.

The iterative adaptation of fitness function (4.1) using FLMS, MFLMS-1, MFLMS-2, NFLMS, SW-FLMS and mFLMS algorithms is presented in Fig. 4.10(a) for $\mu = 0.001$. It is seen that NFLMS algorithm is stable and convergent while, the other algorithms do not provide smooth convergence for $\mu = 0.001$. In order to reduce these fluctuations, the step size is reduced to 0.0005 for the FLMS, MFLMS-1, MFLMS-2, mFLMS and SW-FLMS algorithms and results are presented in Fig. 4.10 (b). The results show that the SW-FLMS method provide smooth convergence while, the FLMS, MFLMS-1, MFLMS-2, mFLMS algorithms do not produce smooth learning curves for $\mu = 0.0005$. The standard FLMS and mFLMS algorithms provide faster convergence than other variants, while, the MFLMS-1 and MFLMS-2 methods give lower steady state error. The step size parameter is further reduced to 0.0001 for FLMS and mFLMS algorithms, and 0.0002 for MFLMS-1 and MFLMS-2 algorithms. Thus, the learning curves presented in Fig.4.10 (c) are based on μ = 0.0001, 0.0001, 0.0005, 0.0002, 0.0002 and 0.001 for FLMS, mFLMS, SW-FLMS, MFLMS-1, MFLMS-2 and NFLMS algorithms, respectively. It is clearly seen that the proposed algorithms provide smooth learning curves for these values of learning rate parameters. It is observed that the proposed mFLMS algorithm is more accurate and convergent than other variants.

The proposed adaptive algorithms are also evaluated based on MSE metric and results are presented in Table 4.5 for different variations in learning rate parameter. It is observed form the results that mFLMS and NFLMS algorithms are more accurate than other proposed variants of standard FLMS, while there is no much difference among FLMS, MFLMS-1, MFLMS-2 and SW-FLMS algorithms in terms of final accuracy for optimal values of step size parameter. However, MFLMS-2 and SW-FLMS algorithms provide better results than standard FLMS.

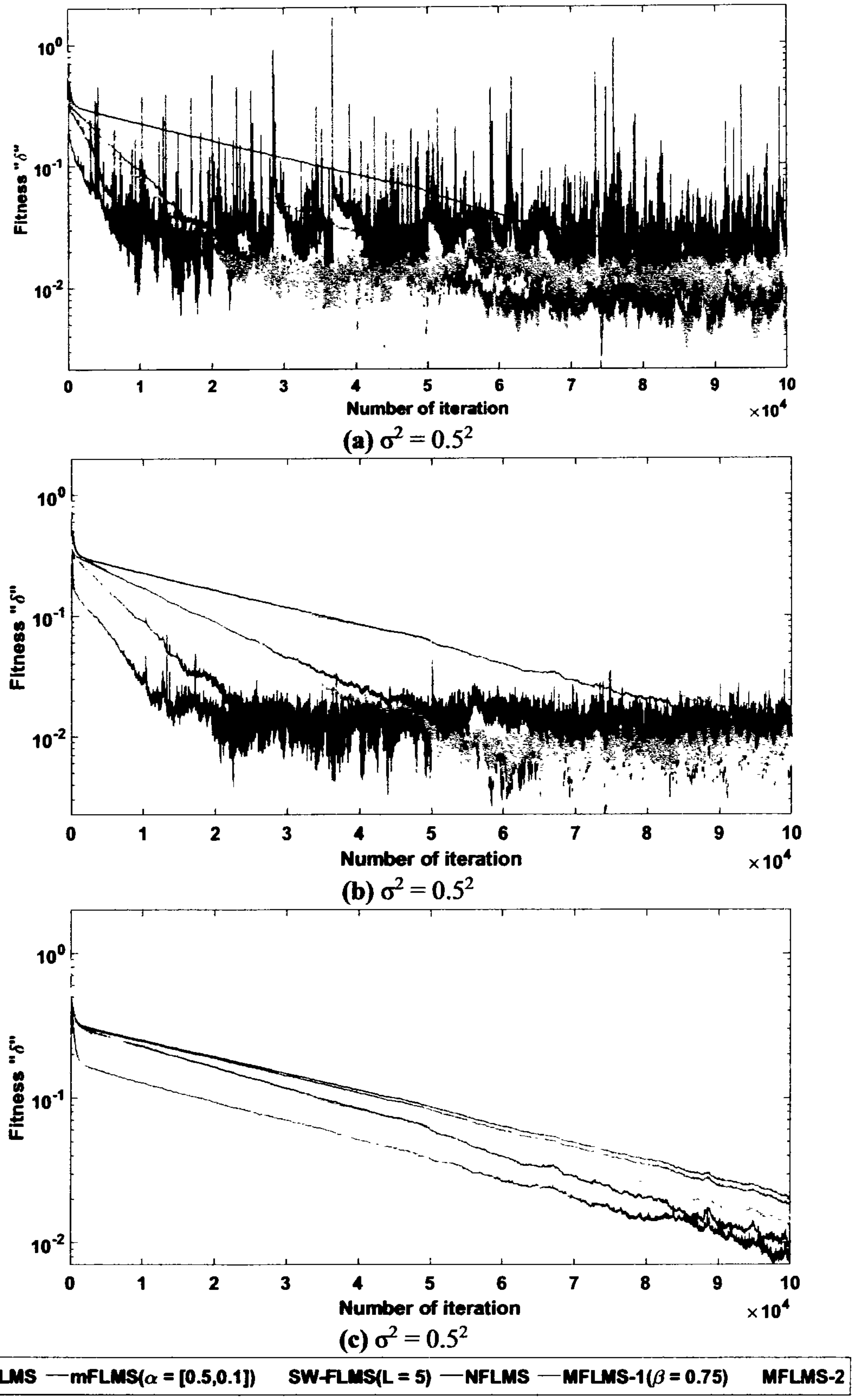

Fig. 4.10 Iterative adaptation of fitness function for different learning rates in case study 6

Table 4.5 Performance comparison of propose algorithms based on MSE for $\sigma^2 = 0.5^2$ in case study 6

μ	Method	Adaptive Parameters								MSE
		θ_1	θ_2	θ_3	θ_4	θ_5	θ_6	θ_7	θ_8	
0.001	**FLMS**	-1.359	0.729	0.992	0.501	0.205	1.691	0.847	0.280	4.35E-04
0.001	**mFLMS** ($\alpha = 0.5, 0.1$)	-1.356	0.727	0.993	0.501	0.203	1.696	0.847	0.275	5.30E-04
0.001	**SW-FLMS** (L = 5)	-1.347	0.738	0.996	0.502	0.201	1.678	0.842	0.321	4.78E-05
0.001	**MFLMS-1** ($\beta = 0.75$)	-1.353	0.732	0.998	0.501	0.202	1.673	0.846	0.306	1.44E-04
0.001	**MFLMS-2**	-1.354	0.731	0.999	0.501	0.202	1.670	0.846	0.308	1.41E-04
0.001	**NFLMS**	-1.344	0.744	0.991	0.509	0.204	1.658	0.839	0.343	9.67E-05
0.0005	**FLMS**	-1.353	0.732	0.999	0.501	0.202	1.672	0.846	0.307	1.43E-04
0.0005	**mFLMS** ($\alpha = 0.5, 0.1$)	-1.353	0.730	1.000	0.500	0.202	1.671	0.847	0.306	1.61E-04
0.0005	**SW-FLMS** (L = 5)	-1.345	0.742	0.980	0.503	0.207	1.650	0.841	0.342	1.82E-04
0.0005	**MFLMS-1** ($\beta = 0.75$)	-1.348	0.737	0.997	0.502	0.201	1.678	0.842	0.318	6.08E-05
0.0005	**MFLMS-2**	-1.348	0.737	0.997	0.502	0.200	1.677	0.842	0.319	5.66E-05
0.001	**NFLMS**	-1.344	0.744	0.991	0.509	0.204	1.658	0.839	0.343	9.67E-05
0.0001	**FLMS**	-1.345	0.743	0.983	0.504	0.206	1.634	0.841	0.350	3.37E-04
0.0001	**mFLMS** ($\alpha = 0.5, 0.1$)	-1.344	0.742	1.016	0.503	0.190	1.674	0.841	0.330	6.50E-05
0.0005	**SW-FLMS** (L = 5)	-1.345	0.742	0.980	0.503	0.207	1.650	0.841	0.342	1.82E-04
0.0002	**MFLMS-1** ($\beta = 0.75$)	-1.345	0.743	0.982	0.504	0.206	1.629	0.840	0.352	4.12E-04
0.0002	**MFLMS-2**	-1.345	0.742	0.984	0.504	0.205	1.643	0.841	0.346	2.28E-04
0.001	**NFLMS**	-1.344	0.744	0.991	0.509	0.204	1.658	0.839	0.343	9.67E-05
True Values		-1.350	0.750	1.000	0.500	0.200	1.680	0.840	0.336	0

4.8 Case study 7: Application to muscle modeling

It is seen in the case study 6 that the proposed mFLMS algorithm provide better results than other proposed variants of FLMS for parameter estimation of Hammerstein systems. Therefore, in this case study, the mFLMS algorithm is applied to identify the parameters of electrically stimulated muscle model. The HCAR structure, discussed in Chapter 2 has been used to model dynamics of stimulated muscle required for rehabilitation of paralyzed muscles by automatically controlled stimulations. The static nonlinear block shows the isometric recruitment curve, defined as the static gain relation between the stimulus activation level and the output torque when muscle is at a fixed length. The linear block of Hammerstein structure represents the dynamic response of electrically stimulated muscle [32]. The electrically stimulated muscle is modeled using HCAR structure with the following parameters [120]:

$$A(z)y(t) = B(z)\bar{x}(t) + \vartheta(t),$$

$$A(z) = 1 + a_1 z^{-1} + a_2 z^{-2} = 1 - z^{-1} + 0.8z^{-2},$$

$$B(z) = b_1 z^{-1} + b_2 z^{-2} = z^{-1} + 0.6z^{-2},$$

$$\begin{aligned}\bar{x}(t) = f[x(t)] &= c_1 f_1[x(t)] + c_2 f_2[x(t)] + c_3 f_3[x(t)] \\ &= 2.8x(t) - 4.8x^2(t) + 5.7x^3(t)\end{aligned},$$

$$\begin{aligned}\boldsymbol{\theta} &= [\theta_1, \theta_2, \theta_3, \theta_4, \theta_5, \theta_6, \theta_7, \theta_8]^T \\ \boldsymbol{\theta} &= [a_1, a_2, c_1, c_2, c_3, b_2c_1, b_2c_2, b_2c_3]^T \\ \boldsymbol{\theta} &= [-1.00, 0.80, 2.80, -4.80, 5.70, 1.68, -2.88, 3.42]^T\end{aligned} \quad . \tag{4.9}$$

The step size is taken as 10^{-5} that is selected after performing a set of trials to obtain the best MSE after convergence. Same variations in noise variance σ^2, proportion of previous gradients α and fractional order fr are used as in case study 3, *i.e.*, $\sigma^2 = 0.01^2$, 0.05^2 and 0.1^2, $\alpha = 0.2, 0.4, 0.6$, and $fr = 0.25, 0.50, 0.75$.

The iterative convergence of the fitness function for first 10000 iterations is presented in Appendix 4.22, for all α and fr variations. It is seen from the results that proposed mFLMS method provides faster convergence than standard FLMS for identification of muscle model. It is also observed that convergence speed increases by increasing the value of α.

The number of iterations required for obtaining specific fitness value of 0.1 and 0.05 are given in Table 4.6 for all noise and α variations. It is seen that the standard FLMS algorithm requires 36239 and 153910 iterations for 0.1 and 0.05 fitness values respectively, while the respective iterations for mFLMS algorithm with $\alpha = 0.6$ are 19552 and 37559 for $\sigma^2 = 0.1^2$. It is inferred from the results that proposed mFLMS algorithm has faster convergence and requires less iterations for HCAR system representing stimulated muscle model.

The MSE values for estimation of muscle model are given in Appendix 4.23 and it is observed from the results presented that mFLMS method is accurate and convergent for all values of fractional orders and higher value of fractional order provides relatively better results.

The learning curves based on fitness (4.1) and MSE (4.2) performance measures are presented in Fig. 4.11 for $fr = 0.50$ and $\sigma^2 = 0.05^2$. It is observed that mFLMS algorithm is faster in convergence than standard FLMS for all values of α. It is inferred from the learning curves that proposed scheme is accurate and convergent for identification of electrically stimulated muscle model for all variations of α and fr.

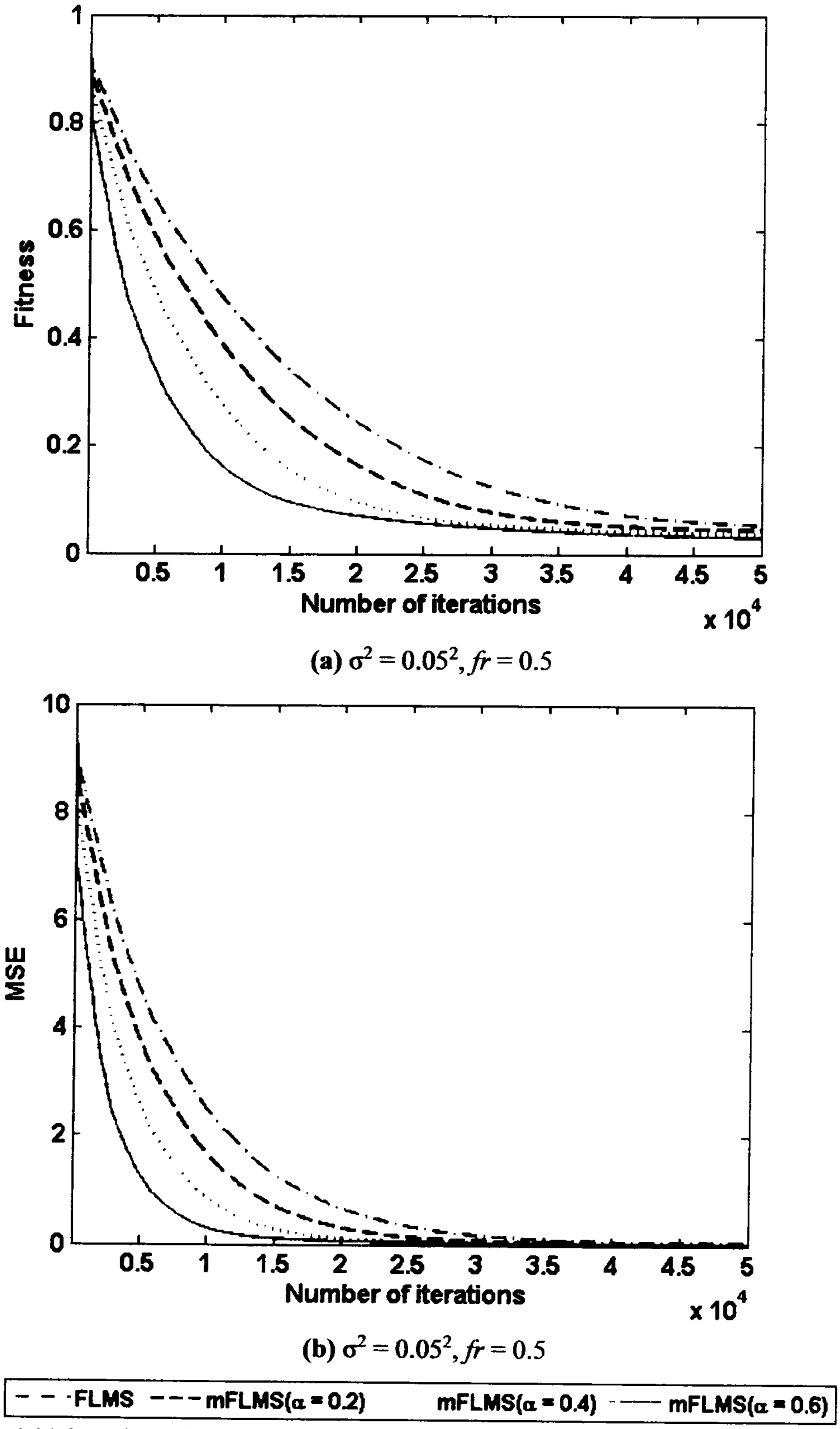

(a) $\sigma^2 = 0.05^2, fr = 0.5$

(b) $\sigma^2 = 0.05^2, fr = 0.5$

Fig. 4.11 Iterative adaptation of fitness and MSE against number of iterations in case study 6

Table 4.6 Performance comparison based on iterations required for specific fitness value in case study 6

Method	α	$\delta = 0.1$			$\delta = 0.05$		
		$\sigma^2 = 0.01^2$	$\sigma^2 = 0.05^2$	$\sigma^2 = 0.1^2$	$\sigma^2 = 0.01^2$	$\sigma^2 = 0.05^2$	$\sigma^2 = 0.1^2$
FLMS		36241	36239	36236	154142	154058	153910
mFLMS	**0.2**	28919	28918	28917	107743	107732	107731
mFLMS	**0.4**	23490	23491	23493	65031	65036	65043
mFLMS	**0.6**	19544	19549	19552	37515	37544	37559

4.9 Summary

In this chapter, proposed fractional adaptive algorithms were applied to different case studies of Hammerstein system identification and simulations results were presented in a variety of graphical illustrations. From case study 6, it was concluded that momentum FLMS provides better results in comparison with other proposed fractional adaptive algorithms. Finally, the momentum FLMS scheme is applied to parameter estimation problem of stimulated muscled model represented through HCAR structure.

Chapter 5.

Application to Power Signal Modeling

It is observed from the results of case studies presented in the last chapter that all the proposed variants of FLMS are accurate and convergent for identification of the Hammerstein systems. Moreover, the mFLMS algorithm is better than other proposed methods in terms of convergence. To further demonstrate the promising properties of the mFLMS algorithm, we consider another application based on signal modeling and parameter estimation of sinusoidal signals.

In this chapter, first an introduction to power signal modeling is presented, then identification model for parameter estimation of power signals is given. Finally, the proposed mFLMS algorithm is applied to parameter estimation of power signal having unknown amplitude and phase. The results obtained through mFLMS are compared with standard LMS, mLMS and FLMS algorithms to show the worth and effectiveness of the design method.

5.1 Introduction

Signal modeling and parameter estimation of sinusoidal signals are important for reliability assessment and quality monitoring of power systems. Frequency, as one of the parameters, is important to be estimated for harmonic measurement and compensation [121] and in phase lock loops for grid signal synchronization with system output [122]. The amplitude estimate is used in fault detection algorithms [123] and in under/over voltage protection algorithms [124]. The phase estimate is used in different scenarios such as PLL algorithms [125] and in the generation of control signals in a controller [126]. Recently, stochastic gradient based algorithms have been proposed for estimating the parameters of the sine combination signal modeling [127]. Before applying the proposed mFLMS to power signal, the identification model is given first.

5.2 Signal Modeling

Parameter estimation of the sinusoidal signals is very important as it helps in assessing the reliability of power systems. Here we consider a sampled multi-harmonic sinusoidal signal with different amplitudes and phase:

$$y(t)=\sum_{k=1}^{N} a_k\left(\sin t\omega_k+\phi_k\right)+\vartheta(t). \tag{5.1}$$

Using trigonometric identity, (5.1) can be represented as:

$$y(t)=\sum_{k=1}^{N} a_k\left(\sin t\omega_k \cos\phi_k+\cos t\omega_k \sin\phi_k\right)+\vartheta(t). \tag{5.2}$$

We assume that the frequency of the signal is known, then (5.2) can be written as:

$$y(t)=\sum_{k=1}^{N} b_k \sin t\omega_k+c_k \cos t\omega_k+\vartheta(t), \tag{5.3}$$

where

$$b_k=a_k \cos\phi_k \text{ and } c_k=a_k \sin\phi_k.$$

We will estimate parameters b_k and c_k since these can give us a_k and ϕ_k using relations:

$$a_k=\sqrt{b_k+c_k} \qquad \phi_k=\tan^{-1}\frac{c_k}{b_k}. \tag{5.4}$$

Defining the parameter vector $\boldsymbol{\theta}$ as:

$$\boldsymbol{\theta} = [b_1, c_1, b_2, c_2, \cdots, b_N, c_N]^T \in R^{2N}, \tag{5.5}$$

and the corresponding information vector as:

$$\boldsymbol{\psi}(t) = [\sin\omega_1 t, \cos\omega_1 t, \sin\omega_2 t, \cos\omega_2 t, \cdots, \sin\omega_N t, \cos\omega_N t]^T \in R^{2N}, \tag{5.6}$$

using equations (5.5) and (5.6) in (5.3), the identification model for power signals is same, as given in (2.8) for Hammerstein system identification.:

5.3 Modeling of power signals

To show the performance of the proposed algorithm, the mFLMS is applied to estimate magnitude and phase of a sinusoidal signal which is a combination of different sinusoidal harmonics having different amplitudes and phases. We compare its performance with standard FLMS, mLMS and LMS algorithms under different noise conditions. Consider the following combination of sine signals with four different frequencies [127]:

$$\begin{aligned} y(t) = {} & 1.8\sin(0.07t + 0.95) + 2.9\sin(0.5t + 0.8) + 4\sin(2t + 0.76) \\ & + 2.5\sin(1.6t + 1.1) + \vartheta(t) \end{aligned} \tag{5.7}$$

The parameter vector (amplitude and phase) of the power signal is:

$$\boldsymbol{\theta} = [a_1, a_2, a_3, a_4, \phi_1, \phi_2, \phi_3, \phi_4]^T = [1.8, 2.9, 4, 2.5, 0.95, 0.8, 0.76, 1.1]^T. \tag{5.8}$$

The mFLMS and mLMS algorithms are investigated for three different values of α (proportion of previous gradients), *i.e.,* [0.2, 0.5, 0.8], as only these two algorithms have momentum terms. The step size for all the algorithms is selected empirically after performing a set of trials to achieve the best MSE value after the convergence, *i.e.,* 10^{-3}. In case of fractional order algorithms, the values for both step size parameters are same, *i.e.,* $\mu_1 = \mu_f = \mu$. For higher values of step size, algorithms either did not converge smoothly or had higher value of MSE. The value of α was also chosen on the similar basis. It is observed that the convergence speed of the mFLMS method increases by increasing the value of α but at the cost of steady state performance, *i.e.*, the higher value of α provides faster convergence while lower value gives better steady state performance. The fractional order based methods are studied for three different fractional orders *i.e.*, $fr = 0.25$, 0.50 and 0.75. All the algorithms are examined for three values of Gaussian noise variance *i.e.*, $\sigma^2 = 0.3^2$, 0.6^2 and 0.9^2. The adaptation process is performed for 4000 iterations.

The learning efficiency of the algorithms for different values of parameters is shown in Figs.5.1 and 5.2. All the subfigures of Figs. 5.1 and 5.2 show plots of fitness function against the number of iterations for fractional order $fr = 0.5$. Detailed results for other values of fr are given in the tables. The comparison of the proposed mFLMS algorithm with standard LMS, mLMS and FLMS methods for $\alpha = 0.2$, 0.5 and 0.8 are given in Fig. 5.1 (a), (b) and (c) respectively for noise variance $\sigma^2 = 0.3^2$, while the respective plots in case of $\sigma^2 = 0.9^2$ are presented in Fig. 5.2 (a), (b) and (c). It is observed that convergence of mLMS and mFLMS methods is faster than their counterparts, *i.e.*, standard LMS and FLMS algorithms, and by increasing the value of α, the momentum versions provide faster convergence. It is also seen that the proposed mFLMS algorithm outperforms all other algorithms in terms of convergence for different variations in parameter values.

The performance of the proposed scheme is also evaluated for initial convergence rate and results of fitness adaptation for first 1000 iterations are presented in Appendices 5.1–5.3 for $\sigma^2 = 0.3^2$, 0.6^2 and 0.9^2 respectively, for various α and fractional order values. It is seen from the results presented in Appendices 5.1–5.3 that initial convergence of mFLMS is much faster than standard adaptive strategies and rate of convergence increases by increasing the proportion of previous gradients (α).

The performance of the proposed mFLMS algorithm is further verified through MSE metric. The results obtained through mFLMS are compared with standard adaptive schemes and given in Table 5.1 for $\sigma^2 = 0.3^2$, while, for $\sigma^2 = 0.6^2$ and 0.9^2 the results are presented in Appendices 5.4 and 5.5 respectively, for different variations in α and fractional order. It is observed that all algorithms are accurate and convergent but accuracy of the methods decreases by increasing noise variance. It is seen that fractional adaptive algorithms *i.e.,* FLMS and mFLMS remain stable for all variations of fractional order and not much difference in accuracy is observed among different fractional orders. However, higher value of fractional order *i.e.,* $fr = 0.75$ gives relatively better results. It can be observed from the results in Appendices 5.1 –5.5 and Table 5.1 that mFLMS algorithm provides faster convergence for higher proportion of previous gradients *i.e.,* $\alpha = 0.8$, while it gives better steady state performance for lower value of alpha *i.e.,* $\alpha = 0.2$. Thus, the middle value *i.e.,* $\alpha = 0.5$ seems to be an appropriate choice that is a good compromise between faster convergence and better steady state performance.

The curve fitting plot for the sinusoidal signal by mFLMS for $\alpha = 0.2$, $fr = 0.5$ and $\sigma^2 = 0.6^2$, is given in Fig. 5.3. It can be noticed from the figure that the proposed mFLMS algorithm accurately follows the original power signal with high precision which validates the correctness and effectiveness of the proposed method.

Table 5.1 Performance comparison based on MSE for $\sigma^2 = 0.3^2$ in power signal estimation

Method	α	**Adaptive Parameters**								**MSE**
		θ_1	θ_2	θ_3	θ_4	θ_5	θ_6	θ_7	θ_8	
LMS		1.6241	2.5608	3.5767	2.1920	0.8940	0.8152	0.7694	1.1025	5.29E-02
mLMS	**0.2**	1.6890	2.6954	3.7477	2.3121	0.9171	0.8099	0.7643	1.1009	1.93E-02
mLMS	**0.5**	1.7662	2.8561	3.9541	2.4563	0.9410	0.8037	0.7584	1.0989	8.97E-04
mLMS	**0.8**	1.7814	2.9025	4.0161	2.4991	0.9380	0.7996	0.7563	1.0981	9.67E-05
FLMS (*fr* = 0.25)		1.7684	2.8862	4.0094	2.4777	0.9416	0.8025	0.7565	1.1048	2.36E-04
mFLMS (*fr* = 0.25)	**0.2**	1.7776	2.8991	4.0161	2.4944	0.9472	0.8009	0.7563	1.0996	1.02E-04
mFLMS (*fr* = 0.25)	**0.5**	1.7794	2.9019	4.0181	2.4987	0.9394	0.7992	0.7567	1.0987	1.11E-04
mFLMS (*fr* = 0.25)	**0.8**	1.7755	2.9046	4.0242	2.5054	0.9209	0.7985	0.7632	1.1003	2.62E-04
FLMS (*fr* = 0.75)		1.7693	2.8730	3.9853	2.4696	0.9418	0.8032	0.7574	1.1010	3.63E-04
mFLMS (*fr* = 0.75)	**0.2**	1.7792	2.8948	4.0071	2.4918	0.9466	0.8017	0.7566	1.0990	7.57E-05
mFLMS (*fr* = 0.75)	**0.5**	1.7812	2.9016	4.0173	2.4980	0.9401	0.7999	0.7563	1.0985	9.63E-05
mFLMS (*fr* = 0.75)	**0.8**	1.7778	2.9051	4.0193	2.5032	0.9220	0.7981	0.7596	1.0997	2.11E-04
True Values		1.8000	2.9000	4.0000	2.5000	0.9500	0.8000	0.7600	1.1000	0

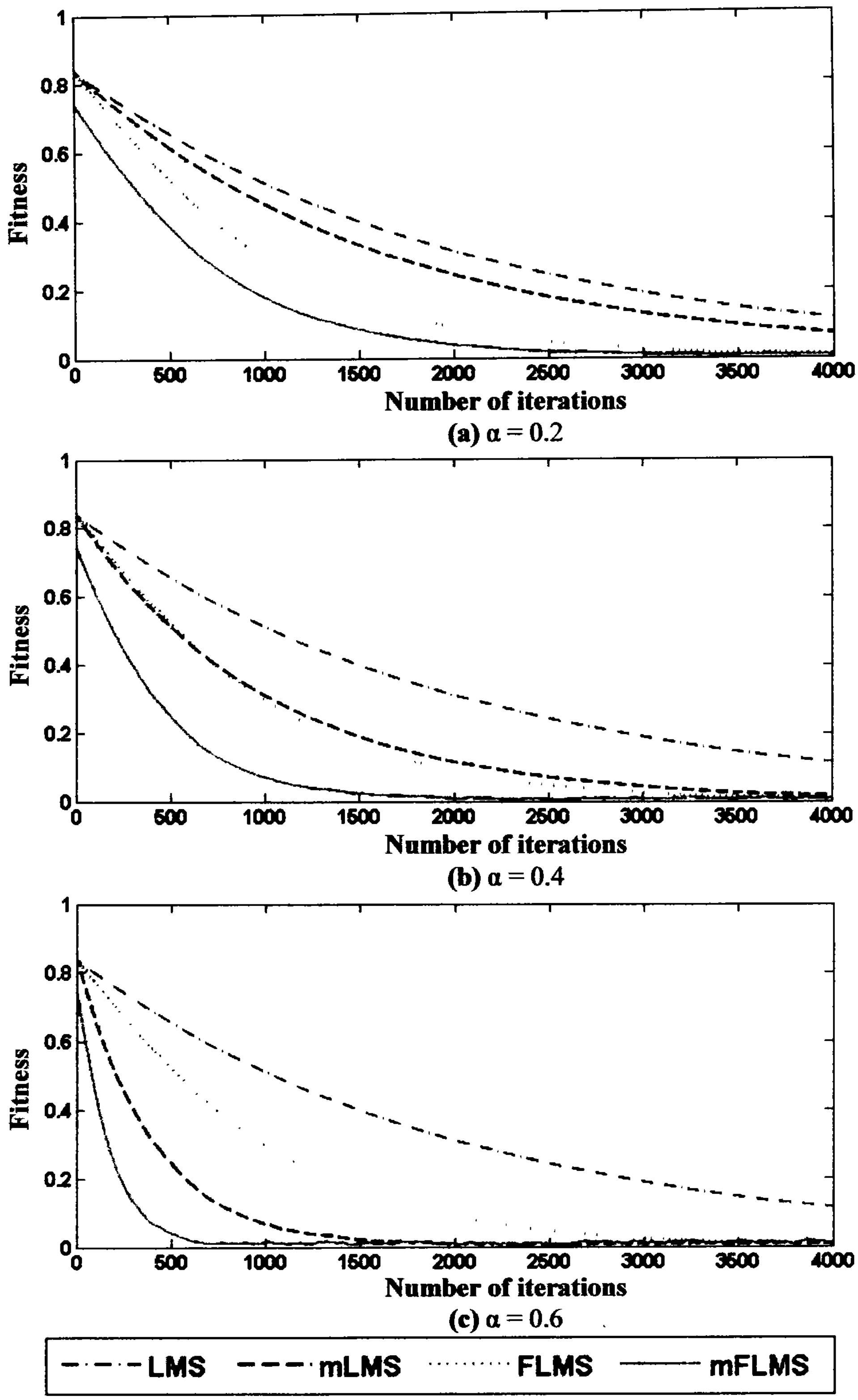

Fig. 5.1 Iterative adaptation of fitness function for $\sigma^2 = 0.3^2$ in of power signal estimation

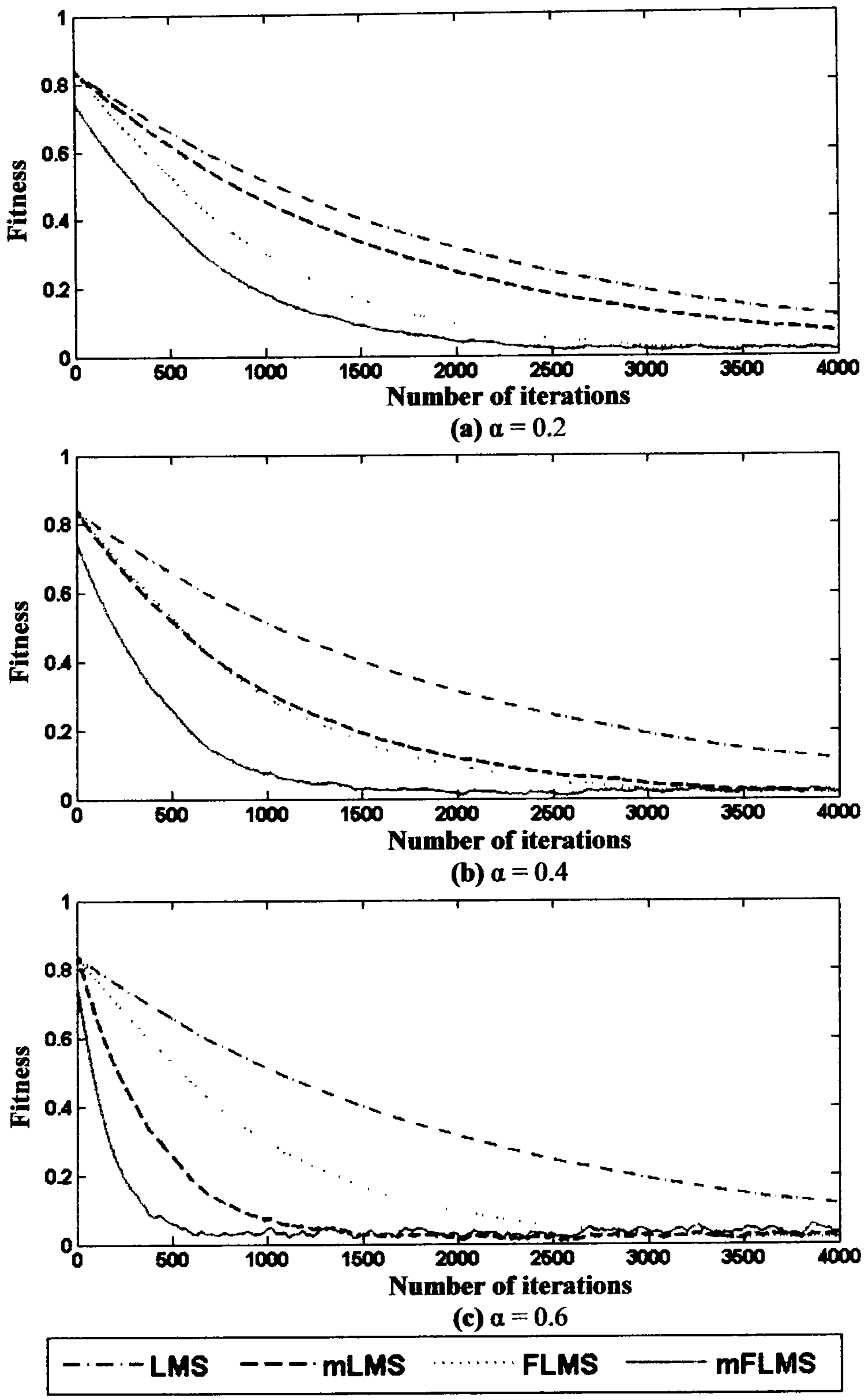

Fig. 5.2 Iterative adaptation of fitness function for $\sigma^2 = 0.9^2$ in power signal estimation

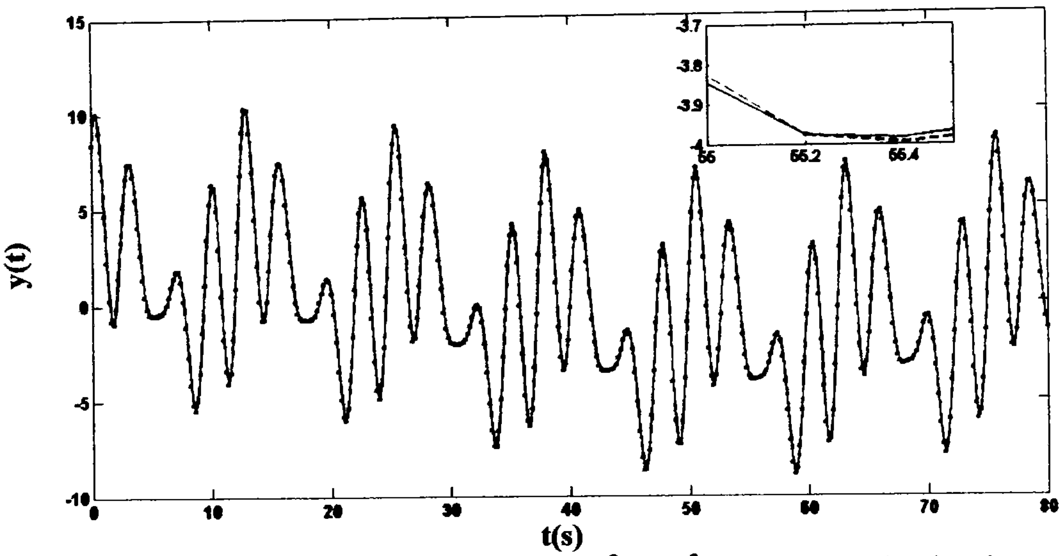

Fig. 5.3 Curve fitting for $\alpha = 0.2$, $fr = 0.5$ and $\sigma^2 = 0.6^2$ in power signal estimation

5.4 Summary

This chapter presented the application of proposed momentum FLMS algorithm to parameter estimation of power signals with unknown amplitude and phase. The results obtained through the momentum FLMS were also compared with standard FLMS, LMS and mLMS algorithms to show the worth and effectiveness of the proposed scheme.

Chapter 6.

Conclusion and Future Work

In this chapter, conclusions drawn for the proposed schemes are presented based on the material presented in last chapters. Few future research directions are also mentioned for researchers interested to work in this field.

6.1 Conclusions

Following are the conclusions drawn from this study:

- The present work may consider to be an advancement in designing an accurate, alternate, and convergent computing mechanism based on deep rooted fractional calculus concepts for nonlinear system identification.
- The mathematical concepts and theories of fractional order calculus are exploited to develop modified FLMS-1 and 2, normalized FLMS, sliding window based FLMS and momentum FLMS algorithms.
- The computational cost of FLMS is reduced in MFLMS-1 and 2, convergence made smoother in NFLMS, while SW-FLMS and mFLMS increases the convergence speed of standard FLMS by effectively utilizing the previous information.
- The correctness of the designed fractional adaptive algorithms is established by efficiently optimizing the parameters of different nonlinear system identification models based on Hammerstein structure.

- The FLMS, MFLMS-1, MFLMS-2, NFLMS, SW-FLMS and MFLMS algorithms estimated the parameters of HCAR system with the MSE values of 3.37×10^{-04}, 4.12×10^{-04}, 2.28×10^{-04}, 9.67×10^{-05}, 1.82×10^{-04} and 6.50×10^{-05} respectively for $\sigma^2 = 0.5^2$. The mFLMS is better among all other variants in terms of convergence speed and accuracy.
- The effective application of proposed momentum FLMS for accurate parameter estimation of power signals with unknown amplitude and phase further establishes the worth and efficacy of the methods.
- The design methods are evaluated for different values of fractional order and it is observed that the proposed fractional methods remain convergent for all fractional orders.
- The fractional adaptive methods are accurate and convergent for different noise levels ranging from low to high, which establish their robustness. However, optimization capability of all proposed algorithms decreases with an increase in noise variance.
- The consistency and reliability of the design methods is proven through the results of statistical analyses based on sufficient independent runs of the algorithms for different performance measures including mean square error, variance account for and Nash-Sutcliffe efficiency.
- Besides the accurate identification, the other advantages of proposed fractional adaptive strategies include, availability of more controlling parameters, wider applicability domain and flexibility in the design procedure based on fractional integrals or derivatives.

6.2 Future Work

Following are few research directions for future development of work in this domain:

- The proposed algorithms may be exploited to address parameter identification problem of input and output nonlinear systems, including Hammerstein CARAR, CARARMA, Box-Jenkins and Weiner models etc.
- The design methods can also be applied to solve other signal processing problems, like, image denoising, image classification, noise removal from biomedical signals, channel estimation, channel equalization and adaptive beamforming.
- This study considered to be a step further for designing new fractional adaptive algorithms such as fractional recursive least square method, fractional kalman filtering approach, fractional diffusion, p-power, leaky and block LMS algorithms etc.
- One may explore the application of latest fractional derivative operators to develop new fractional order adaptive strategies for problems arising in communication, signal processing and control systems.

BIBLIOGRAPHY

[1] S. A. Billings, *Nonlinear System Identification : NARMAX Methods in the Time, Frequency, and Spatio-Temporal Domains.* Wiley, 2013.

[2] B. Zhang and S. A. Billings, "Identification of continuous-time nonlinear systems: The nonlinear difference equation with moving average noise (NDEMA) framework," *Mechanical Systems and Signal Processing*, vol. 60–61, pp. 810–835, Aug. 2015.

[3] Y. Wang and F. Ding, "Parameter Estimation Algorithms for Hammerstein–Wiener Systems With Autoregressive Moving Average Noise," *Journal of Computational and Nonlinear Dynamics*, vol. 11, no. 3, p. 31012, 2015.

[4] I. W. Hunter and M. J. Korenberg, "The identification of nonlinear biological systems: Wiener and Hammerstein cascade models," *Biological Cybernetics*, vol. 55, no. 2–3, pp. 135–144.

[5] K. P. Fruzzetti, A. Palazoğlu, and K. A. McDonald, "Nolinear model predictive control using Hammerstein models," *Journal of Process Control*, vol. 7, no. 1, pp. 31–41, Feb. 1997.

[6] J. Zhao, X. Ma, S. Zhao, and J. Fei, "Hammerstein identification of supercharged boiler superheated steam pressure using Laguerre-Fuzzy model," *International Journal of Heat and Mass Transfer*, vol. 70, pp. 33–39, Mar. 2014.

[7] M. Rébillat, R. Hennequin, É. Corteel, B. F. G. G. Katz, M. Rbillat, R. Hennequin, T. Corteel, and B. F. G. G. Katz, "Identification of cascade of Hammerstein models for the description of nonlinearities in vibrating devices," *Journal of Sound and Vibration*, vol. 330, no. 5, pp. 1018–1038, Feb. 2011.

[8] C. M. Holcomb, R. A. De Callafon, and R. R. Bitmead, "Closed-Loop Identification of Hammerstein Systems with Application to Gas Turbines," *IFAC Proceedings Volumes*, vol. 47, no. 3, pp. 493–498, Jan. 2014.

[9] T. Liang and V. Dinavahi, "Real-Time System-on-Chip Emulation of Electro-Thermal Models for Power Electronic Devices Via Hammerstein Configuration," *IEEE Journal of Emerging and Selected Topics in Power Electronics*, pp. 1–1, 2017.

[10] O. Ait Maatallah, A. Achuthan, K. Janoyan, and P. Marzocca, "Recursive wind speed forecasting based on Hammerstein Auto-Regressive model," *Applied Energy*, vol. 145, pp. 191–197, May 2015.

[11] S. Boubaker, "Identification of nonlinear Hammerstein system using mixed integer-real coded particle swarm optimization: application to the electric daily peak-load forecasting," *Nonlinear Dynamics*, vol. 90, no. 2, 2017.

[12] X. Wang and F. Ding, "Modelling and multi-innovation parameter identification for Hammerstein nonlinear state space systems using the filtering technique," *Mathematical and Computer Modelling of Dynamical Systems*, vol. 22, no. 2, pp. 113–140, Mar. 2016.

[13] Y. Mao and F. Ding, "Multi-innovation stochastic gradient identification for Hammerstein controlled autoregressive autoregressive systems based on the filtering technique," *Nonlinear Dynamics*, vol. 79, no. 3, pp. 1745–1755, Feb. 2015.

[14] D. Wang, F. Ding, and Y. Chu, "Data filtering based recursive least squares algorithm for Hammerstein systems using the key-term separation principle," *Information Sciences*, vol. 222, pp. 203–212, Feb. 2013.

[15] Y. Mao and F. Ding, "A novel data filtering based multi-innovation stochastic gradient algorithm for Hammerstein nonlinear systems," *Digital Signal Processing*, vol. 46, pp. 215–225, Nov. 2015.

[16] D. Wang, "Hierarchical parameter estimation for a class of MIMO Hammerstein systems based on the reframed models," *Applied Mathematics Letters*, vol. 57, pp. 13–19, Jul. 2016.

[17] H. Chen and F. Ding, "Hierarchical Least Squares Identification for Hammerstein Nonlinear Controlled Autoregressive Systems," *Circuits, Systems, and Signal Processing*, vol. 34, no. 1, pp. 61–75, Jan. 2015.

[18] Y. Mao and F. Ding, "A novel parameter separation based identification algorithm for Hammerstein systems," *Applied Mathematics Letters*, vol. 60, pp. 21–27, Oct. 2016.

[19] D. Baleanu, J. Machado, and A. Luo, *Fractional dynamics and control*. Springer Science & Business Media, 2011.

[20] M. D. Ortigueira, C. M. Ionescu, J. T. Machado, and J. J. Trujillo, "Fractional signal processing and applications," *Signal Processing*, vol. 107, no. 107, p. 197, Feb. 2015.

[21] Y. Luo, Y. Q. Chen, C. Y. Wang, and Y. G. Pi, "Tuning fractional order proportional integral controllers for fractional order systems," *Journal of Process Control*, vol. 20, no. 7, pp. 823–831, Aug. 2010.

[22] S. Zheng, X. Tang, and B. Song, "Graphical tuning method for non-linear fractional-order PID-type controllers free of analytical model," *Transactions of the Institute of Measurement and Control*, vol. 38, no. 12, pp. 1442–1459, Dec. 2016.

[23] Y. Chen, D. Xue, and A. Visioli, "Guest Editorial for Special Issue on Fractional Order Systems and Controls," *IEEE/CAA JOURNAL OF AUTOMATICA SINICA*, vol. 3, no. 3, 2016.

[24] A. Cordero, E. Gómez, and J. R. Torregrosa, "Efficient High-Order Iterative Methods for Solving Nonlinear Systems and Their Application on Heat Conduction Problems," *Complexity*, vol. 2017, pp. 1–11, 2017.

[25] F. Khani and M. Haeri, "Robust model predictive control of nonlinear processes represented by Wiener or Hammerstein models," *Chemical Engineering Science*, vol. 129, pp. 223–231, Jun. 2015.

[26] Y. Tang, C. Bu, M. Liu, L. Zhang, and Q. Lian, "Application of ELM–Hammerstein model to the identification of solid oxide fuel cells," *Neural Computing and Applications*, Jul. 2016.

[27] Z. Zou, D. Zhao, X. Liu, Y. Guo, C. Guan, W. Feng, and N. Guo, "Pole-placement self-tuning control of nonlinear Hammerstein system and its application to pH process control," *Chinese Journal of Chemical Engineering*, vol. 23, no. 8, pp. 1364–1368, Aug. 2015.

[28] Q. Zhang, Q. Wang, and G. Li, "Nonlinear modeling and predictive functional control of Hammerstein system with application to the turntable servo system," *Mechanical Systems and Signal Processing*, vol. 72–73, pp. 383–394, May 2016.

[29] N. Togun, S. Baysec, and T. Kara, "Nonlinear modeling and identification of a spark ignition engine torque," *Mechanical Systems and Signal Processing*, vol. 26, pp. 294–304, 2012.

[30] K. Jalaleddini and R. E. Kearney, "Subspace Identification of SISO Hammerstein Systems: Application to Stretch Reflex Identification," *IEEE Transactions on Biomedical Engineering*, vol. 60, no. 10, pp. 2725–2734, Oct. 2013.

[31] D. Aryani, L. Wang, and T. Patikirikorala, "On identification of Hammerstein and Wiener model with application to virtualised software system," *International Journal of Systems Science*, vol. 48, no. 6, pp. 1146–1161, Apr. 2017.

[32] F. Le, I. Markovsky, C. T. Freeman, and E. Rogers, "Recursive identification of Hammerstein systems with application to electrically stimulated muscle," *Control Engineering Practice*, vol. 20, no. 4, pp. 386–396, Apr. 2012.

[33] H. Hu and R. Ding, "Least squares based iterative identification algorithms for input nonlinear controlled autoregressive systems based on the auxiliary model," *Nonlinear Dynamics*, vol. 76, no. 1, pp. 777–784, Apr. 2014.

[34] Y. Xiao, G. Song, Y. Liao, and R. Ding, "Multi-innovation stochastic gradient parameter estimation for input nonlinear controlled autoregressive models," *International Journal of Control, Automation and Systems*, vol. 10, no. 3, pp. 639–643, Jun. 2012.

[35] F. Ding and T. Chen, "Identification of Hammerstein nonlinear ARMAX systems,"

Automatica, vol. 41, no. 9, pp. 1479–1489, Sep. 2005.

[36] F. Ding, Y. Shi, and T. Chen, "Gradient-Based Identification Methods for Hammerstein Nonlinear ARMAX Models," *Nonlinear Dynamics*, vol. 45, no. 1–2, pp. 31–43, Jul. 2006.

[37] K. Narendra and P. Gallman, "An iterative method for the identification of nonlinear systems using a Hammerstein model," *IEEE Transactions on Automatic Control*, vol. 11, no. 3, pp. 546–550, Jul. 1966.

[38] S. A. Billings and S. Y. Fakhouri, "Non-linear system identification using the Hammerstein model," *International Journal of Systems Science*, vol. 10, no. 5, pp. 567–578, May 1979.

[39] W. Greblicki and M. Pawlak, "Identification of discrete Hammerstein systems using kernel regression estimates," *IEEE Transactions on Automatic Control*, vol. 31, no. 1, pp. 74–77, Jan. 1986.

[40] M. Pawlak, "On the series expansion approach to the identification of Hammerstein systems," *IEEE Transactions on Automatic Control*, vol. 36, no. 6, pp. 763–767, Jun. 1991.

[41] Zi-Qiang Lang, "A nonparametric polynomial identification algorithm for the Hammerstein system," *IEEE Transactions on Automatic Control*, vol. 42, no. 10, pp. 1435–1441, 1997.

[42] J. Voros, "Recursive identification of hammerstein systems with discontinuous nonlinearities containing dead-zones," *IEEE Transactions on Automatic Control*, vol. 48, no. 12, pp. 2203–2206, Dec. 2003.

[43] H.-F. Chen, "Pathwise Convergence of Recursive Identification Algorithms for Hammerstein Systems," *IEEE Transactions on Automatic Control*, vol. 49, no. 10, pp. 1641–1649, Oct. 2004.

[44] W.-X. Zhao and H.-F. Chen, "Recursive Identification for Hammerstein System With ARX Subsystem," *IEEE Transactions on Automatic Control*, vol. 51, no. 12, pp. 1966–1974, Dec. 2006.

[45] H.-X. Li, "Identification of Hammerstein models using genetic algorithms," *IEE Proceedings - Control Theory and Applications*, vol. 146, no. 6, pp. 499–504, Nov. 1999.

[46] X. Hong and S. Chen, "The system identification and control of Hammerstein system using non-uniform rational B-spline neural network and particle swarm optimization," *Neurocomputing*, vol. 82, pp. 216–223, Apr. 2012.

[47] S. J. Nanda, G. Panda, and B. Majhi, "Improved identification of Hammerstein

plants using new CPSO and IPSO algorithms," *Expert Systems with Applications*, vol. 37, no. 10, pp. 6818–6831, Oct. 2010.

[48] J. Sun and X. Liu, "A novel APSO-aided maximum likelihood identification method for Hammerstein systems," *Nonlinear Dynamics*, vol. 73, no. 1–2, pp. 449–462, Jul. 2013.

[49] A. Gotmare, R. Patidar, and N. V. George, "Nonlinear system identification using a cuckoo search optimized adaptive Hammerstein model," *Expert Systems with Applications*, vol. 42, no. 5, pp. 2538–2546, Apr. 2015.

[50] P. S. Pal, R. Kar, D. Mandal, and S. P. Ghoshal, "A hybrid backtracking search algorithm with wavelet mutation-based nonlinear system identification of Hammerstein models," *Signal, Image and Video Processing*, vol. 11, no. 5, pp. 929–936, Jul. 2017.

[51] E. Cuevas, P. Díaz, O. Avalos, D. Zaldívar, and M. Pérez-Cisneros, "Nonlinear system identification based on ANFIS-Hammerstein model using Gravitational search algorithm," *Applied Intelligence*, pp. 1–22, Jun. 2017.

[52] D. Wang and F. Ding, "Extended stochastic gradient identification algorithms for Hammerstein–Wiener ARMAX systems," *Computers & Mathematics with Applications*, vol. 56, no. 12, pp. 3157–3164, Dec. 2008.

[53] Dong-Qing Wang, Hua-Bo Liu, and Feng Ding, "Highly Efficient Identification Methods for Dual-Rate Hammerstein Systems," *IEEE Transactions on Control Systems Technology*, vol. 23, no. 5, pp. 1952–1960, Sep. 2015.

[54] F. Ding, X. P. Liu, and G. Liu, "Identification methods for Hammerstein nonlinear systems," *Digital Signal Processing*, vol. 21, no. 2, pp. 215–238, Mar. 2011.

[55] J. Chen, X. Wang, and R. Ding, "Gradient based estimation algorithm for Hammerstein systems with saturation and dead-zone nonlinearities," *Applied Mathematical Modelling*, vol. 36, no. 1, pp. 238–243, Jan. 2012.

[56] F. Ding and T. Chen, "Performance analysis of multi-innovation gradient type identification methods," *Automatica*, vol. 43, no. 1, pp. 1–14, Jan. 2007.

[57] J. Chen, L. Lv, and R. Ding, "Multi-innovation stochastic gradient algorithms for dual-rate sampled systems with preload nonlinearity," *Applied Mathematics Letters*, vol. 26, no. 1, pp. 124–129, Jan. 2013.

[58] Y. Liu, Y. Xiao, and X. Zhao, "Multi-innovation stochastic gradient algorithm for multiple-input single-output systems using the auxiliary model," *Applied Mathematics and Computation*, vol. 215, no. 4, pp. 1477–1483, Oct. 2009.

[59] Er-Wei Bai and Minyue Fu, "A blind approach to Hammerstein model

identification," *IEEE Transactions on Signal Processing*, vol. 50, no. 7, pp. 1610–1619, Jul. 2002.

[60] D. Wang, Y. Chu, G. Yang, and F. Ding, "Auxiliary model based recursive generalized least squares parameter estimation for Hammerstein OEAR systems," *Mathematical and Computer Modelling*, vol. 52, no. 1–2, pp. 309–317, Jul. 2010.

[61] D. Wang, Y. Chu, and F. Ding, "Auxiliary model-based RELS and MI-ELS algorithm for Hammerstein OEMA systems," *Computers & Mathematics with Applications*, vol. 59, no. 9, pp. 3092–3098, May 2010.

[62] F. Ding, Y. Shi, and T. Chen, "Auxiliary model-based least-squares identification methods for Hammerstein output-error systems," *Systems & Control Letters*, vol. 56, no. 5, pp. 373–380, May 2007.

[63] F. Ding, "Hierarchical multi-innovation stochastic gradient algorithm for Hammerstein nonlinear system modeling," *Applied Mathematical Modelling*, vol. 37, no. 4, pp. 1694–1704, Feb. 2013.

[64] D. Wang and F. Ding, "Hierarchical Least Squares Estimation Algorithm for Hammerstein–Wiener Systems," *IEEE Signal Processing Letters*, vol. 19, no. 12, pp. 825–828, Dec. 2012.

[65] J. Sabatier, O. P. Agrawal, and J. A. T. Machado, Eds., *Advances in Fractional Calculus*. Dordrecht: Springer Netherlands, 2007.

[66] I. Podlubny, *Fractional Differential Equations: An Introduction to Fractional Derivatives, Fractional Differential Equations, to Methods of Their Solution and Some of Their Applications*. 1998.

[67] J. T. Machado, V. Kiryakova, and F. Mainardi, "Recent history of fractional calculus," *Communications in Nonlinear Science and Numerical Simulation*, vol. 16, no. 3, pp. 1140–1153, Mar. 2011.

[68] B. M. Vinagre, I. Petráš, I. Podlubny, and Y. Q. Chen, "Using Fractional Order Adjustment Rules and Fractional Order Reference Models in Model-Reference Adaptive Control," *Nonlinear Dynamics*, vol. 29, no. 1/4, pp. 269–279, 2002.

[69] F. Ge, Y. Chen, and C. Kou, "Regional controllability analysis of fractional diffusion equations with Riemann–Liouville time fractional derivatives," *Automatica*, vol. 76, pp. 193–199, Feb. 2017.

[70] M. D. Ortigueira, "Fractional discrete-time linear systems," in *1997 IEEE International Conference on Acoustics, Speech, and Signal Processing*, vol. 3, pp. 2241–2244.

[71] M. D. Ortigueira, "Introduction to fractional linear systems. Part 2: Discrete-time

case," *IEE Proceedings - Vision, Image and Signal Processing*, vol. 147, no. 1, pp. 71–78, Feb. 2000.

[72] M. D. Ortigueira and J. A. T. Machado, "Fractional signal processing and applications," *Signal Processing*, pp. 2285–2286, 2003.

[73] M. D. Ortigueira and J. T. Machado, "Fractional calculus applications in signals and systems," *Signal Processing*, vol. 86, no. 10, pp. 2503–2504, 2006.

[74] R. Zahoor and I. Qureshi, "A modified least mean square algorithm using fractional derivative and its application to system identification," *European Journal of Scientific Research*, vol. 35, no. 1, pp. 14–21, 2009.

[75] M. A. Z. Raja and N. I. Chaudhary, "Adaptive strategies for parameter estimation of Box–Jenkins systems," *IET Signal Processing*, vol. 8, no. 9, pp. 968–980, Dec. 2014.

[76] B. Shoaib, I. M. Qureshi, Ihsanulhaq, and Shafqatullah, "A modified fractional least mean square algorithm for chaotic and nonstationary time series prediction," *Chinese Physics B*, vol. 23, no. 3, p. 30502, Mar. 2014.

[77] S. Khan, M. Usman, I. Naseem, R. Togneri, and M. Bennamoun, "VP-FLMS: A Novel Variable Power Fractional LMS Algorithm," in *2017 Ninth International Conference on Ubiquitous and Future Networks (ICUFN)*, 2017, pp. 290–295.

[78] J. Ahmad, M. Usman, S. Khan, I. Naseem, and H. J. Syed, "RVP-FLMS: A robust variable power fractional LMS algorithm," in *2016 6th IEEE International Conference on Control System, Computing and Engineering (ICCSCE)*, 2016, pp. 494–497.

[79] J. Ahmad, S. Khan, M. Usman, I. Naseem, M. Moinuddin, and H. J. Syed, "FCLMS: Fractional complex LMS algorithm for complex system identification," in *2017 IEEE 13th International Colloquium on Signal Processing & its Applications (CSPA)*, 2017, pp. 39–43.

[80] N. I. Chaudhary, M. A. Z. Raja, M. S. Aslam, and N. Ahmed, "Novel generalization of Volterra LMS algorithm to fractional order with application to system identification," *Neural Computing and Applications*, vol. 29, no. 6, pp. 41–58, Mar. 2018.

[81] N. I. Chaudhary, M. S. Aslam, and M. A. Z. Raja, "Modified Volterra LMS algorithm to fractional order for identification of Hammerstein non-linear system," *IET Signal Processing*, vol. 11, no. 8, pp. 975–985, Oct. 2017.

[82] S. Cheng, Y. Wei, Y. Chen, Y. Li, and Y. Wang, "An innovative fractional order LMS based on variable initial value and gradient order," *Signal Processing*, vol. 133, pp. 260–269, Apr. 2017.

[83] S. Cheng, Y. Wei, Y. Chen, S. Liang, and Y. Wang, "A universal modified LMS algorithm with iteration order hybrid switching," *ISA Transactions*, vol. 67, pp. 67–75, Mar. 2017.

[84] S. Cheng, Y. Wei, Y. Chen, X. LI, and Y. Wang, "A Novel Fractional Order Normalized LMS Algorithm with Direction Optimization," *IFAC-PapersOnLine*, vol. 49, no. 9, pp. 180–185, Jan. 2016.

[85] Y. Yang, B. Yang, and M. Niu, "Spline adaptive filter with fractional-order adaptive strategy for nonlinear model identification of magnetostrictive actuator," *Nonlinear Dynamics*, vol. 90, no. 3, pp. 1647–1659, Nov. 2017.

[86] F. Kretschmer and B. Lewis, "An Improved Algorithm for Adaptive Processing," *IEEE Transactions on Aerospace and Electronic Systems*, vol. AES-14, no. 1, pp. 172–177, Jan. 1978.

[87] Y. Tan, Z. He, and B. Tian, "A Novel Generalization of Modified LMS Algorithm to Fractional Order," *IEEE Signal Processing Letters*, vol. 22, no. 9, pp. 1244–1248, Sep. 2015.

[88] Y. Pu, J. Zhou, Y. Zhang, and N. Zhang, "Fractional extreme value adaptive training method: Fractional steepest descent approach," *IEEE Transactions on Neural Networks and Learning Systems*, vol. 26, no. 4, pp. 653–662, 2015.

[89] Y. Chen, Q. Gao, Y. Wei, and Y. Wang, "Study on fractional order gradient methods," *Applied Mathematics and Computation*, vol. 314, pp. 310–321, Dec. 2017.

[90] M. A. Z. Raja and N. I. Chaudhary, "Two-stage fractional least mean square identification algorithm for parameter estimation of CARMA systems," *Signal Processing*, vol. 107, pp. 327–339, Feb. 2015.

[91] N. I. Chaudhary and M. A. Z. Raja, "Design of fractional adaptive strategy for input nonlinear Box–Jenkins systems," *Signal Processing*, vol. 116, pp. 141–151, Nov. 2015.

[92] S. M. Shah, "Riemann–Liouville operator-based fractional normalised least mean square algorithm with application to decision feedback equalisation of multipath channels," *IET Signal Processing*, vol. 10, no. 6, pp. 575–582, Aug. 2016.

[93] S. M. Shah, R. Samar, S. M. R. Naqvi, and J. A. Chambers, "Fractional order constant modulus blind algorithms with application to channel equalisation," *Electronics Letters*, vol. 50, no. 23, pp. 1702–1704, Oct. 2014.

[94] S. M. Shah, R. Samar, N. M. Khan, and M. A. Z. Raja, "Design of fractional-order variants of complex LMS and NLMS algorithms for adaptive channel equalization," *Nonlinear Dynamics*, vol. 88, no. 2, pp. 839–858, Apr. 2017.

[95] S. K. Dubey and N. K. Rout, "FLMS algorithm for acoustic echo cancellation and its comparison with LMS," in *2012 1st International Conference on Recent Advances in Information Technology (RAIT)*, 2012, pp. 852–856.

[96] M. Geravanchizadeh and S. Ghalamiosgouei, "Speech enhancement by modified convex combination of fractional adaptive filtering," *Iranian Journal of Electrical & Electronic Engineering*, vol. 10, no. 4, pp. 256–266, 2014.

[97] S. Ghalami Osgouei and M. Geravanchizadeh, "Speech enhancement using convex combination of fractional least-mean-squares algorithm," in *2010 5th International Symposium on Telecommunications*, 2010, pp. 869–872.

[98] M. Geravanchizadeh and S. Ghalamiosgouei, "A New Fractional Adaptive Filtering Method and its Application in Speech Enhancement," *International Journal of Information & Communication Technology Research*, vol. 7, no. 2, pp. 1–9, Jun. 2015.

[99] B. Shoaib, I. M. Qureshi, Shafqatullah, and Ihsanulhaq, "Adaptive step-size modified fractional least mean square algorithm for chaotic time series prediction," *Chinese Physics B*, vol. 23, no. 5, p. 50503, May 2014.

[100] S. Khan, J. Ahmad, I. Naseem, and M. Moinuddin, "A Novel Fractional Gradient-Based Learning Algorithm for Recurrent Neural Networks," *Circuits, Systems, and Signal Processing*, pp. 1–20, May 2017.

[101] S. M. Shah, R. Samar, N. M. Khan, and M. A. Z. Raja, "Fractional-order adaptive signal processing strategies for active noise control systems," *Nonlinear Dynamics*, vol. 85, no. 3, pp. 1363–1376, Aug. 2016.

[102] M. T. Akhtar, "An adaptive algorithm, based on modified tanh non-linearity and fractional processing, for impulsive active noise control systems," *Journal of Low Frequency Noise, Vibration and Active Control*, p. 146134841772595, Aug. 2017.

[103] M. S. Aslam and M. A. Z. Raja, "A new adaptive strategy to improve online secondary path modeling in active noise control systems using fractional signal processing approach," *Signal Processing*, vol. 107, pp. 433–443, Feb. 2015.

[104] S. S. Haykin, *Adaptive filter theory*. Pearson Education India, 2008.

[105] M. D. Ortigueira, *Fractional Calculus for Scientists and Engineers*, vol. 84. Dordrecht: Springer Netherlands, 2011.

[106] H. Srivastava and J. Trujillo, *Theory and applications of fractional differential equations*. 2006.

[107] M. Tarrab and A. Feuer, "Convergence and performance analysis of the normalized LMS algorithm with uncorrelated Gaussian data," *IEEE Transactions on*

Information Theory, vol. 34, no. 4, pp. 680–691, Jul. 1988.

[108] D. T. M. Slock, "On the convergence behavior of the LMS and the normalized LMS algorithms," *IEEE Transactions on Signal Processing*, vol. 41, no. 9, pp. 2811–2825, 1993.

[109] S. C. Douglas, "A family of normalized LMS algorithms," *IEEE Signal Processing Letters*, vol. 1, no. 3, pp. 49–51, Mar. 1994.

[110] P. E. An, B. Brown, and C. J. Harris, "On the convergence rate performance of the normalized least-mean-square adaptation," *IEEE Transactions on Neural Networks*, vol. 8, no. 5, pp. 1211–1214, 1997.

[111] P. S. R. Diniz, *Adaptive filtering: algorithms and practical implementation.* Springer, 2013.

[112] W. A. Gardner, "Learning characteristics of stochastic-gradient-descent algorithms: A general study, analysis, and critique," *Signal Processing*, vol. 6, no. 2, pp. 113–133, Apr. 1984.

[113] G. Clark, S. Mitra, and S. Parker, "Block implementation of adaptive digital filters," *IEEE Transactions on Acoustics, Speech, and Signal Processing*, vol. 29, no. 3, pp. 744–752, Jun. 1981.

[114] W. Mikhael and F. Wu, "Fast algorithms for block FIR adaptive digital filtering," *IEEE Transactions on Circuits and Systems*, vol. 34, no. 10, pp. 1152–1160, Oct. 1987.

[115] S. Roy and J. J. Shynk, "Analysis of the momentum LMS algorithm," *IEEE Transactions on Acoustics, Speech, and Signal Processing*, vol. 38, no. 12, pp. 2088–2098, 1990.

[116] M. A. Tugay and Y. Tanik, "Properties of the momentum LMS algorithm," *Signal Processing*, vol. 18, no. 2, pp. 117–127, Oct. 1989.

[117] T. Kailath, *Linear systems.* Prentice-Hall, 1980.

[118] E. I. Jury, *Theory and application of the Z - transform method.* Wiley, 1964.

[119] W. Xiong, W. Fan, and R. Ding, "Least-Squares Parameter Estimation Algorithm for a Class of Input Nonlinear Systems," *Journal of Applied Mathematics*, vol. 2012, pp. 1–14, Aug. 2012.

[120] F. Le, "Identification of electrically stimulated muscle after stroke," University of Southampton, School of Electronics and Computer Science, 2011.

[121] E. L. Owen, "A history of harmonics in power systems," *IEEE Industry Applications*

Magazine, vol. 4, no. 1, pp. 6–12, Jan. 1998.

[122] S. Vazquez, J. A. Sanchez, M. R. Reyes, J. I. Leon, and J. M. Carrasco, "Adaptive Vectorial Filter for Grid Synchronization of Power Converters Under Unbalanced and/or Distorted Grid Conditions," *IEEE Transactions on Industrial Electronics*, vol. 61, no. 3, pp. 1355–1367, Mar. 2014.

[123] M. Shahbazi, P. Poure, S. Saadate, and M. R. Zolghadri, "FPGA-Based Fast Detection With Reduced Sensor Count for a Fault-Tolerant Three-Phase Converter," *IEEE Transactions on Industrial Informatics*, vol. 9, no. 3, pp. 1343–1350, Aug. 2013.

[124] M. N. Kabir, Y. Mishra, G. Ledwich, Z. Y. Dong, and K. P. Wong, "Coordinated Control of Grid-Connected Photovoltaic Reactive Power and Battery Energy Storage Systems to Improve the Voltage Profile of a Residential Distribution Feeder," *IEEE Transactions on Industrial Informatics*, vol. 10, no. 2, pp. 967–977, May 2014.

[125] L. Feola, R. Langella, and A. Testa, "On the Effects of Unbalances, Harmonics and Interharmonics on PLL Systems," *IEEE Transactions on Instrumentation and Measurement*, vol. 62, no. 9, pp. 2399–2409, Sep. 2013.

[126] Y. Yang, K. Zhou, and M. Cheng, "Phase Compensation Resonant Controller for PWM Converters," *IEEE Transactions on Industrial Informatics*, vol. 9, no. 2, pp. 957–964, May 2013.

[127] L. Xu and F. Ding, "Recursive Least Squares and Multi-innovation Stochastic Gradient Parameter Estimation Methods for Signal Modeling," *Circuits, Systems, and Signal Processing*, vol. 36, no. 4, pp. 1735–1753, Apr. 2017.

APPENDIX

Appendix 4.1 Performance comparison based on MSE values in case study 1

σ^2	Method	α	Adaptive Parameters								MSE
			θ_1	θ_2	θ_3	θ_4	θ_5	θ_6	θ_7	θ_8	
0.01^2	LMS		-1.350	0.750	0.995	0.500	0.202	1.668	0.840	0.342	2.75E-05
	mLMS	(0.1, 0.9)	-1.350	0.750	1.000	0.500	0.200	1.680	0.840	0.336	4.27E-08
	mLMS	(0.3, 0.7)	-1.350	0.750	1.000	0.500	0.200	1.680	0.840	0.336	3.30E-08
	mLMS	(0.5, 0.5)	-1.350	0.750	1.000	0.500	0.200	1.680	0.840	0.336	3.01E-08
0.05^2	LMS		-1.351	0.751	0.993	0.501	0.201	1.669	0.841	0.343	2.94E-05
	mLMS	(0.1, 0.9)	-1.349	0.751	1.001	0.499	0.200	1.680	0.841	0.338	1.10E-06
	mLMS	(0.3, 0.7)	-1.351	0.750	1.002	0.501	0.201	1.680	0.841	0.335	1.04E-06
	mLMS	(0.5, 0.5)	-1.351	0.750	1.001	0.501	0.201	1.680	0.841	0.335	9.27E-07
0.1^2	LMS		-1.345	0.751	0.994	0.500	0.203	1.671	0.840	0.340	2.17E-05
	mLMS	(0.1, 0.9)	-1.353	0.749	0.999	0.500	0.200	1.676	0.838	0.338	4.11E-06
	mLMS	(0.3, 0.7)	-1.347	0.748	0.999	0.499	0.198	1.677	0.840	0.333	4.38E-06
	mLMS	(0.5, 0.5)	-1.347	0.748	0.999	0.498	0.198	1.678	0.841	0.333	3.94E-06
	True Values		-1.350	0.750	1.000	0.500	0.200	1.680	0.840	0.336	0

Appendix 4.2 Performance comparison based on fitness achieved at specific iterations in case study 1

σ^2	Method	*A*	Fitness achieved at specific iterations									
			1000	**2000**	**3000**	**4000**	**5000**	**6000**	**7000**	**8000**	**9000**	**10000**
0.01^2	**LMS**		0.224	0.191	0.167	0.146	0.130	0.115	0.101	0.089	0.078	0.069
	mLMS	**(0.1, 0.9)**	0.220	0.185	0.159	0.123	0.098	0.076	0.059	0.045	0.035	0.027
	mLMS	**(0.3, 0.7)**	0.207	0.169	0.140	0.107	0.084	0.065	0.049	0.038	0.029	0.022
	mLMS	**(0.5, 0.5)**	0.188	0.145	0.111	0.087	0.068	0.054	0.041	0.032	0.025	0.019
0.05^2	**LMS**		0.224	0.191	0.167	0.146	0.130	0.115	0.101	0.089	0.078	0.068
	mLMS	**(0.1, 0.9)**	0.220	0.185	0.159	0.123	0.098	0.076	0.059	0.044	0.034	0.026
	mLMS	**(0.3, 0.7)**	0.206	0.169	0.140	0.107	0.084	0.065	0.049	0.037	0.028	0.021
	mLMS	**(0.5, 0.5)**	0.188	0.145	0.111	0.086	0.068	0.054	0.041	0.032	0.024	0.018
0.1^2	**LMS**		0.224	0.191	0.166	0.146	0.130	0.115	0.100	0.088	0.077	0.067
	mLMS	**(0.1, 0.9)**	0.219	0.185	0.159	0.123	0.098	0.076	0.058	0.043	0.033	0.025
	mLMS	**(0.3, 0.7)**	0.206	0.169	0.139	0.107	0.083	0.065	0.049	0.036	0.028	0.020
	mLMS	**(0.5, 0.5)**	0.187	0.145	0.110	0.086	0.068	0.054	0.041	0.031	0.024	0.017

Appendix 4.3 Performance comparison based on the values of statistical parameters in case study 1

	Method	*A*	$\sigma^2 = 0.01^2$			$\sigma^2 = 0.05^2$			$\sigma^2 = 0.1^2$		
			MIN	MEAN	SD	MIN	MEAN	SD	MIN	MEAN	SD
MSE	**LMS**		2.75E-05	1.28E-04	5.48E-05	2.94E-05	1.30E-04	5.56E-05	2.17E-05	1.35E-04	5.78E-05
	mLMS	**(0.1, 0.9)**	4.27E-08	4.43E-07	9.23E-07	1.10E-06	8.80E-06	3.47E-05	4.11E-06	3.79E-05	1.71E-04
	mLMS	**(0.3, 0.7)**	3.30E-08	2.36E-07	1.34E-07	1.04E-06	4.35E-06	3.09E-06	4.38E-06	1.72E-05	1.23E-05
	mLMS	**(0.5, 0.5)**	3.01E-08	2.41E-07	1.13E-07	9.27E-07	3.61E-06	1.97E-06	3.94E-06	1.41E-05	7.91E-06
ENSE	**LMS**		4.10E-05	1.92E-04	8.18E-05	4.38E-05	1.94E-04	8.29E-05	3.24E-05	2.02E-04	8.63E-05
	mLMS	**(0.1, 0.9)**	6.37E-08	6.61E-07	1.38E-06	1.64E-06	1.31E-05	5.19E-05	6.14E-06	5.65E-05	2.55E-04
	mLMS	**(0.3, 0.7)**	4.93E-08	3.52E-07	2.00E-07	1.56E-06	6.49E-06	4.61E-06	6.54E-06	2.56E-05	1.83E-05
	mLMS	**(0.5, 0.5)**	4.49E-08	3.59E-07	1.69E-07	1.38E-06	5.38E-06	2.94E-06	5.88E-06	2.10E-05	1.18E-05

Appendix 4.4 Performance comparison based on MSE values for $\sigma^2 = 0.1^2$ in case study 2

μ	Method	fr/β	Design parameters								MSE
			θ_1	θ_2	θ_3	θ_4	θ_5	θ_6	θ_7	θ_8	
(10^{-03},10^{-05})	**FLMS**	**0.25**	-1.349	0.749	0.999	0.500	0.199	1.680	0.840	0.335	3.48E-08
		0.75	-1.349	0.749	0.999	0.500	0.199	1.680	0.840	0.335	3.50E-08
	MFLMS-1	**0.25/0.25**	-1.350	0.750	1.000	0.499	0.200	1.680	0.840	0.335	8.00E-09
		0.75/0.25	-1.349	0.749	0.999	0.500	0.199	1.680	0.840	0.335	3.29E-08
		0.25/0.75	-1.349	0.749	0.999	0.500	0.199	1.680	0.840	0.335	3.03E-08
		0.75/0.75	-1.349	0.749	0.999	0.500	0.199	1.680	0.840	0.335	3.35E-08
	MFLMS-2	**0.25**	-1.350	0.750	1.000	0.499	0.200	1.680	0.840	0.335	6.18E-09
		0.75	-1.350	0.750	1.000	0.499	0.200	1.680	0.840	0.335	1.07E-08
	True values		-1.350	0.750	1.000	0.500	0.200	1.680	0.840	0.336	0

Appendix 4.5 Performance comparison based on MSE values for $\sigma^2 = 0.5^2$ in case study 2

μ	Method	fr/β	Design parameters								MSE
			θ_1	θ_2	θ_3	θ_4	θ_5	θ_6	θ_7	θ_8	
(10^{-03},10^{-05})	**FLMS**	**0.25**	-1.340	0.743	0.992	0.502	0.199	1.677	0.844	0.336	2.74E-05
		0.75	-1.341	0.743	0.995	0.503	0.198	1.679	0.845	0.334	2.34E-05
	MFLMS-1	**0.25/0.25**	-1.349	0.749	1.003	0.496	0.200	1.682	0.842	0.332	5.34E-06
		0.75/0.25	-1.341	0.743	0.9960	0.502	0.198	1.681	0.844	0.334	2.12E-05
		0.25/0.75	-1.341	0.744	0.996	0.501	0.198	1.681	0.844	0.333	1.94E-05
		0.75/0.75	-1.341	0.743	0.996	0.503	0.197	1.681	0.844	0.333	2.14E-05
	MFLMS-2	**0.25**	-1.349	0.749	1.003	0.497	0.199	1.681	0.842	0.333	4.34E-06
		0.75	-1.349	0.749	1.003	0.496	0.201	1.682	0.842	0.332	7.15E-06
	True values		-1.350	0.750	1.000	0.500	0.200	1.680	0.840	0.336	0

Appendix 4.6 Performance comparison based on MSE values for $\sigma^2 = 0.9^2$ in case study 2

μ	Method	fr/β	Design parameters								MSE
			θ_1	θ_2	θ_3	θ_4	θ_5	θ_6	θ_7	θ_8	
(10^{-03},10^{-05})	**FLMS**	**0.25**	-1.319	0.692	0.921	0.503	0.247	1.805	0.852	0.325	3.47E-03
		0.75	-1.349	0.765	1.008	0.522	0.182	1.649	0.829	0.333	2.73E-04
	MFLMS-1	**0.25/0.25**	-1.346	0.740	0.997	0.493	0.205	1.664	0.828	0.325	7.86E-05
		0.75/0.25	-1.348	0.766	0.989	0.520	0.190	1.642	0.829	0.338	3.19E-04
		0.25/0.75	-1.348	0.765	0.993	0.516	0.183	1.664	0.830	0.330	1.42E-04
		0.75/0.75	-1.350	0.760	1.000	0.522	0.182	1.653	0.829	0.333	2.31E-04
	MFLMS-2	**0.25**	-1.345	0.744	1.000	0.494	0.203	1.663	0.828	0.327	7.09E-05
		0.75	-1.347	0.744	0.995	0.490	0.207	1.666	0.827	0.321	9.37E-05
	True values		-1.350	0750	1.000	0.500	0.200	1.680	0.840	0.336	0

Appendix 4.7 Performance comparison based on statistical parameters through ENSE in case study 2

μ	METHOD	*fr/β*	$\sigma^2 = 0.1^2$			$\sigma^2 = 0.5^2$			$\sigma^2 = 0.9^2$		
			MIN	MEAN	STD	MIN	MEAN	STD	MIN	MEAN	STD
(10^{-03}, 10^{-05})	**FLMS**	**0.25**	5.2E-08	6.3E-07	1.0E-06	4.1E-05	4.2E-04	8.6E-04	5.2E-03	5.4E-03	3.5E-04
		0.75	5.2E-08	6.5E-07	1.1E-06	3.5E-05	3.4E-04	4.8E-04	4.1E-04	1.3E-02	7.4E-02
	MFLMS-1	**0.25/0.25**	1.2E-08	8.3E-08	4.7E-08	8.0E-06	5.2E-05	3.0E-05	1.2E-04	5.6E-04	3.3E-04
		0.25/0.75	4.9E-08	5.2E-07	7.9E-07	3.2E-05	2.7E-04	3.6E-04	4.8E-04	3.7E-03	3.8E-03
		0.75/0.25	4.5E-08	3.3E-07	3.9E-07	2.9E-05	1.8E-04	1.8E-04	2.1E-04	2.1E-03	2.1E-03
		0.75/0.75	5.0E-08	5.2E-07	8.0E-07	3.2E-05	2.9E-04	3.9E-04	3.4E-04	3.2E-03	4.9E-03
	MFLMS-2	**0.25**	9.2E-09	8.2E-08	4.9E-08	6.5E-06	5.1E-05	3.1E-05	1.1E-04	5.6E-04	3.5E-04
		0.75	1.6E-08	9.1E-08	5.1E-08	1.1E-05	5.7E-05	3.2E-05	1.4E-04	6.1E-04	3.5E-04

Appendix 4.8 Performance comparison based on statistical parameters through EVAF in case study 2

μ	METHOD	fr/β	$\sigma^2 = 0.1^2$			$\sigma^2 = 0.5^2$			$\sigma^2 = 0.9^2$		
			MIN	MEAN	STD	MIN	MEAN	STD	MIN	MEAN	STD
(10^{-03}, 10^{-05})	**FLMS**	**0.25**	5.1E-06	5.7E-05	9.5E-05	4.1E-03	3.5E-02	5.1E-02	5.0E-01	5.3E-01	3.3E-02
		0.75	5.1E-06	5.8E-05	9.8E-05	3.5E-03	3.1E-02	4.4E-02	4.0E-02	1.2E+00	7.4E+00
	MFLMS-1	**0.25/0.25**	1.2E-06	7.4E-06	4.7E-06	5.8E-04	4.6E-03	3.0E-03	2.9E-03	5.0E-02	3.3E-02
		0.25/0.75	4.8E-06	4.7E-05	7.3E-05	3.1E-03	2.5E-02	3.2E-02	4.5E-02	3.3E-01	3.3E-01
		0.75/0.25	4.5E-06	3.0E-05	3.7E-05	2.9E-03	1.7E-02	1.7E-02	2.0E-02	2.0E-01	2.1E-01
		0.75/0.75	4.9E-06	4.7E-05	7.3E-05	3.2E-03	2.7E-02	3.7E-02	3.4E-02	2.9E-01	4.9E-01
	MFLMS-2	**0.25**	9.1E-07	7.3E-06	4.9E-06	5.8E-04	4.5E-03	3.1E-03	2.7E-03	4.9E-02	3.4E-02
		0.75	1.5E-06	8.1E-06	5.1E-06	6.7E-04	5.1E-03	3.2E-03	3.9E-03	5.4E-02	3.5E-02

Appendix 4.9 Comparison for different step size parameters based on MSE values for $\sigma^2 = 0.5^2$ and $fr = 0.5$ in case study 3

Method	μ = **1E-02**		μ = **1E-03**		μ = **1E-04**		μ = **1E-05**	
	MEAN	**SD**	**MEAN**	**SD**	**MEAN**	**SD**	**MEAN**	**SD**
FLMS	NaN	NaN	8.60E-04	8.32E-04	7.39E-02	NaN	1.95E-01	7.49E-02
NFLMS	4.04E-04	1.54E-04	5.76E-02	2.62E-02	1.89E-01	7.38E-02	3.66E-01	8.79E-02
MFLMS-1(β = 0.25)	NaN	NaN	1.47E-03	9.18E-04	1.23E-01	5.52E-02	2.19E-01	8.12E-02
MFLMS-1(β = 0.75)	NaN	NaN	1.44E-03	6.96E-04	1.21E-01	4.81E-02	2.17E-01	7.67E-02
NMFLMS-1(β = 0.25)	5.76E-04	3.06E-04	1.09E-01	5.08E-02	2.16E-01	8.05E-02	4.87E-01	9.96E-02
NMFLMS-1(β = 0.75)	5.41E-04	2.45E-04	1.07E-01	4.35E-02	2.13E-01	7.59E-02	4.36E-01	9.75E-02
MFLMS-2	NaN	NaN	1.69E-03	1.23E-03	1.24E-01	6.01E-02	2.21E-01	8.50E-02
NMFLMS-2	6.70E-04	4.08E-04	1.10E-01	5.58E-02	2.20E-01	8.43E-02	5.47E-01	8.69E-02

Appendix 4.10 Performance comparison for different fractional orders based on MSE values for $\sigma^2 = 0.5^2$ in case study 3

fr	**FLMS**	**NFLMS**	**MFLMS-1 (β = 0.25)**	**MFLMS-1 (β = 0.75)**	**NMFLMS-1 (β = 0.25)**	**NMFLMS-1 (β = 0.75)**	**MFLMS-2**	**NMFLMS-2**
0.1	NaN	3.71E-04	3.27E-03	1.80E-03	1.25E-03	6.33E-04	6.79E-03	3.01E-03
0.2	7.48E-04	3.75E-04	2.68E-03	1.73E-03	9.99E-04	6.10E-04	4.67E-03	1.91E-03
0.3	8.05E-04	3.79E-04	2.21E-03	1.67E-03	8.16E-04	5.90E-04	3.29E-03	1.28E-03
0.4	8.47E-04	3.82E-04	1.87E-03	1.63E-03	6.86E-04	5.75E-04	2.42E-03	9.10E-04
0.5	8.67E-04	3.84E-04	1.64E-03	1.59E-03	5.98E-04	5.65E-04	1.87E-03	6.96E-04
0.6	8.56E-04	3.84E-04	1.49E-03	1.58E-03	5.44E-04	5.60E-04	1.55E-03	5.76E-04
0.7	8.14E-04	3.83E-04	1.42E-03	1.58E-03	5.17E-04	5.61E-04	1.40E-03	5.16E-04
0.8	7.43E-04	3.81E-04	1.43E-03	1.61E-03	5.16E-04	5.69E-04	1.37E-03	5.01E-04
0.9	6.54E-04	3.77E-04	1.53E-03	1.65E-03	5.44E-04	5.84E-04	1.47E-03	5.27E-04

Appendix 4.11 Performance comparison based on MSE values for $\sigma^2 = 0.2^2$ in case study 3

Method	Design parameters								MSE
	θ_1	θ_2	θ_3	θ_4	θ_5	θ_6	θ_7	θ_8	
FLMS	-1.346	0.749	1.005	0.494	0.208	1.685	0.837	0.337	2.02E-05
NFLMS	-1.346	0.750	1.000	0.495	0.196	1.682	0.833	0.334	1.60E-05
MFLMS-1(β = 0.25)	-1.352	0.751	1.003	0.493	0.195	1.663	0.843	0.348	6.89E-05
MFLMS-1(β = 0.75)	-1.352	0.751	0.997	0.492	0.197	1.648	0.843	0.355	1.85E-04
NMFLMS-1(β = 0.25)	-1.345	0.745	0.990	0.502	0.205	1.675	0.841	0.341	2.86E-05
NMFLMS-1(β = 0.75)	-1.345	0.745	0.993	0.502	0.203	1.670	0.842	0.344	3.49E-05
MFLMS-2	-1.352	0.751	1.016	0.493	0.189	1.673	0.843	0.344	7.03E-05
NMFLMS-2	-1.351	0.746	1.003	0.493	0.198	1.671	0.846	0.344	3.39E-05
True values	-1.350	0.750	1.000	0.500	0.200	1.680	0.840	0.336	0

Appendix 4.12 Performance comparison based on MSE values for $\sigma^2 = 0.5^2$ in case study 3

Method	Design parameters								MSE
	θ_1	θ_2	θ_3	θ_4	θ_5	θ_6	θ_7	θ_8	
FLMS	-1.362	0.749	1.002	0.503	0.193	1.675	0.843	0.341	1.60E-04
NFLMS	-1.352	0.750	0.998	0.504	0.209	1.672	0.838	0.338	6.74E-05
MFLMS-1(β = 0.25)	-1.352	0.751	1.003	0.493	0.195	1.663	0.843	0.348	1.00E-04
MFLMS-1(β = 0.75)	-1.352	0.751	0.997	0.492	0.197	1.648	0.843	0.355	2.08E-04
NMFLMS-1(β = 0.25)	-1.345	0.745	0.990	0.502	0.205	1.675	0.841	0.341	5.50E-05
NMFLMS-1(β = 0.75)	-1.345	0.745	0.993	0.502	0.203	1.670	0.842	0.344	5.36E-05
MFLMS-2	-1.352	0.751	1.016	0.493	0.189	1.673	0.843	0.344	1.14E-04
NMFLMS-2	-1.345	0.745	0.987	0.502	0.207	1.677	0.841	0.340	6.08E-05
True values	-1.350	0.750	1.000	0.500	0.200	1.680	0.840	0.336	0

Appendix 4.13 Performance comparison based on MSE values for $\sigma^2 = 0.8^2$ in case study 3

Method	Design parameters								MSE
	θ_1	θ_2	θ_3	θ_4	θ_5	θ_6	θ_7	θ_8	
FLMS	-1.356	0.754	1.005	0.497	0.192	1.663	0.841	0.341	4.57E-04
NFLMS	-1.352	0.750	0.998	0.504	0.209	1.672	0.838	0.338	1.93E-04
MFLMS-1(β = 0.25)	-1.352	0.751	1.003	0.493	0.195	1.663	0.843	0.348	1.99E-04
MFLMS-1(β = 0.75)	-1.352	0.751	0.997	0.492	0.197	1.648	0.843	0.355	3.02E-04
NMFLMS-1(β = 0.25)	-1.351	0.754	0.982	0.503	0.210	1.660	0.840	0.352	9.36E-05
NMFLMS-1(β = 0.75)	-1.345	0.745	0.993	0.502	0.203	1.670	0.842	0.344	1.03E-04
MFLMS-2	-1.352	0.751	1.016	0.493	0.189	1.673	0.843	0.344	2.32E-04
NMFLMS-2	-1.348	0.752	0.989	0.499	0.205	1.651	0.837	0.350	8.39E-05
True values	-1.350	0.750	1.000	0.500	0.200	1.680	0.840	0.336	0

Appendix 4.14 Performance comparison through statistics based on ENSE values in case study 3

	Method	$\sigma^2 = 0.2^2$			$\sigma^2 = 0.5^2$			$\sigma^2 = 0.8^2$		
		MIN	**MEAN**	**SD**	**MIN**	**MEAN**	**SD**	**MIN**	**MEAN**	**SD**
ENSE	**FLMS**	3.02E-05	NaN	NaN	2.39E-04	NaN	NaN	6.82E-04	NaN	NaN
	NFLMS	2.38E-05	8.47E-05	4.04E-05	1.01E-04	5.25E-04	2.49E-04	2.87E-04	1.36E-03	6.40E-04
	MFLMS-1($\beta = 0.25$)	1.03E-04	2.41E-03	1.56E-03	1.50E-04	2.50E-03	1.66E-03	2.97E-04	2.68E-03	1.82E-03
	MFLMS-1($\beta = 0.75$)	2.76E-04	2.38E-03	1.18E-03	3.10E-04	2.49E-03	1.27E-03	4.50E-04	2.73E-03	1.45E-03
	NMFLMS-1($\beta = 0.25$)	4.28E-05	6.07E-04	3.83E-04	8.20E-05	7.99E-04	4.81E-04	1.40E-04	1.17E-03	6.46E-04
	NMFLMS-1($\beta = 0.75$)	5.22E-05	6.15E-04	2.94E-04	8.00E-05	8.26E-04	4.08E-04	1.54E-04	1.23E-03	5.86E-04
	MFLMS-2	1.05E-04	2.79E-03	2.22E-03	1.70E-04	2.86E-03	2.34E-03	3.46E-04	3.02E-03	2.49E-03
	NMFLMS-2	5.06E-05	7.27E-04	5.77E-04	9.07E-05	9.11E-04	6.65E-04	1.25E-04	1.27E-03	8.22E-04

Appendix 4.15 Performance comparison through statistics based on EVAF values in case study 3

	Method	$\sigma^2 = 0.2^2$			$\sigma^2 = 0.5^2$			$\sigma^2 = 0.8^2$		
		MIN	**MEAN**	**SD**	**MIN**	**MEAN**	**SD**	**MIN**	**MEAN**	**SD**
EVAF	**FLMS**	2.69E-03	NaN	NaN	1.70E-02	NaN	NaN	4.81E-02	NaN	NaN
	NFLMS	1.60E-03	7.46E-03	3.75E-03	9.29E-03	4.64E-02	2.32E-02	2.49E-02	1.21E-01	5.89E-02
	MFLMS-1(β = 0.25)	9.92E-03	2.29E-01	1.47E-01	1.39E-02	2.34E-01	1.55E-01	2.70E-02	2.48E-01	1.68E-01
	MFLMS-1(β = 0.75)	2.62E-02	2.26E-01	1.11E-01	2.80E-02	2.34E-01	1.19E-01	3.88E-02	2.53E-01	1.34E-01
	NMFLMS-1(β = 0.25)	4.27E-03	5.78E-02	3.61E-02	7.40E-03	7.47E-02	4.47E-02	1.37E-02	1.08E-01	6.01E-02
	NMFLMS-1(β = 0.75)	5.19E-03	5.85E-02	2.78E-02	7.52E-03	7.73E-02	3.84E-02	1.30E-02	1.14E-01	5.54E-02
	MFLMS-2	1.05E-02	2.65E-01	2.10E-01	1.68E-02	2.68E-01	2.18E-01	3.37E-02	2.80E-01	2.30E-01
	NMFLMS-2	4.98E-03	6.93E-02	5.47E-02	8.16E-03	8.54E-02	6.19E-02	1.24E-02	1.18E-01	7.62E-02

Appendix 4.16 Performance comparison based on fitness achieved at specific iterations for $\sigma^2 = 0.01^2$ in case study 5

fr	Method	α	Fitness achieved at specific iterations									
			1000	**2000**	**3000**	**4000**	**5000**	**6000**	**7000**	**8000**	**9000**	**10000**
0.25	**FLMS**		0.2361	0.1809	0.1350	0.1003	0.0737	0.0542	0.0410	0.0303	0.0226	0.0168
	mFLMS	**0.2**	0.2023	0.1414	0.0960	0.0644	0.0431	0.0284	0.0197	0.0133	0.0091	0.0060
	mFLMS	**0.4**	0.1599	0.0955	0.0554	0.0308	0.0181	0.0101	0.0062	0.0041	0.0027	0.0017
	mFLMS	**0.6**	0.1115	0.0530	0.0256	0.0123	0.0068	0.0037	0.0023	0.0017	0.0012	0.0008
0.50	**FLMS**		0.2359	0.1804	0.1346	0.0999	0.0736	0.0541	0.0411	0.0305	0.0228	0.0170
	mFLMS	**0.2**	0.2009	0.1406	0.0957	0.0644	0.0433	0.0287	0.0200	0.0136	0.0093	0.0063
	mFLMS	**0.4**	0.1557	0.0934	0.0544	0.0303	0.0177	0.0097	0.0059	0.0037	0.0023	0.0014
	mFLMS	**0.6**	0.1029	0.0482	0.0226	0.0103	0.0055	0.0029	0.0018	0.0014	0.0011	0.0007
0.75	**FLMS**		0.2381	0.1831	0.1379	0.1034	0.0773	0.0575	0.0442	0.0333	0.0252	0.0190
	mFLMS	**0.2**	0.2024	0.1436	0.0994	0.0683	0.0471	0.0319	0.0227	0.0158	0.0110	0.0076
	mFLMS	**0.4**	0.1541	0.0947	0.0565	0.0329	0.0198	0.0112	0.0070	0.0043	0.0026	0.0015
	mFLMS	**0.6**	0.0966	0.0452	0.0209	0.0091	0.0047	0.0024	0.0015	0.0012	0.0010	0.0007

Appendix 4.17 Performance comparison based on fitness achieved at specific iterations for $\sigma^2 = 0.05^2$ in case study 5

fr	Method	α	Fitness achieved at specific iterations									
			1000	**2000**	**3000**	**4000**	**5000**	**6000**	**7000**	**8000**	**9000**	**10000**
0.25	**FLMS**		0.2356	0.1809	0.1354	0.1007	0.0750	0.0550	0.0416	0.0309	0.0232	0.0169
	mFLMS	**0.2**	0.2017	0.1416	0.0967	0.0648	0.0449	0.0295	0.0204	0.0141	0.0098	0.0063
	mFLMS	**0.4**	0.1591	0.0960	0.0566	0.0312	0.0204	0.0111	0.0071	0.0055	0.0042	0.0028
	mFLMS	**0.6**	0.1105	0.0542	0.0273	0.0125	0.0083	0.0044	0.0035	0.0037	0.0048	0.0028
0.50	**FLMS**		0.2354	0.1804	0.1350	0.1004	0.0750	0.0550	0.0418	0.0311	0.0234	0.0171
	mFLMS	**0.2**	0.2003	0.1408	0.0964	0.0649	0.0452	0.0298	0.0209	0.0144	0.0100	0.0065
	mFLMS	**0.4**	0.1550	0.0940	0.0555	0.0308	0.0201	0.0109	0.0071	0.0052	0.0039	0.0026
	mFLMS	**0.6**	0.1019	0.0494	0.0244	0.0106	0.0076	0.0040	0.0033	0.0035	0.0048	0.0028
0.75	**FLMS**		0.2377	0.1831	0.1383	0.1038	0.0786	0.0584	0.0449	0.0338	0.0257	0.0191
	mFLMS	**0.2**	0.2019	0.1438	0.1000	0.0687	0.0487	0.0330	0.0236	0.0164	0.0115	0.0078
	mFLMS	**0.4**	0.1534	0.0952	0.0575	0.0333	0.0220	0.0125	0.0083	0.0054	0.0040	0.0025
	mFLMS	**0.6**	0.0956	0.0464	0.0226	0.0092	0.0073	0.0038	0.0032	0.0033	0.0046	0.0027

Appendix 4.18 Performance comparison based on fitness achieved at specific iterations for $\sigma^2 = 0.1^2$ in case study 5

fr	Method	α	Fitness achieved at specific iterations									
			1000	**2000**	**3000**	**4000**	**5000**	**6000**	**7000**	**8000**	**9000**	**10000**
0.25	**FLMS**		0.2350	0.1810	0.1359	0.1013	0.0766	0.0561	0.0424	0.0315	0.0241	0.0171
	mFLMS	**0.2**	0.2010	0.1419	0.0976	0.0653	0.0471	0.0307	0.0214	0.0150	0.0110	0.0070
	mFLMS	**0.4**	0.1582	0.0968	0.0581	0.0316	0.0234	0.0124	0.0085	0.0074	0.0067	0.0047
	mFLMS	**0.6**	0.1092	0.0559	0.0295	0.0132	0.0124	0.0067	0.0059	0.0066	0.0097	0.0055
0.50	**FLMS**		0.2348	0.1805	0.1355	0.1010	0.0767	0.0562	0.0427	0.0319	0.0244	0.0174
	mFLMS	**0.2**	0.1997	0.1411	0.0972	0.0655	0.0474	0.0312	0.0221	0.0154	0.0112	0.0073
	mFLMS	**0.4**	0.1542	0.0948	0.0569	0.0313	0.0233	0.0125	0.0087	0.0072	0.0065	0.0045
	mFLMS	**0.6**	0.1006	0.0511	0.0268	0.0114	0.0124	0.0067	0.0059	0.0066	0.0097	0.0055
0.75	**FLMS**		0.2371	0.1832	0.1387	0.1044	0.0802	0.0595	0.0459	0.0345	0.0266	0.0194
	mFLMS	**0.2**	0.2012	0.1441	0.1007	0.0693	0.0508	0.0343	0.0248	0.0172	0.0125	0.0084
	mFLMS	**0.4**	0.1526	0.0959	0.0587	0.0338	0.0250	0.0141	0.0100	0.0071	0.0065	0.0043
	mFLMS	**0.6**	0.0944	0.0482	0.0251	0.0100	0.0123	0.0066	0.0059	0.0062	0.0094	0.0053

Appendix 4.19 Performance comparison through MSE values for $\sigma^2 = 0.01^2$ in case study 5

fr	Method	α	Adaptive Parameters								MSE
			θ_1	θ_2	θ_3	θ_4	θ_5	θ_6	θ_7	θ_8	
0.25	**FLMS**		-1.350	0.751	1.000	0.499	0.200	1.640	0.841	0.356	2.57E-04
	mFLMS	**0.2**	-1.350	0.751	1.004	0.500	0.198	1.666	0.841	0.343	3.33E-05
	mFLMS	**0.4**	-1.350	0.751	1.004	0.500	0.198	1.680	0.841	0.337	2.51E-06
	mFLMS	**0.6**	-1.350	0.751	1.001	0.500	0.199	1.681	0.841	0.336	5.80E-07
0.50	**FLMS**		-1.350	0.751	0.999	0.499	0.200	1.639	0.841	0.357	2.63E-04
	mFLMS	**0.2**	-1.350	0.751	1.003	0.500	0.198	1.665	0.841	0.344	3.58E-05
	mFLMS	**0.4**	-1.350	0.751	1.003	0.500	0.198	1.679	0.841	0.337	1.71E-06
	mFLMS	**0.6**	-1.350	0.751	1.001	0.500	0.199	1.681	0.841	0.336	4.63E-07
0.75	**FLMS**		-1.350	0.751	0.998	0.499	0.201	1.634	0.841	0.359	3.29E-04
	mFLMS	**0.2**	-1.350	0.751	1.002	0.499	0.199	1.662	0.841	0.345	5.26E-05
	mFLMS	**0.4**	-1.350	0.751	1.002	0.500	0.199	1.677	0.841	0.338	2.06E-06
	mFLMS	**0.6**	-1.350	0.751	1.001	0.500	0.199	1.681	0.841	0.336	3.99E-07
	True Values		-1.350	0.750	1.000	0.500	0.200	1.680	0.840	0.336	0

Appendix 4.20 Performance comparison through MSE values for $\sigma^2 = 0.05^2$ in case study 5

fr	Method	α	Adaptive Parameters								MSE
			θ_1	θ_2	θ_3	θ_4	θ_5	θ_6	θ_7	θ_8	
0.25	**FLMS**		-1.349	0.752	1.000	0.498	0.198	1.640	0.844	0.358	2.61E-04
	mFLMS	**0.2**	-1.349	0.753	1.004	0.499	0.196	1.667	0.845	0.344	3.64E-05
	mFLMS	**0.4**	-1.349	0.753	1.004	0.500	0.196	1.681	0.845	0.337	7.04E-06
	mFLMS	**0.6**	-1.349	0.755	1.002	0.501	0.197	1.682	0.846	0.336	7.31E-06
0.50	**FLMS**		-1.349	0.753	0.999	0.498	0.198	1.639	0.844	0.358	2.68E-04
	mFLMS	**0.2**	-1.349	0.753	1.004	0.499	0.197	1.666	0.845	0.345	3.91E-05
	mFLMS	**0.4**	-1.349	0.753	1.003	0.499	0.197	1.680	0.845	0.338	6.06E-06
	mFLMS	**0.6**	-1.349	0.755	1.002	0.501	0.197	1.682	0.846	0.336	7.07E-06
0.75	**FLMS**		-1.350	0.753	0.998	0.498	0.199	1.634	0.844	0.360	3.35E-04
	mFLMS	**0.2**	-1.349	0.753	1.002	0.499	0.197	1.662	0.845	0.347	5.57E-05
	mFLMS	**0.4**	-1.349	0.754	1.002	0.500	0.197	1.678	0.845	0.339	5.79E-06
	mFLMS	**0.6**	-1.349	0.755	1.002	0.501	0.197	1.682	0.846	0.336	6.74E-06
	True Values		-1.350	0.750	1.000	0.500	0.200	1.680	0.840	0.336	0

Appendix 4.21 Performance comparison through MSE values for $\sigma^2 = 0.1^2$ in case study 5

fr	Method	α	Adaptive Parameters								MSE
			θ_1	θ_2	θ_3	θ_4	θ_5	θ_6	θ_7	θ_8	
0.25	**FLMS**		-1.348	0.755	0.999	0.497	0.196	1.641	0.848	0.359	2.68E-04
	mFLMS	**0.2**	-1.348	0.755	1.005	0.498	0.194	1.668	0.849	0.346	4.52E-05
	mFLMS	**0.4**	-1.348	0.757	1.004	0.499	0.194	1.682	0.850	0.339	1.99E-05
	mFLMS	**0.6**	-1.348	0.759	1.003	0.501	0.194	1.684	0.852	0.337	2.77E-05
0.50	**FLMS**		-1.348	0.755	0.999	0.496	0.196	1.640	0.849	0.360	2.77E-04
	mFLMS	**0.2**	-1.348	0.756	1.004	0.498	0.195	1.667	0.849	0.346	4.83E-05
	mFLMS	**0.4**	-1.348	0.757	1.004	0.499	0.195	1.681	0.850	0.339	1.89E-05
	mFLMS	**0.6**	-1.348	0.759	1.003	0.501	0.194	1.684	0.852	0.337	2.74E-05
0.75	**FLMS**		-1.348	0.755	0.998	0.496	0.197	1.635	0.848	0.362	3.45E-04
	mFLMS	**0.2**	-1.348	0.756	1.003	0.498	0.196	1.663	0.849	0.348	6.42E-05
	mFLMS	**0.4**	-1.349	0.757	1.003	0.499	0.195	1.680	0.850	0.340	1.71E-05
	mFLMS	**0.6**	-1.348	0.760	1.003	0.501	0.194	1.684	0.852	0.337	2.62E-05
	True Values		-1.350	0.750	1.000	0.500	0.200	1.680	0.840	0.336	0

Table 4.22 Performance comparison based on fitness achieved at specific iterations for $\sigma^2 = 0.05^2$ in case study 6

fr	Method	*α*	Fitness achieved at specific iterations									
			1000	**2000**	**3000**	**4000**	**5000**	**6000**	**7000**	**8000**	**9000**	**10000**
0.25	**FLMS**		0.8568	0.7994	0.7445	0.6980	0.6548	0.6128	0.5804	0.5459	0.5115	0.4808
	mFLMS	**0.2**	0.8286	0.7553	0.6881	0.6335	0.5847	0.5377	0.5012	0.4634	0.4256	0.3924
	mFLMS	**0.4**	0.7795	0.6812	0.5977	0.5348	0.4805	0.4289	0.3880	0.3484	0.3097	0.2773
	mFLMS	**0.6**	0.6863	0.5500	0.4532	0.3892	0.3354	0.2890	0.2539	0.2252	0.2008	0.1832
0.50	**FLMS**		0.8554	0.7974	0.7426	0.6963	0.6533	0.6111	0.5774	0.5416	0.5056	0.4735
	mFLMS	**0.2**	0.8273	0.7537	0.6872	0.6332	0.5847	0.5364	0.4985	0.4594	0.4204	0.3866
	mFLMS	**0.4**	0.7789	0.6822	0.6006	0.5388	0.4834	0.4300	0.3884	0.3478	0.3081	0.2751
	mFLMS	**0.6**	0.6902	0.5591	0.4641	0.3979	0.3401	0.2888	0.2495	0.2155	0.1847	0.1617
0.75	**FLMS**		0.8546	0.7956	0.7408	0.6950	0.6527	0.6101	0.5763	0.5406	0.5050	0.4734
	mFLMS	**0.2**	0.8266	0.7533	0.6881	0.6355	0.5872	0.5390	0.5015	0.4630	0.4248	0.3918
	mFLMS	**0.4**	0.7802	0.6864	0.6077	0.5474	0.4919	0.4387	0.3979	0.3578	0.3187	0.2863
	mFLMS	**0.6**	0.6972	0.5729	0.4803	0.4119	0.3523	0.2988	0.2587	0.2225	0.1889	0.1630

Appendix 4.23 Performance comparison through MSE values for $\sigma^2 = 0.05^2$ in case study 6

fr	Method	α	Adaptive Parameters								MSE
			θ_1	θ_2	θ_3	θ_4	θ_5	θ_6	θ_7	θ_8	
0.25	**FLMS**		-0.999	0.800	2.471	-4.801	5.856	1.566	-2.879	3.475	1.85E-02
	mFLMS	**0.2**	-0.999	0.800	2.553	-4.800	5.817	1.613	-2.880	3.452	1.00E-02
	mFLMS	**0.4**	-1.000	0.800	2.648	-4.800	5.772	1.664	-2.880	3.428	3.55E-03
	mFLMS	**0.6**	-1.000	0.800	2.745	-4.800	5.726	1.705	-2.880	3.409	5.49E-04
0.50	**FLMS**		-0.999	0.800	2.573	-4.800	5.808	1.620	-2.879	3.449	8.43E-03
	mFLMS	**0.2**	-1.000	0.800	2.626	-4.800	5.783	1.655	-2.879	3.433	4.72E-03
	mFLMS	**0.4**	-1.000	0.800	2.690	-4.800	5.752	1.692	-2.880	3.415	1.88E-03
	mFLMS	**0.6**	-1.000	0.800	2.758	-4.800	5.720	1.721	-2.880	3.401	5.20E-04
0.75	**FLMS**		-1.000	0.800	2.682	-4.795	5.756	1.676	-2.885	3.423	2.13E-03
	mFLMS	**0.2**	-1.000	0.800	2.711	-4.799	5.742	1.700	-2.881	3.411	1.28E-03
	mFLMS	**0.4**	-1.000	0.800	2.745	-4.800	5.726	1.725	-2.880	3.399	7.71E-04
	mFLMS	**0.6**	-1.000	0.800	2.783	-4.800	5.708	1.743	-2.880	3.391	6.48E-04
	True Values		-1.000	0.800	2.800	-4.800	5.700	1.680	-2.880	3.420	0

Appendix 5.1 Performance comparison based on fitness achieved at specific iterations for $\sigma^2 = 0.3^2$ in power signal estimation

Method	**α**	**Fitness achieved at specific iterations**									
		100	**200**	**300**	**400**	**500**	**600**	**700**	**800**	**900**	**1000**
LMS		0.7978	0.7598	0.7226	0.6867	0.6546	0.6209	0.5910	0.5624	0.5344	0.5088
mLMS	**0.2**	0.7881	0.7415	0.6964	0.6534	0.6154	0.5761	0.5416	0.5091	0.4775	0.4490
mLMS	**0.5**	0.7600	0.6891	0.6238	0.5631	0.5116	0.4604	0.4163	0.3774	0.3403	0.3084
mLMS	**0.8**	0.6602	0.5137	0.4021	0.3104	0.2443	0.1864	0.1424	0.1113	0.0860	0.0677
FLMS (*fr* = 0.25)		0.7774	0.7165	0.6543	0.5933	0.5385	0.4809	0.4308	0.3846	0.3408	0.3028
mFLMS (*fr* = 0.25)	**0.2**	0.6646	0.5902	0.5178	0.4504	0.3919	0.3331	0.2842	0.2431	0.2061	0.1752
mFLMS (*fr* = 0.25)	**0.5**	0.6191	0.5049	0.4027	0.3149	0.2475	0.1861	0.1402	0.1085	0.0830	0.0646
mFLMS (*fr* = 0.25)	**0.8**	0.4550	0.2444	0.1281	0.0645	0.0372	0.0185	0.0107	0.0102	0.0126	0.0160
FLMS (*fr* = 0.75)		0.7653	0.6960	0.6291	0.5665	0.5124	0.4573	0.4108	0.3687	0.3293	0.2954
mFLMS (*fr* = 0.75)	**0.2**	0.6559	0.5781	0.5065	0.4424	0.3882	0.3346	0.2905	0.2532	0.2193	0.1906
mFLMS (*fr* = 0.75)	**0.5**	0.6075	0.4936	0.3978	0.3180	0.2569	0.2008	0.1578	0.1264	0.0998	0.0797
mFLMS (*fr* = 0.75)	**0.8**	0.4438	0.2525	0.1451	0.0795	0.0488	0.0235	0.0112	0.0092	0.0109	0.0142

Appendix 5.2 Performance comparison based on fitness achieved at specific iterations for $\sigma^2 = 0.6^2$ in power signal estimation

Method	α	Fitness achieved at specific iterations									
		100	**200**	**300**	**400**	**500**	**600**	**700**	**800**	**900**	**1000**
LMS		0.7979	0.7600	0.7235	0.6875	0.6560	0.6217	0.5913	0.5629	0.5347	0.5093
mLMS	**0.2**	0.7882	0.7418	0.6976	0.6544	0.6172	0.5770	0.5418	0.5096	0.4778	0.4496
mLMS	**0.5**	0.7602	0.6895	0.6257	0.5646	0.5142	0.4617	0.4165	0.3778	0.3407	0.3091
mLMS	**0.8**	0.6604	0.5148	0.4064	0.3131	0.2492	0.1879	0.1415	0.1111	0.0861	0.0692
FLMS (*fr* = 0.25)		0.7775	0.7170	0.6561	0.5949	0.5412	0.4823	0.4310	0.3852	0.3412	0.3037
mFLMS (*fr* = 0.25)	**0.2**	0.6648	0.5910	0.5201	0.4525	0.3954	0.3348	0.2842	0.2437	0.2066	0.1762
mFLMS (*fr* = 0.25)	**0.5**	0.6192	0.5062	0.4064	0.3179	0.2527	0.1880	0.1393	0.1088	0.0839	0.0674
mFLMS (*fr* = 0.25)	**0.8**	0.4548	0.2474	0.1367	0.0698	0.0457	0.0247	0.0205	0.0184	0.0247	0.0318
FLMS (*fr* = 0.75)		0.7655	0.6965	0.6310	0.5680	0.5151	0.4587	0.4110	0.3693	0.3297	0.2961
mFLMS (*fr* = 0.75)	**0.2**	0.6559	0.5789	0.5087	0.4444	0.3914	0.3362	0.2905	0.2538	0.2197	0.1913
mFLMS (*fr* = 0.75)	**0.5**	0.6074	0.4948	0.4012	0.3208	0.2615	0.2026	0.1573	0.1266	0.1002	0.0812
mFLMS (*fr* = 0.75)	**0.8**	0.4434	0.2554	0.1529	0.0840	0.0568	0.0269	0.0172	0.0157	0.0213	0.0282

Appendix 5.3 Performance comparison based on fitness achieved at specific iterations for $\sigma^2 = 0.90^2$ in power signal estimation

Method	α	Fitness achieved at specific iterations									
		100	200	300	400	500	600	700	800	900	1000
LMS		0.7980	0.7603	0.7245	0.6884	0.6574	0.6225	0.5915	0.5633	0.5351	0.5098
mLMS	**0.2**	0.7883	0.7421	0.6988	0.6554	0.6189	0.5780	0.5421	0.5101	0.4782	0.4502
mLMS	**0.5**	0.7603	0.6900	0.6276	0.5661	0.5168	0.4630	0.4166	0.3783	0.3410	0.3098
mLMS	**0.8**	0.6606	0.5159	0.4108	0.3159	0.2542	0.1895	0.1407	0.1110	0.0865	0.0717
FLMS (*fr* = 0.25)		0.7777	0.7175	0.6578	0.5964	0.5440	0.4837	0.4313	0.3858	0.3416	0.3046
mFLMS (*fr* = 0.25)	**0.2**	0.6649	0.5918	0.5224	0.4545	0.3990	0.3365	0.2843	0.2443	0.2071	0.1774
mFLMS (*fr* = 0.25)	**0.5**	0.6193	0.5075	0.4101	0.3210	0.2579	0.1900	0.1387	0.1094	0.0854	0.0711
mFLMS (*fr* = 0.25)	**0.8**	0.4548	0.2510	0.1459	0.0756	0.0552	0.0323	0.0313	0.0270	0.0368	0.0476
FLMS (*fr* = 0.75)		0.7656	0.6970	0.6329	0.5695	0.5179	0.4601	0.4111	0.3699	0.3301	0.2970
mFLMS (*fr* = 0.75)	**0.2**	0.6559	0.5796	0.5109	0.4464	0.3947	0.3379	0.2907	0.2544	0.2201	0.1922
mFLMS (*fr* = 0.75)	**0.5**	0.6074	0.4960	0.4048	0.3236	0.2662	0.2045	0.1569	0.1270	0.1009	0.0833
mFLMS (*fr* = 0.75)	**0.8**	0.4431	0.2585	0.1611	0.0889	0.0654	0.0319	0.0257	0.0230	0.0318	0.0422

Appendix 5.4 Performance comparison based on MSE for $\sigma^2 = 0.6^2$ in power signal estimation

Method	α	Adaptive Parameters								MSE
		θ_1	θ_2	θ_3	θ_4	θ_5	θ_6	θ_7	θ_8	
LMS		1.6173	2.5622	3.5830	2.1881	0.8936	0.8181	0.7670	1.1016	5.28E-02
mLMS	**0.2**	1.6813	2.6969	3.7556	2.3085	0.9164	0.8127	0.7617	1.0998	1.91E-02
mLMS	**0.5**	1.7555	2.8577	3.9658	2.4534	0.9386	0.8059	0.7553	1.0974	9.13E-04
mLMS	**0.8**	1.7631	2.9051	4.0323	2.4984	0.9258	0.7993	0.7526	1.0961	3.87E-04
FLMS (*fr* = 0.25)		1.7551	2.8878	4.0257	2.4742	0.9381	0.8038	0.7528	1.1034	4.64E-04
mFLMS (*fr* = 0.25)	**0.2**	1.7619	2.9006	4.0334	2.4915	0.9421	0.8014	0.7525	1.0981	3.46E-04
mFLMS (*fr* = 0.25)	**0.5**	1.7591	2.9036	4.0360	2.4972	0.9286	0.7984	0.7534	1.0973	4.38E-04
mFLMS (*fr* = 0.25)	**0.8**	1.7526	2.9086	4.0475	2.5104	0.8912	0.7970	0.7664	1.1007	1.02E-03
FLMS (*fr* = 0.75)		1.7572	2.8747	3.9990	2.4662	0.9388	0.8050	0.7541	1.0994	4.75E-04
mFLMS (*fr* = 0.75)	**0.2**	1.7651	2.8965	4.0225	2.4889	0.9419	0.8030	0.7530	1.0974	2.49E-04
mFLMS (*fr* = 0.75)	**0.5**	1.7628	2.9033	4.0347	2.4960	0.9300	0.7997	0.7527	1.0969	3.85E-04
mFLMS (*fr* = 0.75)	**0.8**	1.7570	2.9101	4.0384	2.5063	0.8933	0.7962	0.7592	1.0995	8.36E-04
True Values		1.8000	2.9000	4.0000	2.5000	0.9500	0.8000	0.7600	1.1000	0

Appendix 5.5 Performance comparison based on MSE for $\sigma^2 = 0.9^2$ in power signal estimation

Method	α	Adaptive Parameters								MSE
		θ_1	θ_2	θ_3	θ_4	θ_5	θ_6	θ_7	θ_8	
LMS		1.6106	2.5637	3.5894	2.1843	0.8933	0.8210	0.7646	1.1007	5.26E-02
mLMS	**0.2**	1.6735	2.6984	3.7635	2.3049	0.9157	0.8155	0.7591	1.0987	1.90E-02
mLMS	**0.5**	1.7448	2.8593	3.9775	2.4505	0.9361	0.8081	0.7522	1.0959	9.99E-04
mLMS	**0.8**	1.7450	2.9078	4.0486	2.4976	0.9133	0.7989	0.7490	1.0942	8.70E-04
FLMS (*fr* = 0.25)		1.7417	2.8892	4.0419	2.4706	0.9346	0.8050	0.7492	1.1019	8.15E-04
mFLMS (*fr* = 0.25)	**0.2**	1.7461	2.9020	4.0506	2.4885	0.9368	0.8020	0.7488	1.0965	7.39E-04
mFLMS (*fr* = 0.25)	**0.5**	1.7389	2.9051	4.0537	2.4955	0.9176	0.7976	0.7502	1.0959	9.79E-04
mFLMS (*fr* = 0.25)	**0.8**	1.7313	2.9121	4.0700	2.5148	0.8610	0.7956	0.7695	1.1012	2.25E-03
FLMS (*fr* = 0.75)		1.7452	2.8763	4.0128	2.4629	0.9357	0.8067	0.7507	1.0979	6.81E-04
mFLMS (*fr* = 0.75)	**0.2**	1.7510	2.8981	4.0379	2.4859	0.9372	0.8042	0.7495	1.0957	5.44E-04
mFLMS (*fr* = 0.75)	**0.5**	1.7446	2.9050	4.0522	2.4940	0.9198	0.7995	0.7491	1.0954	8.64E-04
mFLMS (*fr* = 0.75)	**0.8**	1.7377	2.9150	4.0573	2.5092	0.8640	0.7943	0.7588	1.0993	2.11E-04
True Values		1.8000	2.9000	4.0000	2.5000	0.9500	0.8000	0.7600	1.1000	0